ISTITUTO ITALIANO PER GLI STUDI FILOSOFICI
SEMINARI DI SCIENZE

10

PETER BILLER, JOSEPH HONERKAMP, FRANCESCO PETRUCCIONE

Stochastic Dynamical Systems

NAPOLI, NELLA SEDE DELL'ISTITUTO

P. BILLER - J. HONERKAMP - F. PETRUCCIONE Stochastic Dynamical Systems

L'Istituto Italiano per gli Studi Filosofici, fondato da Gerardo Marotta, ha sede in Palazzo Serra di Cassano, via Monte di Dio 14, Napoli.

ISTITUTO ITALIANO PER GLI STUDI FILOSOFICI
SEMINARI DI SCIENZE

10

PETER BILLER, JOSEPH HONERKAMP, FRANCESCO PETRUCCIONE

Stochastic Dynamical Systems

NAPOLI, NELLA SEDE DELL'ISTITUTO

La stampa di questo volume è stata realizzata grazie a un contributo della FIME-Leasing

ISBN 88-7723-031-2

Fakultät für Physic der Universität Freiburg
Hermann-Herder-Strasse 3, W-7800 Freiburg im Breisgau
Federal Republic of Germany
and
Freiburger Materialforschungszentrum
Stefan-Maier-Str. 31
W-7800 Freiburg im Breisgau
Federal Republic of Germany

FOREWORD

Stochastic Dynamical Systems is the field where one studies complex systems such as polymeric fluids or the atmosphere with the concepts of mathematical stochastics and probability theory. Because experimental data, with their corresponding errors, can be interpreted as realizations of stochastic variables, typical problems of data analysis can be studied and developed within this approach.

Furthermore, the equations of motion are formulated as stochastic equations in this field. This takes into account that a complex system can never be completely isolated. It is always disturbed by external influences which may be modelled simply as a fluctuating quantity known as noise.

Given such models, the extraction of experimentally accessible quantities and the identification of the model from experimental data must be accomplished. In the first of this series of lectures some basic notions are introduced and prominent problems of stochastic dynamical systems are presented such as: ill-posed problems in data analysis, time series analysis formulation, and simulations of stochastic differential equations. In the following lectures these topics are discussed more deeply. In data analysis the limits of the simple least-square method are explained and the modern techniques of treating inverse problems are outlined. The stochastic differential equations, their formulation, and the various aspects of their simulation are discussed within the field of rheology.

The lectures on *Stochastic Dynamical Systems*, which are reproduced here, were held in Naples at Palazzo Serra di Cassano, the site of the Istituto Italiano per gli Studi Filosofici, in October 1990.

Finally, we offer our deepest personal thanks to Avv. G. Marotta, the President of the Istituto Italiano per gli Studi Filosofici, for inviting us to his prestigious institute, and for his generous hospitality. We also express our gratitude to Prof. A. Gargano and Prof. G. Marrucci for the friendly local organization.

Freiburg, November 1990

P. BILLER
J. HONERKAMP
F. PETRUCCIONE

Contents

Chapter 1

Stochastic Dynamical Systems: An Introduction

J.Honerkamp [¶]

Most people associate science with precise predictions. We know this e.g. from astronomy which is also the field where modern science was born. On the other hand, real life is unpredictable and full of irregularities. This is most clearly expressed in a game of chance. However, we have learned to introduce concepts of probability to tell something about the outcome of some event in a game of chance. If we throw a coin many times we expect that the fraction of heads is near 0.5, we say the probability for getting heads with one throw is 1/2. If a die is rolled the probability of e.g. 'five' is 1/6, if the die is fair. If we roll the die 6000 times we expect nearly 1000 times the outcome 'five', but the outcome of every single throw is completely uncertain.

What does this have to do with science? Are probability concepts only relevant for games, for statistical aspects in description of real life phenomena? We will show in this and the following lectures that this is not true. We will try to demonstrate that probabilistic concepts and methods are cornerstones for treating complex systems like polymeric fluids, the climate on earth or the human body as quantitatively as possible. So if we would like to extend our scientific attitude — which means building mathemati-

[¶]This introductory lecture was given in Italian by F.Petruccione

cal models for the systems to be analyzed — to such complex systems we must necessarily introduce probabilistic notions and a good background in such ideas will be very helpful in understanding the behaviour of such systems.

1.1 Random variables

The basic notion of probability theory is the random variable, sometimes also called a stochastic variable. This must be distinguished from a random or stochastic number. We observe random numbers in throwing a die many times, namely the numbers from 1 to 6 in a random sequence. We say the random number is a realization of a random variable. The variable is a mathematical, abstract object, defined by the possible outcomes in realizations and by the probabilities associated to each of these outcomes. Hence the number (in German called 'Augenzahl') is the random variable in our die-experiment, the possible outcomes are the numbers $(1, 2, \ldots, 6)$ with probability $1/6$ for each. In rolling the die we observe a realization of this random variable. We get a random number, namely a number, that was obtained by chance.

Thus, chance does not mean complete arbitrariness. Getting something by chance means that a random variable is realized. A random variable is defined by the possible outcomes and their probabilities. We must know how probable the events are and which events are possible at all. An event 'seven' e.g. can never appear with a die. There are still rules in the matter of chance or random events, but probabilistic rules.

This way of thinking is not so well known, not even among scientists, though in nearly any experiment one meets a random number, which will show up if one repeats the same experiment again and again. You will usually get always slightly different results and if you plot a histogram you will get a distribution as e.g. in fig.1.1. Hence the experimental results are realizations of a random variable; the true value of the quantity, of course, which we would like to obtain, is not random. The randomness comes in because there are always some uncontrollable influences on our experimental device, that add to the true value and which can be represented by a random number. Experimental measurements are therefore

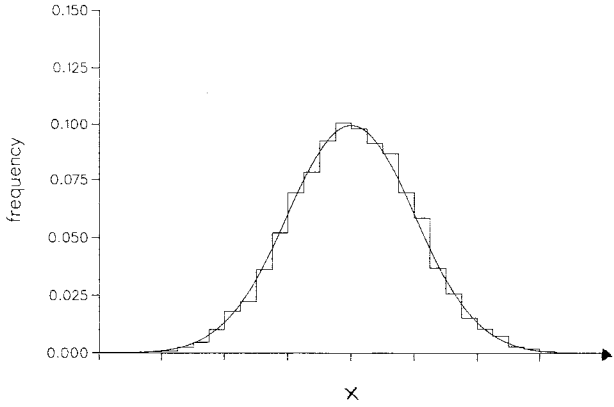

Figure 1.1: A typical histogram collecting the various results scattered around a mean value x. The solid line represents a Gaussian distribution

realizations of a random variable, and we may write

$$Y = x + \eta\,, \tag{1.1}$$

where x shall stand for the true value of the quantity we measure, η is the random variable that represents the external influences and Y is therefore the random variable, whose realizations we actually observe in our measurements.

In order to define the random variable η we have to specify its possible outcomes and their probabilities. We have reasons to believe that these experimental uncertainties are best represented by a random variable η where the probability that a realization will be in the interval $(z, z + dz)$ will be

$$p(z)dz = \frac{1}{\sqrt{2\pi}\sigma}\, e^{-\frac{1}{2}\frac{z^2}{\sigma^2}} dz. \tag{1.2}$$

$p(z)$ is a function which nicely fits the histogram of fig.1.1 (solid line).

The width of the curve is measured by the parameter σ and this is, at the same time, a measure for the uncertainty, the statistical error of the experimental result. There are well established rules by which one can estimate x and σ from the histogram, and formulating an experimental result means giving an estimate $\hat{x}$ of x, the true value, and an estimate $\hat{\sigma}$ of σ, the experimental error. This error also measures how good the estimate $\hat{x}$ of x is, because one may show that with 68% probability the true value will lie in the interval

$$(\hat{x} - \hat{\sigma}, \hat{x} + \hat{\sigma}) \ . \tag{1.3}$$

All these considerations are very elementary and more or less well known to every scientist. But nevertheless, the consequences of the fact that experimental results should be viewed as realizations of a random variable are often not taken seriously enough.

1.2 Inverse problems

We will demonstrate the fruitfulness of stochastic notions with a problem that we will shortly outline in this lecture and discuss more deeply in the next two lectures. It is a very prominent problem of stochastic systems where these experimental errors play a crucial role and where we are not yet dealing with a *dynamical* stochastic system. Dynamical systems are introduced afterwards and a similar relevant problem will be presented.

This prominent problem I want to introduce now is the so-called inverse problem. Inverse problems arise very frequently in science because many quantities which one would like to examine are not directly measurable. Such quantities are e.g. the sizes of particles in a suspension, the density of human tissue or the relaxation times of some dynamical process. In many cases one is interested in the distribution of these quantities, e.g. in the frequency of a given particle size, in the density of the tissue as a function of the location or in the weight with which the dynamical process with a given relaxation time contributes to the whole dynamical process.

Though these distributions are not directly measurable one can get information about them e.g. by scattering of light, X-rays or neutrons. The quantity measured by such experiments is the intensity of the scattered or

transmitted light (or X-rays or neutrons). Hence one has somehow to infer from these experimental results the distribution one is looking for. By theoretical considerations one normally finds how the distribution affects the experimental result. If we call the distribution function $h(\tau)$ where τ stands e.g. for the particle size and if we denote the intensity of scattered neutrons by $G(\omega)$ where ω characterizes the scattering angle then the relation between these two functions can frequently be written as

$$G(\omega) = \int d\tau\, K(\omega, \tau) h(\tau) \tag{1.4}$$

where the kernel $K(\omega, \tau)$ is given by the theory or the model. There are plenty of examples where such a relation is assumed.

The inverse problem now consists in the estimation of the function $h(\tau)$ from the experimental data for $G(\omega)$. These data will be obtained at some discrete ω_i, $i = 1, \ldots, N$ and they will be corrupted by unavoidable errors. Hence the information consists of the data $\{g_i^\sigma, i = 1, \ldots, N\}$ with

$$g_i^\sigma = G(\omega_i) + \sigma_i \epsilon_i \tag{1.5}$$

where σ_i is the standard error and ϵ_i a random number, a realization of a standard Gaussian random variable. From this information one has to infer the function $h(\tau)$.

Thus, an inverse problem is a frequently occurring and typical problem. One likes to know a function which characterizes the system we study. This function, however, cannot be measured directly but has to be extracted from measurements of some other quantity. From the relation between $h(\tau)$ and $G(\omega)$ one immediately recognizes that, given $h(\tau)$, one may easily infer the quantity $G(\omega)$ we expect to measure, but the inverse problem, going from the measurements of $G(\omega)$ to the distribution $h(\tau)$, turns out to be a difficult task. This is especially true because the measurements are always corrupted by experimental errors. We will see in the following lectures that, if this inversion is not done with enough care and enough background of stochastic methods, one will not get reasonable answers. One has to control the uncertainty in the answer $h(\tau)$ in dependence on the experimental error in the measurements of $G(\omega)$. Then it will become evident that the usually applied methods such as the least-square minimization will not work. There are many distributions compatible with the data. One has to introduce more information than the data alone to

get a unique solution. One may e.g. require that the solution has some properties like a special smoothness or maximum entropy.

The phenomenon that the information contained in the experimental data is not enough to obtain a unique solution is the reason why such inverse problems are also called ill-posed problems. We will study the proper treatment of ill-posed problems in the third lecture and we will elaborate the further requirements which lead to uniqueness. But there is an interesting moral in this. Probing nature by means of an experiment will sometimes not give us a unique answer. The information will always be incomplete. Only by imposing further arguments can we find a definite answer.

1.3 Stochastic processes and time series

Until now we have considered random variables and the usefulness of this notion in problems where time plays no role. But there also exists the concept of a time-dependent random variable, say $Y(t)$, that means that at each time t there is a random variable with a probability distribution $p(y,t)$. Some realizations of such a time dependent random variable are drawn in fig.1.2 . Each realization corresponds to a different trajectory or path in space and looks very irregular because in this example there is little correlation for neighbouring times. We call a time dependent random variable a stochastic process or a random process. (One should also mention that for a proper definition of a stochastic process not only $p(y,t)$, but also all higher distributions $p(y_1,t_1,y_2,t_2)$, etc. must be given.)

One observes realizations of a stochastic process e.g. if one measnres a time dependent quantity $x(t)$. Because at each time t we have a different experimental error $\epsilon(t)$ we would introduce

$$Y(t) = x(t) + \epsilon(t) \tag{1.6}$$

as the time dependent random variable, where at each time $\epsilon(t)$ may be a Gaussian random number, independent from $\epsilon(t')$ for $t' \neq t$. This is, of course, a very simple stochastic process, because the standard Gaussian stochastic process $\epsilon(t)$, which is also known as white noise, is adding to a well defined time dependent quantity. For $x(t) = \cos\omega t$ this looks like fig.1.3, and from this picture we would anticipate that it is a deterministic signal

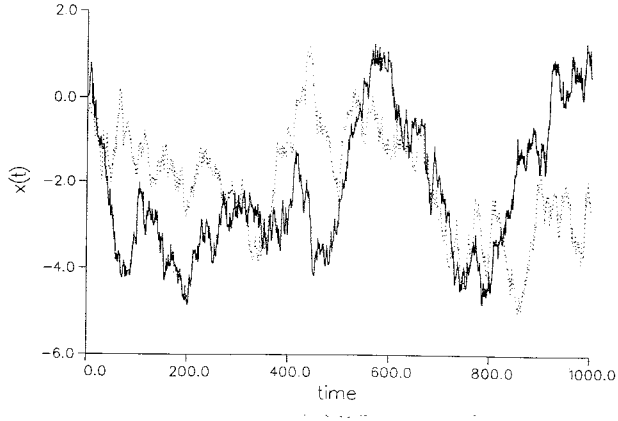

Figure 1.2: Two realizations of a typical stochastic process

superposed by some noise. This is the case of an observational noise, which is only the time-dependent version of the above mentioned experimental error. A really interesting stochastical dynamical system is much more than this. To introduce it let us write $x(t) = \cos\omega t$ as a dynamical system, e.g. as

$$x(t) = a\,x(t-1) + b\,x(t-2) \tag{1.7}$$

with appropriate parameters a, b. This is a discrete version of a differential equation and it is called a dynamical system because given x at former times, namely $x(t-1)$, $x(t-2)$, one may calculate $x(t)$, and because this can also be done without any ambiguity, we call this a deterministic dynamical system. Hence, the system

$$\begin{aligned} x(t) &= a\,x(t-1) + b\,x(t-2) \\ Y(t) &= x(t) + \epsilon(t) \end{aligned} \tag{1.8}$$

would also describe a process as shown in fig.1.3. But now let us introduce

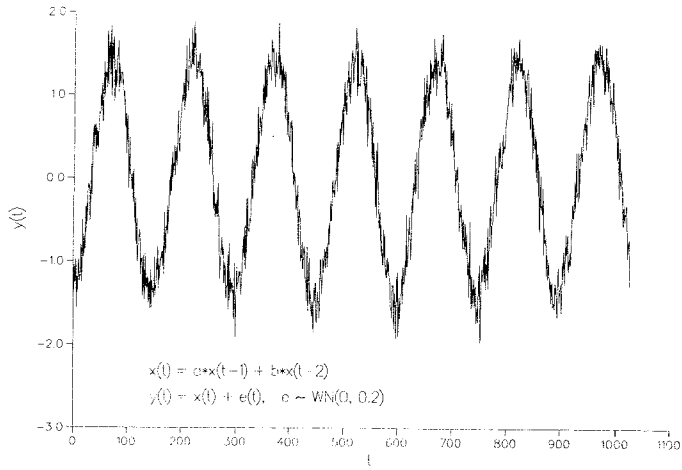

Figure 1.3: A simple sinusoidal function of time corrupted by a white noise

a random variable in the dynamic equation too, so that we change the dynamics to

$$X(t) \;=\; a\,X(t-1) + b\,X(t-2) + \eta(t)\;, \tag{1.9}$$

where $\eta(t)$ is e.g. also a white noise process independent of $\epsilon(t)$. Then with given $x(t-1)$ and $x(t-2)$ a definite determination of $x(t)$ is no longer possible. We can give only probabilities for the value of $x(t)$, that means, even if $x(t-1)$ and $x(t-2)$ are already known, $x(t)$ is a random number, a realization of the random variable $X(t)$. Hence by introducing a random variable into the dynamic equation $X(t)$ becomes a random variable too (and therefore we have written capital letters X in eqn.1.9, to distinguish random variables from realizations).

If we now calculate realizations of this process then we get something like that seen in fig.1.4. You see the great difference from a *pure* cosine wave which we would obtain without the white noise in the dynamical equation,

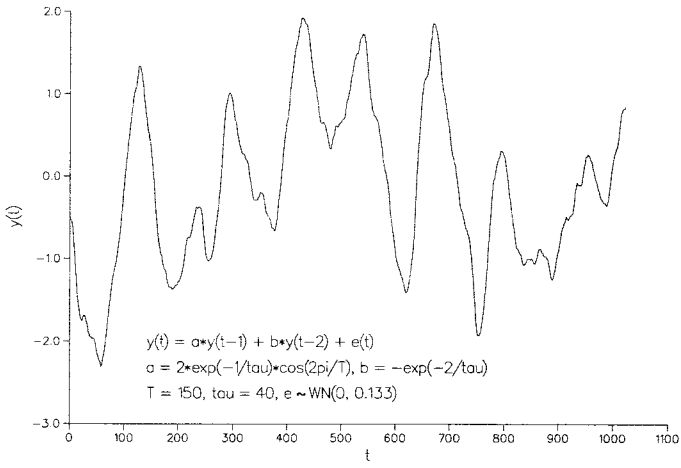

Figure 1.4: A realization of a stochastic process as given in equ.1.9.

but you see also the difference from the case in fig.(1.3) where only the observational noise is present. There is still some oscillation in the signal but irregularly, stochastically; it is a signal of a stochastic oscillator. The frequency of this oscillator is by construction the same as of the other two signals. But there is one difference now. I have changed the parameters a, b a little bit, but in such a manner that the frequency will not be modified. However, a damping is introduced. Hence without the white noise the trajectory of the system $X(t)$ would look as in fig.1.5. This is necessary because the addition of the white noise in the dynamical equation acts like an external drive, as an input of energy and without a damping the trajectory would diverge.

A linear, stochastically driven oscillator is the most elementary stochastic dynamical system. Taking into account also the unavoidable observa-

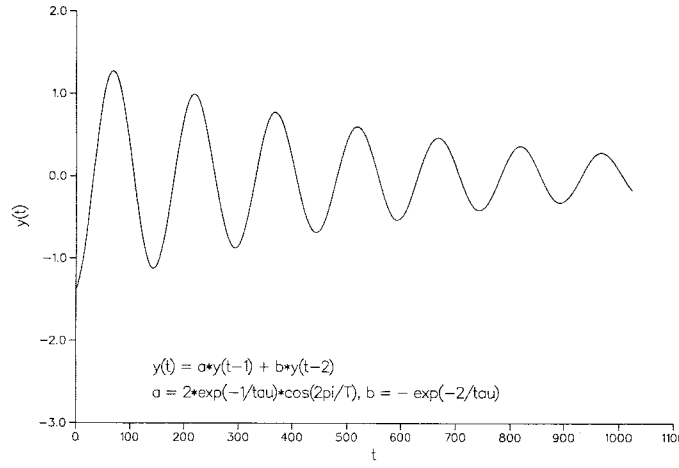

Figure 1.5: A damped cosine wave described by a dynamical system without the white noise

tional error we would formulate such a system as

$$\begin{aligned} X(t) &= a\,X(t-1) + b\,X(t-2) + \eta(t) \\ Y(t) &= X(t) + \epsilon(t) \quad . \end{aligned} \tag{1.10}$$

By superimposing such systems one may describe a wide variety, namely the whole class of linear stochastic systems. If we observe time-dependent processes in nature which already look very random one may ask whether they can be modelled by such a linear stochastic system.

Time dependent processes which look random are observed very frequently. In meteorology and climatology one registers the mean temperature or pressure of every day, month or year. The sequence of such values associated to different but equidistant times is called a time series. In fig.1.6 two prominent time series of climatology are shown, the first one is the difference of the atmospheric pressure at two meteorologic stations,

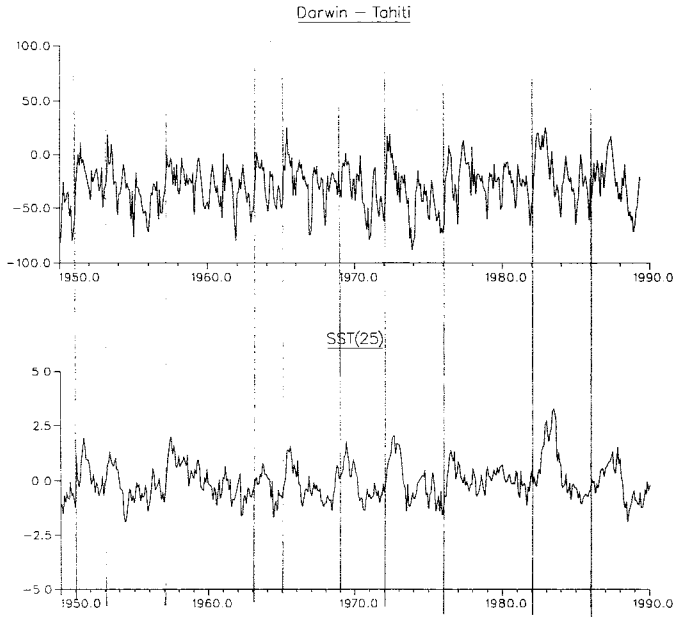

Figure 1.6: (a): Difference of the atmospheric pressures in Darwin and Tahiti; (b) the sea surface anomalies (SST, anomaly = difference from a mean value) at some point on the equator in front of the south american coast

Darwin in Australia and Tahiti. The second one is the difference of the sea surface temperature from a mean value at some location on the equator in front of the South American coast. One recognizes wild fluctuations but also regularities, at least some correlations. There are years where both quantities become large. These are the years when the so-called El-Niño phenomenon appears, a warm sea flow off the west coast of Peru causing heavy damage to the fishing and all industry depending on it.

Meteorology and climatology are the traditional fields where time series are registered. Modern analysis of such time series consists of finding a stochastic process of which the time series could be a realization. One calls this the identification problem and it means the fitting of parameters of a stochastic dynamical system to a time series. There are many other time series, also in other scientific fields. In medicine there are the electrocardiogram and electroencephalogram series which all of you have at least heard of but there are also less well known ones, e.g. those measuring the acceleration of the hand, observing by this means the fluctuations which are very small for normal persons but can become very large for persons with a certain disease, called Parkinson tremor. Fig.1.7 shows such time series from a normal person above and from a Parkinson tremor patient below. Apart from the different amplitudes (the difference in scale is not shown but the amplitude of a Parkinson time series is about 1000 times larger as for a series from a normal person) they look quite different. It turns out that the first series can really be described by a linear stochastic oscillator system whereas the Parkinson time series has been identified as a chaotic signal.

I would like to show you still another time series, namely a typical speech signal. If one measures the sound pressure with a rate of, say 13 kHz, one obtains a time series as given in fig.1.8. These are very instationary, because any phonem corresponds to a different stochastic process (see fig.1.9). Recognition of these different processes means speech recognition. This is a difficult but very exciting and also commercially attractive task.

In presenting these different time series and interpreting them as realizations of stochastic processes we have at the same time already mentioned some aims which are the motivation for the analysis. Whenever one has really found a mathematical model for the observed process, one can

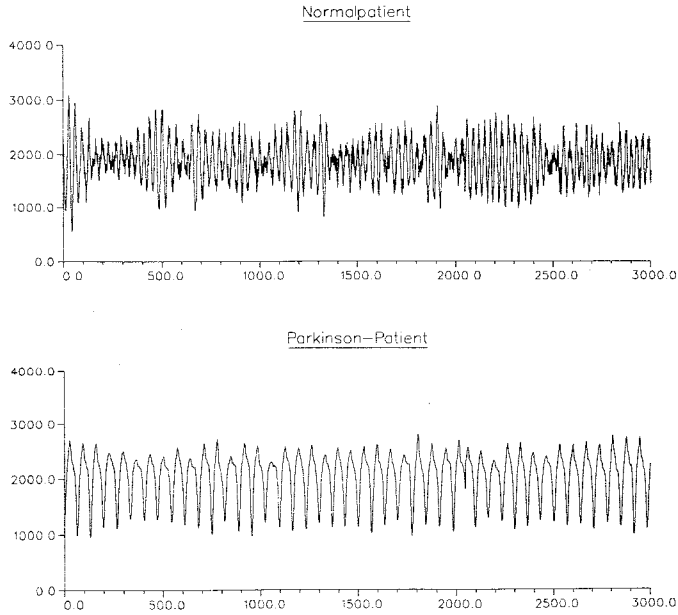

Figure 1.7: Tremor time series (tremor = small fluctuations of a hand): (a) for a normal person; (b) for a person with Parkinson's disease. The ratio of the scales is 1000

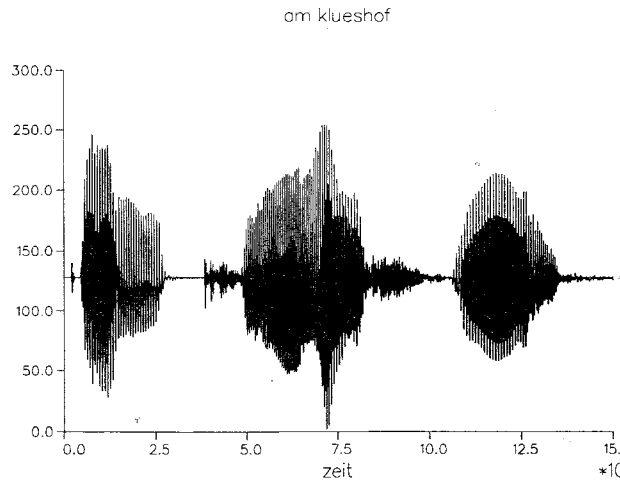

Figure 1.8: A typical speech signal

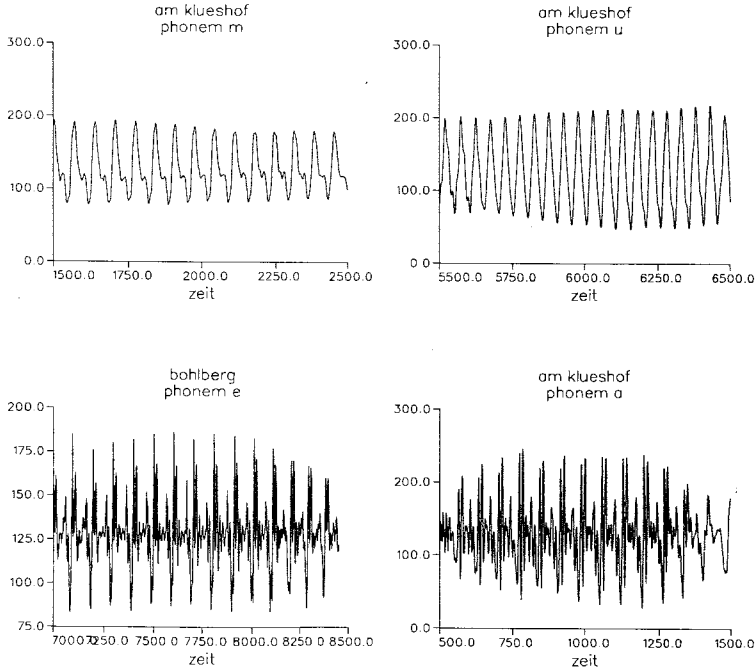

Figure 1.9: Small parts from the time series in fig. 1.8 which correspond to different phonems.

- make predictions, this is e.g. interesting in climatology and meteorology. One wants e.g. to forecast the El-Niño events or other climatological signals.
- characterize the system and study the change of the characteristic parameters of the model in dependence on external influences. This is relevant to the tremor time series analysis.
- classify the time series or parts of it. This is a task which is necessary for speech recognition.
- code the time series. If with the identified model one can reconstruct the signal without too much distortion one may store or transmit the parameters of the model instead of the series. This may reduce the amount of information to be stored or transmitted considerably.

1.4 Continuous time stochastic processes

By considering the time series we have introduced a discrete time parameter because observations are being made at discrete, mostly equidistant time points. Also the stochastic models were adapted to this viewpoint and were formulated with a discrete time parameter. Dynamical systems formulated with a *continuous* time parameter are differential equations as e.g.

$$\dot{x}(t) = -\alpha\, x(t) \tag{1.11}$$

Given x at $t = 0$ one may calculate $x(t)$ for any $t > 0$ from such an equation (here we get $x(t) = x(0)e^{-\alpha t}$, an exponentially decreasing function). Again we may turn such a deterministic differential equation into a stochastic differential equation by adding e.g. white noise to the right hand side of eq.(1.11), leading to

$$\dot{X}(t) = -\alpha\, X(t) + \eta(t) \tag{1.12}$$

By this means $X(t)$ becomes a stochastic process, a random variable for each time. Instead of a decreasing function $x(t)$ as the solution of eqn.(1.12) we now obtain as realizations of $\{X(t), t > 0\}$ trajectories as shown in fig. 1.10 . The relaxation to zero dictated by the deterministic part of the equation $(-\alpha\, x(t))$ is always disturbed by the noise. We get a stationary state of fluctuations about zero.

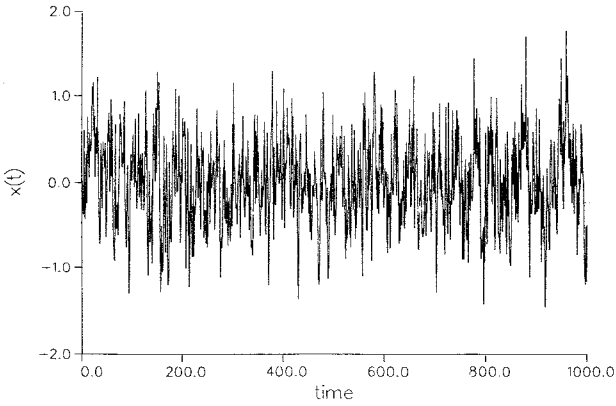

Figure 1.10: A realization of the stochastic process given by equ. 1.10.

Many such stochastic differential equations have been formulated up until now. The additional noise in these equations simulates the external influences, which cannot be taken into consideration in more detail. This is justified, if there are many different influences, say forces, which are all independent and add up to such a force fluctuating on a small time scale like a white noise. There are many situations where such a picture is a good approximation to the real situation: small particles in a fluid, pollutants in the air, macromolecules in a solution or in a polymeric melt. In rheology where one studies the flow behaviour of polymeric fluids this approach of formulating stochastic differential equations for the macromolecules has been very fruitful. The macromolecule is modelled as a chain of beads connected by springs which simulate the forces between the beads. For each bead one writes down the equation of motion in the classical manner, but one adds the noise term to simulate the external stochastic influences. By this a set of stochastic differential equations is obtained. The fourth

lecture will deal with such stochastic equations in rheology.

In this context one is not interested in a realization of $X(t)$, but more in statistical properties of such trajectories. One can show that experimentally accessible quantities are expressed by quantities like $< X^2(t) >$ or $< X(t)X(t+\tau) >$ where $< O(x) >$ means the expectation value of $O(X)$ to be calculated by e.g.

$$< O(X(t)) >= \int dx\, O(x) p(x,t) \ . \tag{1.13}$$

One will see that only the simplest of the stochastic differential equations can be treated analytically, that means, by giving closed mathematical expressions for such expectation values.

But a very powerful method, even for the most complicated stochastic differential equations is the simulation of the equation. One generates thousands or millions of realizations of the stochastic process formulated by the set of equations and evaluates the statistical properties. By this means one obtains again estimates of the expectation values which have to be treated like experimental values. One has to determine an interval, in which e.g. with 68% probability the true value of the expectation value lies. A proper discussion of the estimators is again a matter, where notions and concepts of stochastics are necessary. In the fifth lecture such simulations are presented and discussed.

1.5 Conclusions

In this introductory lecture we have pointed out that 'Stochastic Dynamical Systems' is a field in which one studies complex systems like polymeric fluids or the atmosphere with the concepts of mathematical stochastics and probability theory. We hope we have shown that these notions are really adequate and useful. (Some books about this topic are e.g. [1, 2, 3].) We introduced the concept of a random variable and of the random or stochastic process and we briefly discussed those prominent topics within this field: the treatment of inverse problems, the identification of a stochastic dynamical system from a time series and the formulation and the simulation of stochastic differential equations. These topics will be studied more deeply in the following four lectures.

Chapter 2

Stochastic Concepts for Analyzing Experimental Data

J. Honerkamp

In this and the following lecture we will discuss various aspects of a characterization of a material by its specific response to external influences. The material we have in mind here is a polymeric melt. The external influences will be some types of deformation. But one will readily recognize that the methods used to analyze the response data, i.e. the raw experimental data and to interpret these in terms of a theoretical model will be very general. Also a couple of very useful concepts and methods of stochastic dynamical systems can be explained within this discussion.

2.1 The relaxation spectrum

A polymeric melt is a very complex material. It is not a pure, Newtonian fluid like water, it is not a solid like a rubber, it has viscous *and* elastic properties. In order to study these viscoelastic properties one may design experiments where some type of deformation is exerted on the material. It will respond with an internal stress which may be characteristic for that material. For a sudden step strain e.g. an internal shear stress will appear, relax and approach zero after a while. The form of this relaxation will be different for different materials. (For a solid these stresses stay

constant, for a Newtonian fluid like water there are no stresses at all.) If the deformation γ_0 is small enough (what this means depends on the material) the internal shear stress $\tau(t)$ is a product of the amount of deformation, γ_0, and of the relaxation modulus, which describes the approach of the stress to zero:

$$\tau(t) = \gamma_0 G(t) \ . \tag{2.1}$$

We call the region of deformation where $\tau(t)$ is proportional to γ_0 the regime of linear viscoelasticity. The relaxation modulus $G(t)$ is defined only for $t \geq 0$ ($t = 0$ is the time where the deformation is applied to the material). The decrease of $G(t)$ with time can be described by a superposition of decreasing exponential functions

$$G(t) = \sum_{\alpha=1}^{M} h_\alpha \, e^{-t/\tau_\alpha} \tag{2.2}$$

where the τ_α, $\alpha = 1, \ldots, M$ are some relaxation times and the h_α, $h_\alpha \geq 0$ are the weights which measure the contribution of a process with the characteristic time τ_α to the whole relaxation process.

Hence, in a first *Ansatz* of a linear viscoelastic theory one resolves the whole relaxation process into a superposition of elementary processes which are governed by some relaxation time. This idea is plausible from the point of view that the constituents of the polymeric melt, the macromolecules, are long chains which, under a sudden deformation of the material, are stretched. The adaption to this new shape of the bulk body will take time and due to the complicated structure and interaction there will be different time scales. Turning it around, if we introduce a relaxation process for every time scale, then there may be more and less dominant relaxation times i.e., different weights for each relaxation time. Hence we may introduce a continuous relaxation spectrum $h(\tau)$, so that the relaxation modulus $G(t)$ is now expressed as

$$G(t) = \int_{-\infty}^{\infty} d\ln\tau \, h(\tau) e^{-t/\tau} \tag{2.3}$$

and we get back a relation like (2.2) if we introduce a grid of relaxation times $[\tau_\alpha, \alpha = 1, \ldots, M]$ and describe the integral in (2.3) as

$$G(t) = \sum_{\alpha=1}^{M} h(\tau_\alpha) m_\alpha e^{-t/\tau_\alpha} \tag{2.4}$$

where m_α are the weights due to the discretization of the integral. The relaxation spectrum $h(\tau)$ or the set $\{h_\alpha = h(\tau_\alpha)$ with suitable chosen $\tau_\alpha\}$ is a candidate for a characterization of the material, and there is some experience which makes us believe that the spectrum is really a good characteristic function. If this is true, then one should be able to judge, alone from the knowledge of the relaxation spectrum, the flow behaviour. At least there should be a simple relationship between the relaxation spectrum and some relevant properties of a flow of these melts in an industrial process. And if the relaxation spectrum is really able to play a central role in the characterization of a material, then also other properties, such as e.g. those of the molecular mass distribution should be inferable from it.

There is another reason why the relaxation spectrum is a useful quantity. The sudden shear deformation is not the only standard influence on a material we can apply. Sometimes there are other types of deformations which are more easily applicable. Each of these standard experiments introduces a material function like the relaxation modulus $G(t)$. The common information content is the relaxation spectrum and once this spectrum is known, all material functions can be calculated. This is the task for which the spectrum is most frequently used today. From one material function one tries to infer the relaxation spectrum. Then the other material functions can be calculated. We will call this the conversion task of the relaxation spectrum contrary to the characterization task we mentioned above.

2.2 Measuring the dynamic moduli

A deformation history for which the corresponding material function is relatively quickly and easy accessible is the oscillatory shear flow. If we denote the instantaneous shear (in the $x-y$ plane, say) by $\gamma(t)$, then in oscillatory shear flow we have

$$\gamma(t) = \gamma_0 \cos \omega t, \quad t \geq 0 \ , \tag{2.5}$$

where ω is the frequency and γ_0 the amplitude. On the other hand the general relationship between internal stress $\tau(t)$ and shear rate $\dot{\gamma}(t)$ reads

(see e.g. [4])

$$\tau(t) = \int_0^t ds\, G(s)\dot{\gamma}(t-s) \tag{2.6}$$

where $G(s)$ is the relaxation modul introduced in section 2.1. In a complex notation we write now $\gamma(t)$ as

$$\gamma(t) = Re\left(\gamma_0 e^{i\omega t - i\varphi}\right), \quad t \geq 0\ , \tag{2.7}$$

where we introduced a phase φ for generality. (Actually we have $\varphi = \pi/2$ in an experiment so that $\gamma(t) = \gamma_0 \sin(\omega t)$). Then we obtain

$$\tau(t) = Re\left\{\int_0^t ds\, G(s) i\omega\gamma_0 e^{-i\varphi} e^{i\omega(t-s)}\right\}. \tag{2.8}$$

In the steady state regime ($t \to \infty$) we get

$$\tau(t) = Re\left(i\omega\gamma_0 e^{i\omega t} e^{-i\varphi}\widetilde{G}(\omega)\right) \tag{2.9}$$

with

$$\widetilde{G}(\omega) = \int_0^\infty ds\, G(s) e^{-i\omega s}. \tag{2.10}$$

If we write

$$\widetilde{G}(\omega) = \frac{1}{\omega}\left(G''(\omega) - iG'(\omega)\right) \tag{2.11}$$

where $G''(\omega)$ is the loss modulus and $G'(\omega)$ the storage modulus, we finally end up with

$$\tau(t) = \gamma_0\left(G'(\omega)\cos(\omega t - \varphi) - G''(\omega)\sin(\omega t - \varphi)\right). \tag{2.12}$$

Hence under an oscillatory shear flow a linear viscoelastic material responds with an internal stress which is also a superposition of a sine and cosine function with the same frequency. For small oscillatory shear flow we have two real material functions, $G'(\omega)$ and $G''(\omega)$, or one complex function $\widetilde{G}(\omega)$.

The extraction of this quantity from the stress signal $\tau(t)$ is usually done by Fourier-transformation:

$$G'(\omega) = \frac{1}{\gamma_0}\frac{1}{nT}\int_0^{nT} dt\, \tau(t)\cos\omega t\,, \tag{2.13a}$$

$$G''(\omega) = \frac{1}{\gamma_0}\frac{1}{nT}\int_0^{nT} dt\, \tau(t)\sin\omega t\,, \quad T = 2\pi/\omega. \tag{2.13b}$$

where n is some integer so that nT is approximately equal to the length of the time signal. We are, however, also interested in the experimental error of the material functions, which is due to statistical fluctuations of the signal. Therefore we prefer another method, a usual linear regression method, for estimating $G'(\omega)$ and $G''(\omega)$ by which the error is also easily obtained. But before we discuss this method let us mention two immediate generalizations.

- If the deformation history is generalized to

$$\gamma(t) = \sum_{i=1}^{K} a_i \cos \omega_i t \tag{2.14}$$

with given (ω_i, a_i), we obtain in the linear regime (in the following we will neglect the phase φ):

$$\tau(t) = \sum_{i=1}^{K} a_i \left(G'(\omega_i) \cos \omega_i t \; - \; G''(\omega_i) \sin \omega_i t \right) . \tag{2.15}$$

The stress signal is a superposition of the signal for each frequency. This is the consequence of the linear relationship. The regression method to be discussed below for estimating $G'(\omega)$ and $G''(\omega)$ can also be applied to this case and with a shear deformation history like (2.14) we will obtain the relaxation moduli $G'(\omega)$, $G''(\omega)$ and their experimental errors at the frequencies ω_i, $i = 1, \ldots, K$.

- Nonlinear behaviour will appear as a nonharmonic periodic time behaviour of $\tau(t)$. Higher harmonics will be observed in the stress signal. This may be represented then e.g. as

$$\begin{aligned} \tau(t) \;\; = \;\; \gamma_0 \big(& G'(\omega) \cos \omega t - G''(\omega) \sin \omega t \\ & + G'_3(\omega) \cos 3\omega t - G''_3(\omega) \sin 3\omega t \\ & + G'_5(\omega) \cos 5\omega t - G''_5(\omega) \sin 5\omega t + \ldots \big) \end{aligned} \tag{2.16}$$

where $G'_3(\omega), \ldots$ may still depend on γ_0. Our procedure to extract $G'(\omega)$ and $G''(\omega)$ from a time series $\tau(t_i)$, $i = 1, \ldots, N$ can easily be generalized to the estimation of the coefficients $G'(\omega), G''(\omega), G'_3(\omega), \ldots$.

In the linear regression method the coefficients $G'(\omega)$ and $G''(\omega)$ are found

from the stress signal $\tau(t_i)$, $i = 1, \ldots, N$ by minimizing the discrepancy

$$\chi^2 = \sum_{i=1}^{N} \frac{1}{\sigma_i^2} \Big(\tau(t_i) - \gamma_0 (G'(\omega) \cos \omega t_i - G''(\omega) \sin \omega t_i) \Big)^2 ; \tag{2.17}$$

that means, $G'(\omega)$ and $G''(\omega)$ are chosen so that χ^2 is minimal. Here σ_i are the experimental errors of $\tau(t_i)$, i.e. the experimental error of the stress measurement at $t = t_i$. We assume this error to be constant, $\sigma_i = \sigma_0$. Under this assumption it is not necessary that the value of the error is known, it can be estimated by the regression method. The formulation of the fit problem as such a minimization problem and its final solution is very well known and every student who will ever be confronted with data will have to learn it. But there are two points which are not so well known but which are extremly important and therefore also deserve to belong to common wisdom.

- The first point is that there is an elegant solution for the coefficients and their errors. In order to introduce this, let me write formula (2.12) at the points t_i where $\tau(t)$ is measured as

$$\tau(t_i) = \sum_{\alpha=1}^{L} K_{i\alpha} G_\alpha \ , \quad i = 1, \ldots, N \ , \tag{2.18}$$

  G_α, $\alpha = 1, \ldots, L$ are the coefficients to be estimated and $K_{i\alpha}$ are the elements of an $N \times L$ matrix $\mathbf{K}$. (In our case L=2 and $K_{i1} = \gamma_0 \cos \omega t_i$, $G_1 = G'(\omega)$, $K_{i2} = -\gamma_0 \sin \omega t_i$, $G_2 = G''(\omega)$). Then we have to minimize

$$\chi^2 = \sum_{i=1}^{N} \frac{1}{\sigma_i^2} \left(\tau(t_i) - \sum_{\alpha=1}^{L} K_{i\alpha} G_\alpha \right)^2 . \tag{2.19}$$

  The coefficients $\{G_\alpha\}$ which minimize χ^2 are now given directly in terms of quantities which appear in the so-called singular value decomposition of the matrix $\mathbf{K}$.

  This decomposition reads

$$\mathbf{K} = \sum_{j=1}^{L} w_j \, \mathbf{u}_j \mathbf{v}_j^T \tag{2.20}$$

  where $\mathbf{u}_j$, $j = 1, \ldots, L$ are the L eigenvectors to the $N \times N$ matrix $\mathbf{K}\,\mathbf{K}^T$ with the largest eigenvalues; $\mathbf{v}_j$, $j = 1, \ldots, L$ are the eigenvectors of the

$L \times L$ matrix $\mathbf{K}^T\mathbf{K}$ and w_j, $j = 1, \ldots, L$ are the singular values, which are related to the eigenvalues a_j of $\mathbf{K}^T\mathbf{K}$ by $w_j = \sqrt{a_j}$.

Numerical algorithms for calculating these quantities for a given matrix $\mathbf{K}$ can be found in nearly every numerical library, (e.g. in the IMSL, the NAG or in [5]) and in terms of these quantities the solution of the regression problem reads

$$G_\alpha = \sum_{j=1}^{L} \frac{1}{w_j} (\mathbf{v}_j)_\alpha \left(\sum_{i=1}^{N} (\mathbf{u}_j)_i \cdot \tau(t_i) \right) . \tag{2.21}$$

The error $\sigma(G_\alpha)$ of G_α can be calculated from

$$\sigma^2(G_\alpha) = \sigma_0^2 \sum_{j=1}^{L} \frac{1}{w_j^2} ((\mathbf{v}_j)_\alpha)^2 . \tag{2.22}$$

and the constant experimental error σ_0 of the stress measurements can be estimated by

$$\sigma_0 = \sqrt{\chi^2_{\min}/(N - L)} . \tag{2.23}$$

where $\chi^2_{\min}$ is the value of χ^2 at its minimum.

- The second point can easily be inferred from these formulae. The solutions G_α are not well defined if some w_j become very small (compared to the largest singular value which will set the scale). Small changes in the experimental value $\tau(t_i)$ (which may be realized in a further, but identical experiment) will lead to large changes in the solution. The solution is badly defined which is also expressed by the fact, as one deduces from (2.22), that the variance, the statistical error of G_α is very large. In the case we are just considering this problem does not arise and we will come to this point later in the next lecture.

We will demonstrate the use of the linear regression method for estimating the material functions including their errors with some examples.

Fig.2.1 shows typical cases of functions $\gamma(t)$ and $\tau(t)$, where $\gamma(t) = \gamma_0 \cos \omega t$ with $\gamma_0 = 10\%$ in (a) and $\gamma_0 = 0.1\%$ in (b). The results for the material functions are

$$G'(\omega) = 645.55 \pm 0.31, \quad G''(\omega) = 1140.00 \pm 0.42 \tag{2.24}$$

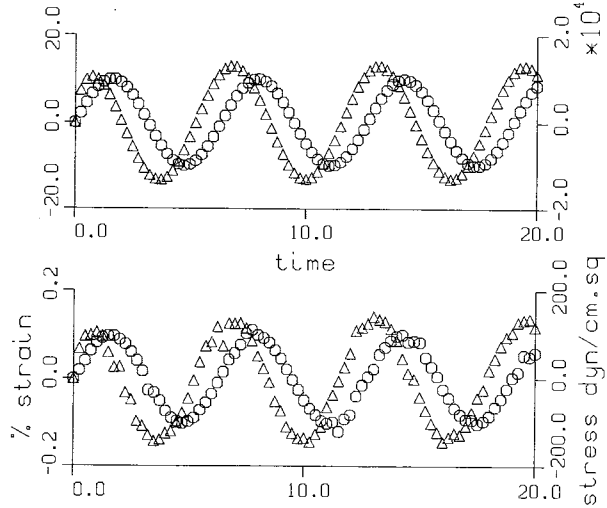

Figure 2.1: Strain and stress as function of time in an oscillatory shear flow, measured at a PS sample (Rheometrics): (a) Strain amplitude 10%; (b) Strain amplitude (0.1%), so that the experimental noise is high

and

$$G'(\omega) = 664.65 \pm 10.23, \quad G''(\omega) = 1212.61 \pm 13.83. \tag{2.25}$$

respectively. Due to the very small strain amplitude in (b) the experimental noise is high. The material functions can still be determined by the least square method. Of course, the statistical errors are much larger.

2.3 The least-square estimation of the spectrum

Having discussed how to obtain the values of the dynamic moduli $G'(\omega), G''(\omega)$ including their statistical experimental errors from the stress time series we will start from these dynamical moduli as the experimental data. If $\omega_i, i = 1, \ldots, N$ are the frequencies of the oscillatory flow we have applied,

our data consist of $\{\omega_i, g_i'^{\sigma}, \sigma_i', g_i''^{\sigma}, \sigma_i''; i = 1, \ldots, N\}$, where e.g. $g_i'^{\sigma}$ denotes the value obtained for $G'(\omega_i)$ and σ_i' is the corresponding error. Our task is now to find from these data the relaxation spectrum, which we already introduced in the discussion of the relaxation modulus

$$G(t) = \sum_{\alpha=1}^{M} h_\alpha e^{-t/\tau_\alpha} . \tag{2.26}$$

From (2.10) we obtain then

$$\begin{aligned} \widetilde{G}(\omega) &= \int_0^\infty ds\, G(s) e^{-i\omega s} = \int_0^\infty ds \sum_{\alpha=1}^{M} h_\alpha e^{-(\frac{1}{\tau_\alpha} + i\omega)s} \\ &= \sum_{\alpha=1}^{M} h_\alpha \frac{1}{\frac{1}{\tau_\alpha} + i\omega} = \sum_{\alpha=1}^{M} h_\alpha \frac{\tau_\alpha (1 - i\omega\tau_\alpha)}{1 + (\omega\tau_\alpha)^2} , \end{aligned} \tag{2.27}$$

so that the dynamic moduli are represented by the spectrum in the following way:

$$G'(\omega) = \sum_{\alpha=1}^{M} h_\alpha \frac{(\omega\tau_\alpha)^2}{1 + (\omega\tau_\alpha)^2} , \qquad G''(\omega) = \sum_{\alpha=1}^{M} h_\alpha \frac{\omega\tau_\alpha}{1 + (\omega\tau_\alpha)^2} . \tag{2.28}$$

The set of relaxation times $\{\tau_\alpha,\, \alpha = 1, \ldots, M\}$ are chosen equidistantly distributed on a logarithmic time scale. In order to find the set of weights $\{h_\alpha,\, \alpha = 1, \ldots, M\}$ for which the differences

$$g_i'^{\sigma} - \sum_{\alpha=1}^{M} h_\alpha \frac{(\omega_i\tau_\alpha)^2}{1 + (\omega_i\tau_\alpha)^2} \quad \text{and} \quad g_i''^{\sigma} - \sum_{\alpha=1}^{M} h_\alpha \frac{\omega_i\tau_\alpha}{1 + (\omega_i\tau_\alpha)^2} \tag{2.29}$$

are as small as possible, we define the discrepancy as

$$\begin{aligned} \chi^2 &= D(\{g_i^\sigma\}, \{h_\alpha\}) \\ &= \sum_{i=1}^{N} \frac{1}{\sigma_i'^2} \left(g_i'^{\sigma} - \sum_{\alpha=1}^{M} h_\alpha \frac{(\omega_i\tau_\alpha)^2}{1 + (\omega_i\tau_\alpha)^2} \right)^2 + \sum_{i=1}^{N} \frac{1}{\sigma_i''^2} \left(g_i''^{\sigma} - \sum_{\alpha=1}^{M} h_\alpha \frac{\omega_i\tau_\alpha}{1 + (\omega_i\tau_\alpha)^2} \right)^2 \end{aligned} \tag{2.30}$$

and look for that set $\{h_\alpha\}$ for which χ^2 is minimal.

We call this set the least-square estimator and as mentioned in sect.2.2 it can easily be found with the singular value decomposition of the $2N \times M$ matrix $\mathbf{K}$ with

$$K_{i\alpha} = \frac{1}{\sigma_i'} \frac{\omega_i\tau_\alpha}{1 + (\omega_i\tau_\alpha)^2} , \qquad i = 1, \ldots, N \tag{2.31a}$$

$$K_{i\alpha} = \frac{1}{\sigma''_{i-N}} \frac{(\omega_{i-N}\tau_\alpha)^2}{1+(\omega_{i-N}\tau_\alpha)^2}, \quad i = N+1,\ldots,2N. \tag{2.31b}$$

The least-square estimator then reads

$$h_\alpha = \sum_{j=1}^{M} \frac{1}{w_j} (\mathbf{v}_j)_\alpha (\mathbf{u}_j \cdot \mathbf{g}^\sigma) \tag{2.32}$$

with $\mathbf{g}^\sigma = (g_1^\sigma, \ldots, g_{2N}^\sigma)$ where

$$g_i^\sigma = g_i'^\sigma / \sigma'_i, \qquad i = 1,\ldots,N \tag{2.33a}$$

$$g_i^\sigma = g''^\sigma_{i-N} / \sigma''_{i-N}, \qquad i = N+1,\ldots,2N, \tag{2.33b}$$

and the $w_j, \mathbf{u}_j, \mathbf{v}_j$, $j = 1,\ldots,M$ are given by the singular value decomposition of the matrix $\mathbf{K}$. The statistical errors $\sigma(h_\alpha)$ are calculated from

$$\sigma^2(h_\alpha) = \sum_{j=1}^{M} \frac{1}{w_j^2} \left((\mathbf{v}_j)_\alpha\right)^2. \tag{2.34}$$

In section 2.2 it was mentioned that there is always the danger that the statistical uncertainties of the least-square estimator are too large so that this estimator is not meaningful anymore. This is now just what happens. The larger M is, i.e. the higher the resolution we choose on the τ-axis, the broader the range which is covered by the singular values and the smaller the smallest singular values become. This is plausible because our problem is the discrete version of the solution of an integral equation of the first kind. We look for the solution $h(\tau)$ of

$$G(\omega) = \int_{-\infty}^{+\infty} d\ln\tau \; K(\omega,\tau) h(\tau), \tag{2.35}$$

which, if the integral is approximated by a discrete sum, takes the form

$$G(\omega_i) = \sum_{\alpha=1}^{M} \ln\left(\frac{\tau_\alpha}{\tau_{\alpha-1}}\right) K(\omega_i,\tau_\alpha) h(\tau_\alpha). \tag{2.36}$$

With increasing M the distance between nearest points $(\tau_\alpha, \tau_{\alpha+1})$ decreases; the columms in the matrix $\mathbf{K}$, therefore, become less independent, leading to smaller singular values (strict dependence leads to a zero singular value). The growth of the errors with increasing M is demonstrated in fig.2.2 for some experimental data, the least-square estimator is shown with $M = 8$

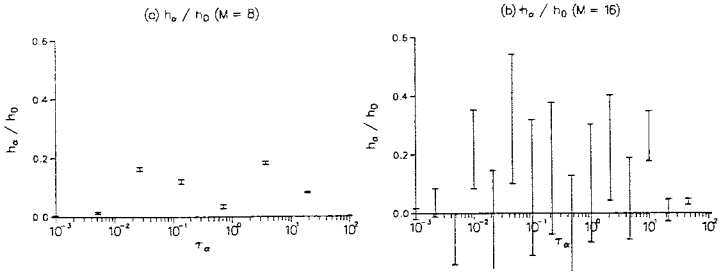

Figure 2.2: Normalized results for a relaxation spectrum derived with a least-square method: (a) $M = 8$ and (b) $M = 16$ gridpoints at the τ-axis

and with $M = 16$. One recognizes the dramatic increase of the errors. That means, there is not only one set of weights $\{h_\alpha\}$ which nicely fits the experimental data, but a continuum of sets in the neighborhood of the least-square estimator. To understand this better and to formulate it more precisely let us look at the discrepancy achieved by the least-square estimator. One can show that one expects a value around $2N - M \leq 2N$ for it. But even, if each individual discrepancy, e.g.

$$g_i^\sigma - \sum_{\alpha=1}^{M} h_\alpha \frac{(\omega_i \tau_\alpha)^2}{1 + (\omega_i \tau_\alpha)^2} \tag{2.37}$$

is of the order of σ_i (so that χ^2 is of the order of $2N$, which is the number of experimental data), the fit $\{h_\alpha\}$ can be considered to be compatible with the experimental data. We will therefore define those sets $\{h_\alpha\}$ as compatible with the data, for which the inequality

$$D(\{g_i^\sigma\}, \{h_\alpha\}) \leq 2N \tag{2.38}$$

holds. Then we could follow from this discussion that there are many sets $\{h_\alpha\}$ of weights which are compatible with the experimental data. The least-square estimator is just one of these (see fig.2.3). If we would repeat the experiment getting slightly different experimental data we could obtain a largely different least-square estimator out of these because small

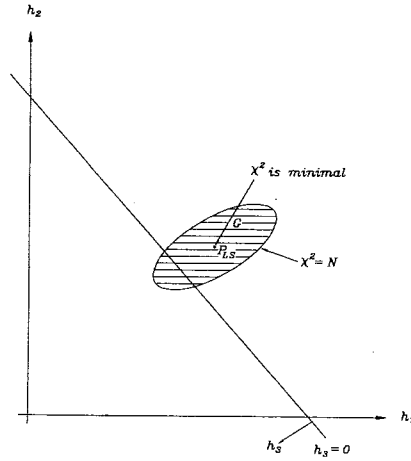

Figure 2.3: Example of a spectrum with three weights $\{ h_1, h_2, h_3, h_1 + h_2 + h_3 = 1 \}$. The interior of the triangle is the allowed region where $h_i \geq 0$. P_{LS} is the least square estimator, G is the region of sets which are compatible with the data.

variations of the data may lead to large variations of the least-square estimator. If this situation arises which is signalized by small singular values compared to the largest one, the problem of fitting the data by a set of weights is called ill-conditioned or ill-posed. The proper treatment of ill-posed problems is discussed thoroughly in the mathematical literature and the main methods are briefly discussed in chapter 3.

2.4 Material functions and the relaxation spectrum

Until now we have studied two material functions, the relaxation modulus $G(t)$ measurable in a sudden shearing displacement experiment, and

the dynamic moduli $G'(\omega), G''(\omega)$, which are measured in oscillatory shear deformation. All these material functions can be expressed through the relaxation spectrum. We have

$$G(t) = \sum_{\alpha=1}^{M} h_\alpha e^{-t/\tau_\alpha} \tag{2.39}$$

and

$$G'(\omega) = \sum_{\alpha=1}^{M} h_\alpha \frac{(\omega\tau_\alpha)^2}{1+(\omega\tau_\alpha)^2}\,, \qquad G''(\omega) = \sum_{\alpha=1}^{M} h_\alpha \frac{\omega\tau_\alpha}{1+(\omega\tau_\alpha)^2}\,. \tag{2.40}$$

If we have determined a material function by one experiment we could estimate the spectrum $\{h_\alpha\}$ and with this information we are able to predict the other material functions. This conversion will be considered in sect. 2.5. Here we would like to list the various material functions as well as some related constants.

From $G(t)$ we may infer the constants

$$G(0) = \sum_{\alpha=1}^{M} h_\alpha \qquad \text{and} \qquad \dot{G}(0) = -\sum_{\alpha=1}^{M} \frac{h_\alpha}{\tau_\alpha}\,, \tag{2.41}$$

which are, however, not experimentally well accessible because of the great experimental uncertainties for small times in the sudden deformation experiment.

Looking at

$$\tilde{G}(\omega) = \frac{1}{\omega}\big(G''(\omega) - iG'(\omega)\big) \tag{2.42}$$

for $\omega \to 0$ we obtain

$$\tilde{G}(\omega) = \big(\eta_0 + O(\omega^2)\big) - i\beta\big(\omega + O(\omega^3)\big) \tag{2.43}$$

with

$$\eta_0 = \sum_{\alpha=1}^{M} h_\alpha \tau_\alpha\,, \tag{2.44a}$$

$$\beta = \sum_{\alpha=1}^{M} h_\alpha \tau_\alpha^2\,. \tag{2.44b}$$

If we plot $|\tilde{G}(\omega)|$ as function of ω we get a curve which for $\omega \to 0$ increases and reaches a plateau at η_0.

Further standard experiments and the related material functions are

1. Stress growth upon inception of steady shear flow: $\gamma(t) = \gamma_0 t$ for $t \geq 0$, $\gamma(t) = 0$ for $t < 0$.
Then we have $\dot{\gamma}(t) = \gamma_0$ for $t > 0$ and

$$\tau(t) = \gamma_0 \int_0^t ds\, G(s) \ . \tag{2.45}$$

With (2.39) we obtain

$$\tau(t) = \gamma_0 \sum_{\alpha=1}^{M} h_\alpha \int_0^t ds\, e^{-s/\tau_\alpha} \equiv \gamma_0 \eta^+(t) \tag{2.46}$$

with

$$\eta^+(t) = \sum_{\alpha=1}^{M} h_\alpha \tau_\alpha (1 - e^{-t/\tau_\alpha}). \tag{2.47}$$

For $t \to \infty$ we obtain

$$\eta^+(t) \to \eta_0 = \sum_{\alpha=1}^{M} h_\alpha \tau_\alpha \ . \tag{2.48}$$

2. Stress relaxation after shear flow:

$$\gamma(t) = \begin{cases} \gamma_0 t\,, & 0 < t < t_1 \\ \gamma_0 t_1\,, & t_1 < t. \end{cases} \tag{2.49}$$

Then

$$\begin{aligned} \tau(t) &= \gamma_0 \int_0^t G(s)\, ds \\ &= \gamma_0 \sum_{\alpha=1}^{M} h_\alpha \tau_\alpha (1 - e^{-t/\tau_\alpha}), \qquad 0 \leq t \leq t_1\,, \end{aligned} \tag{2.50a}$$

$$\begin{aligned} \tau(t) &= \gamma_0 \int_{t-t_1}^t G(s)\, ds \\ &= \gamma_0 \sum_{\alpha=1}^{M} h_\alpha \tau_\alpha (e^{(t-t_1)/\tau\alpha} - e^{-t/\tau_\alpha}), \qquad t \geq t_1\,. \end{aligned} \tag{2.50b}$$

3. We may apply a given stress τ_0 for $t > 0$ and measure the deformation $\gamma(t)$. In a linear regime then

$$\gamma(t) = \tau_0 J(t) \tag{2.51}$$

where the creep or compliance function $J(t)$ can be respresented as

$$J(t) = \frac{t}{\eta_0} + J(0) + \sum_{\alpha=1}^{M} l_\alpha (1 - e^{-t/\tau_\alpha}) \ . \tag{2.52}$$

Here a retardation spectrum $\{l_\alpha\}$ is introduced, it serves for representing $J(t)$ in a simple form, but it is not independent from the relaxation spectrum [6]. For the Fourier-transform we obtain

$$\tilde{J}(\omega) = \frac{1}{\eta_0} \frac{1}{(i\omega)^2} + \frac{1}{i\omega}\Big(J(0) + \sum_{\alpha=1}^{M} l_\alpha\Big) - \sum_{\alpha=1}^{M} l_\alpha \frac{\tau_\alpha}{1 + i\omega\tau_\alpha} \tag{2.53}$$

and one can show, that the relation

$$\tilde{J}(\omega) = \frac{1}{(i\omega)^2 \tilde{G}(\omega)} \tag{2.54}$$

holds by which also follows that the factor in front of t in $J(t)$ and of $\frac{1}{(i\omega)^2}$ in $\tilde{J}(\omega)$ is just $\frac{1}{\eta_0}$. $\tilde{J}(\omega)$ is a complex quantity as $\tilde{G}(\omega)$ and one may introduce similar to $G'(\omega)$ and $G''(\omega)$ two real dynamical creep functions $J'(\omega)$ and $J''(\omega)$ by

$$\tilde{J}(\omega) = \frac{1}{\omega}\big(-J''(\omega) - iJ'(\omega)\big) \ . \tag{2.55}$$

Then we obtain

$$J''(\omega) = \frac{1}{\eta_0 \omega} + \sum_{\alpha=1}^{M} l_\alpha \frac{\omega\tau_\alpha}{1 + (\omega\tau_\alpha)^2} \ , \tag{2.56a}$$

$$J'(\omega) = J(0) - \sum_{\alpha=1}^{M} l_\alpha \frac{(\omega\tau_\alpha)^2}{1 + (\omega\tau_\alpha)^2} \ , \tag{2.56b}$$

and because of

$$-(\omega\tilde{J}(\omega)) = J''(\omega) + iJ'(\omega) = \frac{1}{\omega\tilde{G}(\omega)} = \frac{1}{G'' - iG'} = \frac{G'' + iG'}{G''^2 + G'^2} \tag{2.57}$$

we have also

$$J''(\omega) = \frac{G''(\omega)}{G''^2(\omega) + G'^2(\omega)} \ , \tag{2.58a}$$

$$J'(\omega) = \frac{G'(\omega)}{G''^2(\omega) + G'^2(\omega)} \ . \tag{2.58b}$$

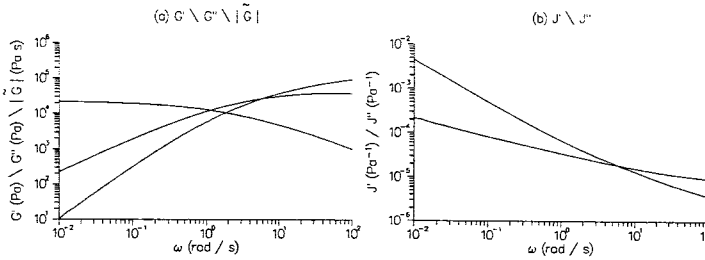

Figure 2.4: The dynamic moduli $G'(\omega)$, $G''(\omega)$ and $|\widetilde{G}(\omega)|$ in (a) and the corresponding $J'(\omega)$, $J''(\omega)$ in (b); (data from Rheometrics).

Fig.2.4 shows $G'(\omega)$, $G''(\omega)$ and $|\widetilde{G}(\omega)|$ for a PDMS-sample, as well as the corresponding $J'(\omega)$, $J''(\omega)$ and $\widetilde{J}(\omega)$.

As this discussion shows, $\widetilde{J}(\omega)$ is easily calculable from $\widetilde{G}(\omega)$, but in order to infer $J(t)$ one has to convert $\widetilde{J}(\omega)$ into $J(t)$. This can only be done by estimating the retardation spectrum from $\widetilde{J}(\omega)$ in order to calculate $J(t)$ from this. We will discuss such problems in the next section.

4. Creep recovery

$$\tau = \begin{cases} \tau_0 & \text{for} \quad 0 < t < t_1 \\ 0 & \text{for} \quad t_1 < t\,. \end{cases} \tag{2.59}$$

Then

$$\gamma(t) = \tau_0 J(t) \qquad 0 \le t \le t_1 \tag{2.60a}$$

$$= \tau_0\big(J(t) - J(t-t_1) + J(0)\big) \qquad , t_1 \le t \tag{2.60b}$$

or

$$\gamma(t) = \tau_0\Big(\frac{t}{\eta_0} + J(0) - \sum_{\alpha=1}^{M} l_\alpha(1 - e^{-t/\tau_\alpha})\Big)\,, \quad 0 \le t \le t_1 \tag{2.61a}$$

$$= \tau_0\Big(\frac{t_1}{\eta_0} + J(0) - \sum_{\alpha=1}^{M} l_\alpha(e^{-(t-t_1)/\tau_\alpha} - e^{-t/\tau_\alpha})\Big)\,, \quad t_1 \le t\,. \tag{2.61b}$$

2.5 Conversion with the least-square estimator

As explained already in sect.2.4 one may determine one material function from another with help of the spectrum. Hence $G(t)$ can be calculated, if the relaxation spectrum is inferred from the dynamic moduli, $J(t)$ is easily obtained if the retardation spectrum has been estimated from $\widetilde{J}(\omega)$.

Sometimes this conversion is done with the least-square estimator of the spectrum or with some methods which try to improve the least-square estimaton. As we have seen in sect. 2.3 the least-square estimator either does not resolve the spectrum well enough or, for higher resolution, it is corrupted by too large errors. The attempts to improve this estimator by introducing the positivity condition or varying the gridpoints τ_α in order to get an even smaller discrepancy, do not change this situation. On the other hand the conversion seems to work very well with the least-square estimator taken for the spectrum. We will study this problem here and do various conversions with the least-square estimator. We will see, that indeed the conversion task can be done satisfactorily by the least-square estimator.

We start with a theoretical spectrum and simulate experimental data $g_i'^{\sigma}, g_i''^{\sigma}$ from it. Then we will determine the least-square estimator from these data and calculate from this the material functions $G(t)$, $\eta^+(t)$ and $\Psi_{1,0}(t)$, which is the first normal stress coefficient extrapolated to zero strain (see [7, 8]). Furthermore we can derive $J'(\omega)$, $J''(\omega)$ from $G'(\omega)$, $G''(\omega)$ and infer from these creep material functions the least-square estimator of the retardation spectrum, by which finally $J(t)$ can be obtained.

As the theoretical spectrum we choose the function

$$h(\tau) = A_1 e^{-\left(\ln(\tau/\tau_1)\right)^2/2b_1^2} + A_2 e^{-\left(\ln(\tau/\tau_2)\right)^2/2b_2^2} \,. \tag{2.62}$$

That means, on a logarithmic τ-axis the spectrum is a superposition of two Gaussian curves with maxima at τ_1 and τ_2 and width b_1 and b_2 respectively. The height of the maxima are dictated by A_1 and A_2.

The synthetic data are then obtained via

$$g_i'^{\sigma} = G'(\omega_i)(1+\sigma_0\eta_i') \tag{2.63a}$$

$$g_i''^{\sigma} = G''(\omega_i)(1+\sigma_0\eta_i''), \quad i = 1,\ldots,N \tag{2.63b}$$

where σ_0 is the relative error, η_i', η_i'' are standard normally distributed ran-

dom numbers and $G'(\omega_i)$, $G''(\omega_i)$ are calculated according to

$$G'(\omega_i) = \int_{-\infty}^{+\infty} d\ln\tau\, h(\tau) \frac{(\omega_i\tau)^2}{1+(\omega_i\tau)^2} \tag{2.64}$$

and

$$G''(\omega_i) = \int_{-\infty}^{+\infty} d\ln\tau\, h(\tau) \frac{\omega_i\tau}{1+(\omega_i\tau)^2} \ , \tag{2.65}$$

where we have chosen

$$\omega_i = \omega_{\min} \left(\frac{\omega_{\max}}{\omega_{\min}}\right)^{\frac{i-1}{N-1}} \quad , \quad i = 1, \ldots, N \tag{2.66}$$

so that we get the frequencies also equally distributed on a logarithmic scale and the integrals in (2.64) and (2.65) are approximated by a sum, e.g.

$$G'(\omega_i) = \sum_{\alpha=1}^{M} h(\tau_\alpha) m_\alpha \frac{(\omega_i\tau_\alpha)^2}{1+(\omega_i\tau_\alpha)^2} \equiv \sum_{\alpha=1}^{M} \left(m_\alpha \frac{(\omega_i\tau_\alpha)^2}{1+(\omega_i\tau_\alpha)^2} \right) h_\alpha \tag{2.67}$$

where $\tau_\alpha = \tau_{\min} \left(\frac{\tau_{max}}{\tau_{\min}}\right)^{\frac{\alpha-1}{M-1}}$, $\alpha = 1, \ldots, M$ and therefore

$$m_\alpha = \ln(\tau_\alpha/\tau_{\alpha-1}) = \frac{1}{M-1} \ln(\frac{\tau_{\max}}{\tau_{\min}}) \ .$$

In the following we will always choose $\sigma_0 = 0.03$ (that means there is a constant relative error of 3%) and $\omega_{\min} = 5 \cdot 10^{-4}, \omega_{\max} = 5 \cdot 10^4$. Fig.2.5 shows in (a) a theoretical spectrum, in (b) some data for $G'(\omega)$ and $G''(\omega)$ derived from it. In (a) also the least-square estimator is shown. Because there are not many grid points τ_α the errors are not too large, but the spectrum is not resolved very well.

In (c) the least-square estimator of the retardation spectrum as derived from $J'(\omega)$ and $J''(\omega)$ is presented whereas $J'(\omega)$ and $J''(\omega)$ are shown in (d). The material functions calculated from these least square estimators are given in fig.2.5 (e)-(h), namely the relaxation modul $G(t)$ in (e), the compliance function $J(t)$ in (f), $\eta^+(t)$ in (g) and $\Psi_{1,0}(t)$ in (h). The solid lines refer always to the calculations by the true spectra (the relaxation spectrum was given, the true retardation spectrum was derived analytically from this), the marks are due to the calculation of these material functions by the least-square estimators of the spectra.

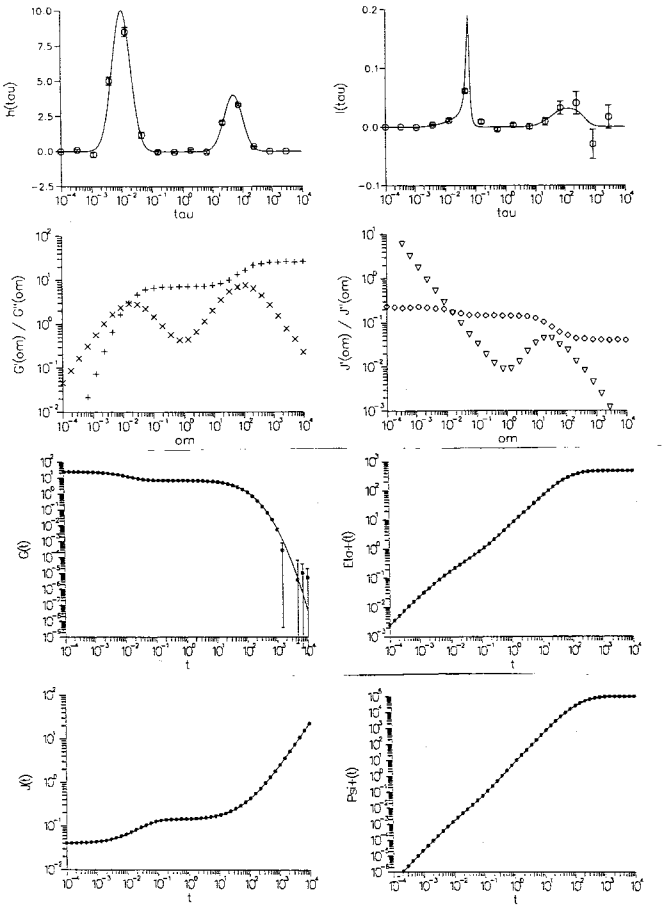

Figure 2.5: (a) a theoretical spectrum; (b) some data for $G'(\omega), (+)$ and $G''(\omega), (x)$ derived from it; (c) the least-square estimator of the retardation spectrum as well as the theoretical result for it calculated from the given relaxation spectrum; (d) the compliance moduli $J'(\omega), (\diamond)$ and $J''(\omega), (\nabla)$; (e) the relaxation modul $G(t)$; (f) the compliance function $J(t)$; (g) $\eta^+(t)$ (h) $\Psi_{1,0}(t)$. The solid lines refer to the calculations by the true, known spectrum, the marks are due to the calculation of these material functions by the least-square estimators of the spectra.

One observes complete agreement. The least-square estimator turns out to be a good converter even with a low resolution for the spectra. Hence it is not necessary to take into account more τ_α-values. By this the errors in the least square estimators only grow and thereby also the errors in the calculated moduli which are now still on the order of the markers.

2.6 Scaling behaviour of material functions

The viscoelastic properties depend on the temperature. If we vary temperature, the dynamic moduli e.g. will change, they are therefore functions of frequency *and* temperature. But experience shows that under variation of frequency and temperature the changes of the material functions are not quite independent. Fig.2.6 shows $G'(\omega)$ for two different temperatures, one recognizes that by vertical and horizontal shift of one curve one may obtain a common curve in broader ω-range. This observation is reflected in the following *Ansatz* for the temperature dependence of the material functions:

$$G'(\omega,T) = c(T)\,T\,F'(a(T)\omega); \qquad G''(\omega,T) = c(T)\,T\,F''(a(T)\omega) \tag{2.68}$$

where F', F'' are functions of one variable. The *Ansatz* therefore reduces the functions of two variables to those of one variable. If such an *Ansatz* is justified by the experimental data, one speaks of a scaling behaviour of the material functions.

Given now experimental data

$$G'(\omega_i,T_j),\ G''(\omega_i,T_j), \quad i=1,\ldots,N,\ j=1,\ldots,M \tag{2.69}$$

the task is to determine the functions $c(T)$, $a(T)$ and $F'(x)$, $F''(x)$. This can be done in the following way. We will demonstrate it for the two data sets $G'(\omega_i,T_1)$, $G'(\omega_i,T_2)$ shown in fig.2.6.

Choose T_1, say, as the reference temperature. Choose some constants a_1 and c_1 (e.g. $a_1=1, c_1=1$), interpreted as $a_1 = a(T_1)$ and $c_1 = c(T_1)$ and set

$$G'(\omega,T_1) = c_1 T_1\,F'(a_1\omega) \tag{2.70}$$

introducing by that the function F' in the range $a_1\omega\,\epsilon\,[\omega_1,\omega_N]$. If the scaling *Ansatz*

$$G'(\omega,T) = c(T)\,T\,F'(a(T)\omega) \tag{2.71}$$

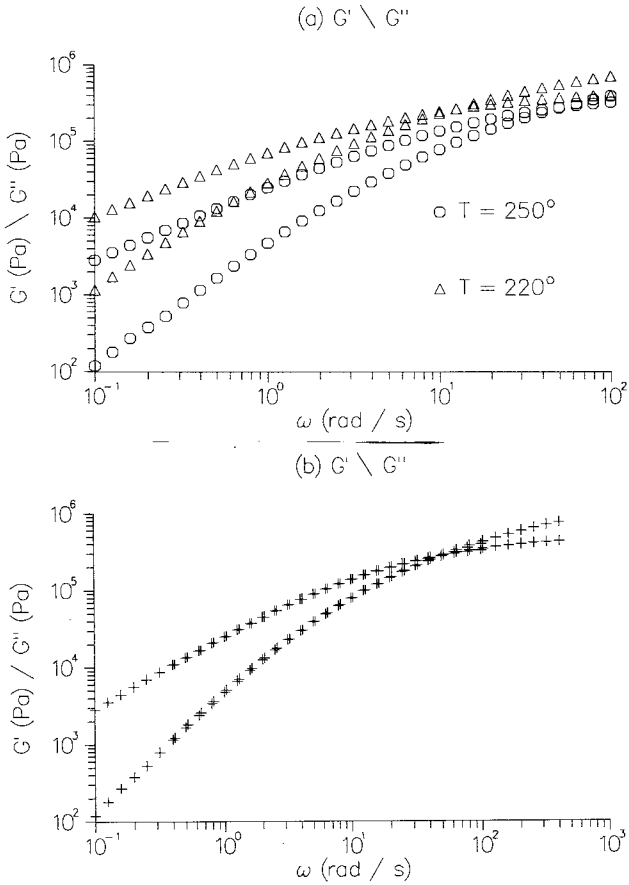

Figure 2.6: Dynamic moduli for two different temperatures (a), and a common curve obtained by suitable vertical and horizontal shifts (b).

is true, then

$$\begin{aligned} G'(\omega, T_2) &= c(T_2)\, T_2\, F'(a(T_2)\omega) \\ &= \frac{c(T_2)}{c(T_1)}\, \frac{T_2}{T_1}\, G'(\frac{a(T_2)}{a(T_1)}\omega, T_1) \end{aligned} \tag{2.72}$$

follows. Define now

$$\epsilon_i = G'(\omega_i, T_2) - \frac{c(T_2)}{c(T_1)}\, \frac{T_2}{T_1}\, G'(\frac{a(T_2)}{a(T_1)}\omega_i, T_1) \tag{2.73}$$

Given $a(T_1)$, $c(T_1)$, ϵ_i should be zero if the scaling behaviour holds and $a(T_2)$ and $c(T_2)$ are chosen properly. Of course, this can only be checked, if $\frac{a(T_2)}{a(T_1)}\omega_i$ still lies in the frequency range where measurements for $T = T_1$ are made and where $G'(\frac{a(T_2)}{a(T_1)}\omega_i, T_1)$ can be obtained by interpolation. We therefore define the quantity

$$V(a(T_2), c(T_2)) = \frac{1}{k} \sum \frac{1}{\sigma_i^2} \epsilon_i^2 \tag{2.74}$$

where the sum runs over all ω_i, for which $\frac{a(T_2)}{a(T_1)}\omega_i \epsilon [\omega_1, \omega_N]$ and k is the number of these terms. We have weighted the difference ϵ_i with the factor $1/\sigma_i$, where σ_i is proportional to the error of $G(\omega_i, T_2)$, hence e.g. $\sigma_i = G(\omega_i, T_2)$ if there is a constant relative error in the measurements of the function $G(\omega, T)$.

Minimization of $V(a(T_2), c(T_2))$ leads to estimates of $a(T_2)$, $c(T_2)$ as well as to errors for this estimate.

Chapter 3

Inverse Problems: From Experimental Data to a Theoretical Model

J. Honerkamp

In chapter 2 we have introduced the least-square estimation of the spectrum. We have seen that this is *not* a good and reliable method to infer a spectrum to be interpreted physically and to characterize the material, though the conversion task could be done with the help of this estimator. In this chapter we will introduce two mathematically well studied methods which lead to more reliable estimations of the spectrum. They are accepted tools for treating inverse problems also in other fields [9, 10, 11].

3.1 The regularization method

In this section we will present a method, known as the regularization method, by which one obtains more reliable answers for the relaxation spectrum than with the least-square method. We consider again the problem to find a function $h(\tau)$, which 'explains' the data $\{g_i^\sigma, \sigma_i, i = 1, \ldots, N\}$, so that

$$g_i^\sigma = \int_{-\infty}^{+\infty} d\ln\tau\, K(\omega_i, \tau) h(\tau) + \epsilon_i\,, \quad i = 1, \ldots, N \tag{3.1}$$

where ϵ_i is the experimental error. As explained in sect.2.3 there are many sets $\{h_\alpha\}$ compatible with the data, namely for which the discrepancy

$$D(\{g_i^\sigma\},h) = \sum_{i=1}^{N} \frac{1}{\sigma_i^2}\Big(g_i^\sigma - \int_{-\infty}^{+\infty} d\ln\tau\, K(\omega_i,\tau)h(\tau)\Big)^2 \;\leq\; N \tag{3.2}$$

where N is the number of experimental data points. In order to choose one specific set out of these one has to introduce another criterium. This can e.g. be smoothness expressed as the condition that the square of the second derivate of $h(\tau)$, integrated over the interval in question, should be as small as possible. Hence we could e.g. minimize

$$J(h) = \int_I d\ln\tau\,\big(h''(\tau)\big)^2\,, \qquad I = (-\infty,+\infty) \tag{3.3}$$

under the condition

$$D(\{g_i^\sigma\},h) = N. \tag{3.4}$$

Such a minimization under a condition can be done by introducing a Lagrangian multiplier λ and by formulating

$$J(h,\lambda) = \int_I d\ln\tau\,\big(h''(\tau)\big)^2 + \lambda\big(D(\{g_i^\sigma\},h) - N\big) \tag{3.5}$$

as the objective function which has to be minimized with given λ. This turns out to be a well-posed problem, the solution may be called $h_\lambda(\tau)$ and then λ has to be determined finally by choosing it so that really

$$D(\{g_i^\sigma\},h) = N.$$

Instead of $J(h,\lambda)$ one could also minimize

$$\begin{aligned} \tilde{J}(h,\lambda) &= \lambda J(h,\frac{1}{\lambda}) + N \\ &= D(\{g_i^\sigma\},h) + \lambda\int_I d\tau\,(Lh)^2 \end{aligned} \tag{3.6}$$

(where L becomes the second derivative operator) again subject to the condition

$$D(\{g_i^\sigma\},h) = N.$$

In this form one recognizes directly the differences to the least-square estimation of the spectrum.

By the term in the objective function, which is added to the discrepancy a further aim is introduced and this will cure the ill-posedness. The condition (3.4), on the other hand, will secure the compatibility of the solution with the data.

This strategy of treating an ill-posed problem is called the regularization method [12, 13, 14, 11] and λ is the regularization parameter. There are many versions of the regularization method. They differ in the operator L in the objective function and in the strategy used to determine the regularization parameter, that means, to secure the compatibility of the solution with the experimental data. Even $L = 1$ is possible (see e.g.[15]) and for this operator a comparison of different strategies used to determine the regularization parameter within ill-posed rheological problems has been made [16]. In this publication also a new strategy for the determination of the regularization parameter, the self-consistent method, has been introduced, which is more robust than the others and still leads to good results in those cases where the other strategies fail. Tests and applications of this regularization method will be discussed in sect.3.3. There we use either $L = 1$ or $L = \frac{d^2}{d\tau^2}$ but always the self-consistent method for the determination of the regularization parameter. The case where no complete knowledge about the errors is available is discussed in sect.3.4.

3.2 The maximum-entropy method

There is another method used to treat ill-posed problems, the maximum-entropy method. This is, however, only applicable, if the function $h(\tau)$ which one is looking for is positive semidefinite, i.e. $h(\tau) \geq 0$. If $h(\tau)$ represents some spectrum, this will be the case.

The maximum-entropy method makes use of the fact, that for any probability distribution $p(x)$ a quantity, called entropy, is defined via

$$S[p] = - < \ln p(x) > = - \int_I dx\, p(x) \ln p(x) \ , \tag{3.7}$$

where I is the interval in which $p(x)$ is defined. Because a spectrum $h(\tau)$ has the same properties as a probability distribution, namely it is

$$h(\tau) \geq 0 \ , \tag{3.8}$$

and one may normalize $h(\tau)$ so that

$$\int_I d\tau\, h(\tau) = 1 \tag{3.9}$$

one may introduce also the entropy of a spectrum in the same manner.

But, normally, the spectrum has a physical dimension and we therefore prefer a notation of a relative entropy

$$S[h \mid h_0] = -\int_I d\tau\, h(\tau) \ln\left(\frac{h(\tau)}{h_0(\tau)}\right) \tag{3.10}$$

where $h_0(\tau)$ is some prior spectrum. One can easily prove that for any spectrum

$$S[h \mid h_0] \leq 0 \tag{3.11}$$

and, of course

$$S[h_0 \mid h_0] = 0\ . \tag{3.12}$$

That means, if we ask for that spectrum which has maximum entropy and which is consistent with the data in the sense that

$$D(\{g_i^\sigma\}, h) = N\ , \tag{3.13}$$

then we obtain that spectrum which is as near as possible to the prior spectrum but compatible with the data. The prior distribution is normally not compatible with the data, especially if we choose this as constant because we have no information at all before taking the data. Again we have here an objective function which has to be minimized, the negative of the entropy, and the consistency of the solution with the data is secured by the condition on the discrepancy. But also the prior distribution comes into play. If we choose this as a constant, then we will find the spectrum which is compatible with the data but which also deviates as little as possible from a constant.

To illustrate the interplay between maximum entropy principle and compatibility condition let us look at an example, where $M = 3$, $\{h_\alpha\} = \{h_1, h_2, h_3,\ h_1 + h_2 + h_3 = 1\}$. The region, where $h_\alpha \geq 0$ is shown in fig.3.1 as the interior of the triangle, where also the lines of equal entropy are drawn. S_0 is the point of maximum entropy without taking care of the experimental data, so S_0 represents the prior distribution. The point P_{LS} may be the least-square estimator and the region G, surrounded by the

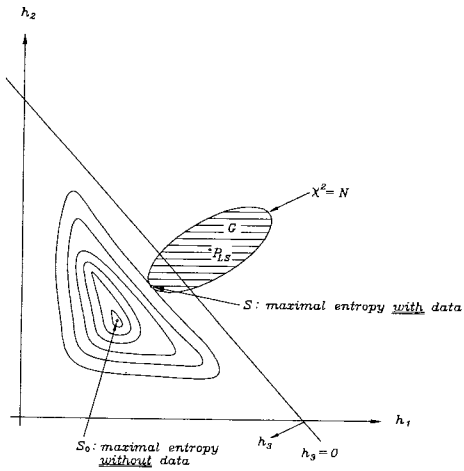

Figure 3.1: Example of a spectrum with three weigths $\{h_1, h_2, h_3;\ h_1 + h_2 + h_3 = 1\}$. The interior of the triangle is the allowed region where $h_\alpha \geq 0$. The closed circles are lines of constant entropy. S_0 is the point of maximum entropy without taking the data into account, P_{LS} is the least square estimator. G is the region of sets $\{h_\alpha\}$ which are compatible with the data. S is the maximum entropy estimator.

ellipse $\{D(\{g_i^\sigma\}, h_\alpha) = N\}$, represents the solutions which are compatible with the data. So there are still many solutions for which $h_\alpha \geq 0$. The point S marks the maximum entropy solution. One recognizes, that there is a unique solution and for it we have not only

$$D(\{g_i^\sigma\}, h_\alpha) \leq N \ , \tag{3.14}$$

but

$$D(\{g_i^\sigma\}, h_\alpha) = N \ . \tag{3.15}$$

As with the regularization method there are also different versions of the entropy method according to different formulations of the compatibility.

An especially robust method which leads to good results in situations where the above introduced, most frequently used version fails, is given by [17]. Instead of (3.13), the compatibility of the solution with the data is formulated as

$$D(\{g_i^\sigma\}, N) = \frac{N}{N - M_{eff}} z \tag{3.16}$$

where

$$z = \min_{h \geq 0} D(\{g_i^\sigma\}, h) \ , \tag{3.17}$$

M_{eff} is an integer which will be explained in a moment and which is less than or equal to M which is the number of gridpoints on the τ-axis so that the discretization of the integral reads

$$\int d\ln\tau \, K(\omega, \tau) h(\tau) = \sum_{\alpha=1}^{M} K'_{i\alpha} h_\alpha \ . \tag{3.18}$$

Within this discretization one may find z from (3.17). The number M_{eff} is then the number of $\{\tau_\alpha\}$, for which the weight h_α at the minimum of z turns out to be not zero.

3.3 Test of the methods with synthetic data

In order to test the regularization and the maximum entropy method we will start with a known spectrum and simulate experimental data from it. Then we will determine the spectrum from these data and compare this estimation with the given spectrum.

The simulation of the data will be done in the same manner as described in sect.2.5.

First we will demonstrate that our modifications of the regularization and maximum entropy method lead to more robust algorithms. For the regularization method we invented the selfconsistent determination of the regularization parameter [16], the maximum-entropy method was modified by another formulation of the compatibility with the data [17]. For the theoretical spectrum as defined in sect.2.5 we choose the parameters

$$A_1 = 10, \tau_1 = 5 \cdot 10^{-3}, b_1 = 1; \ A_2 = 10, \tau_2 = 10, b_2 = 1 \ . \tag{3.19}$$

and in fig.3.2 we show what can happen with the unmodified versions and what are the results with the modified versions. That means, there

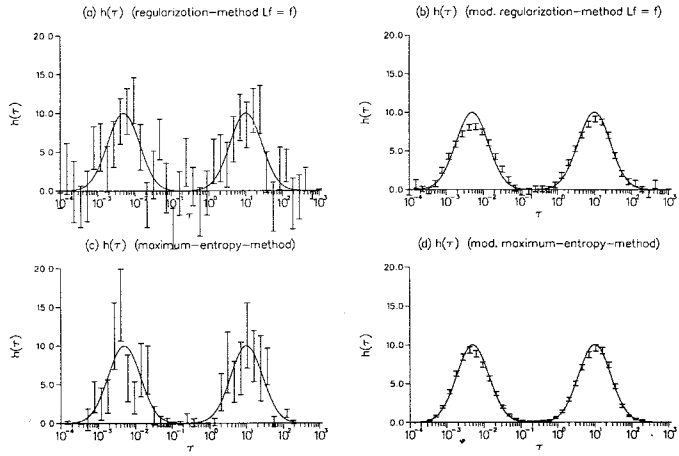

Figure 3.2: Possible results of unmodified and modified versions of the regularization and maximum entropy methods: (a) Reconstruction of a spectrum with the regularization method as explained in sect.3.1; (b) Reconstruction from the same data with the selfcousistent determination of the regularization parameter; (c) Reconstruction of a spectrum with maximum entropy method as explained in sect.3.2; (d) Recoustruction from the same data with the modified maximum entropy method.

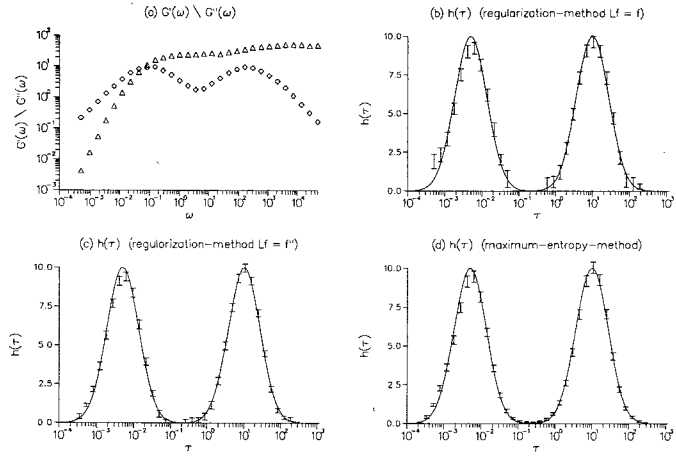

Figure 3.3: Simulated experimental data (a) and reconstructions of the spectrum (markers with error bars): in (b) by the regularization method with $L = 1$, in (c) with L equal to the second derivative and in (d) the reconstruction by the maximum entropy method. The solid line refers always to the theoretical spectrum.

are cases where the data are so unrepresentative that the unmodified, commonly used methods fail whereas the modified versions still lead to satisfactory results.

Next we compare the methods with three different spectra:

1. We consider a very harmless spectrum with parameters as in eqn.3.19. The simulated experimental data and the spectra, the input spectrum as well as the reconstructed ones by the various methods, are shown in fig.3.3. All methods are able to reconstruct the spectrum very well.

2. We consider a spectrum where the peaks are very narrow, the para-

meters are

$$A_1 = 10,\ \tau_1 = 0.1,\ b_1 = 0.75;\ A_2 = 10,\ \tau_2 = 2,\ b_2 = 0.75\ .$$

The results are shown in fig.3.4.

3. We test the methods with a spectrum where the two peaks are of very different heights. The parameters are now

$$A_1 = 10,\ \tau_1 = 5 \cdot 10^{-3},\ b_1 = 1;\ A_2 = 0.5,\ \tau_2 = 50,\ b_2 = 1\ .$$

Fig.3.5 shows the results.

It turns out that the regularization method with $Lh = h''$ and the maximum entropy method are both able to reconstruct these more difficult spectra whereas the regularization method with $Lh = h$ has problems with peaks of very different heights.

Finally let us observe what happens if we do not have enough data to reconstruct the spectrum in its full range. This is regularly the case. We take the same spectrum as in fig.3.5 and take into account only the data until $\omega = 3$ (see fig.3.6). Now the large peak of the spectrum can not be reconstructed because in that τ region there is no information from the data. But the small peak is reproduced very well by the regularization method with $Lh = h''$ and by the maximum entropy method.

3.4 Error models

In the introduction of the regularization, the maximum entropy and also the least-square method the knowledge about the errors σ_i', σ_i'' of the experimental data $g_i'^{\sigma}$, $g_i''^{\sigma}$ is always used. Frequently, however, one does not know these. But sometimes one may assume that the relative error is constant, then we have

$$\sigma_i' = g_i'^{\sigma}\sigma_0 \tag{3.20}$$

where σ_0 is the relative error. If this is the only unknown the methods are still applicable. In general an overall factor σ_0 in the error model

$$\sigma_i' = \sigma_0 \cdot \tilde{\sigma}_i' \tag{3.21}$$

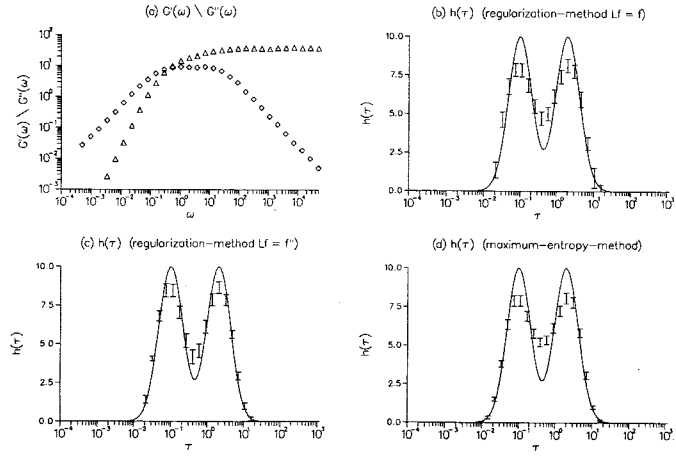

Figure 3.4: Simulated experimeutal data (the peaks of the spectrum are very narrow to each other) (a) and reconstructions of the spectrum (markers with error bars): in (b) by the regularization method with $L = 1$, in (c) with L equal to the second derivative aud in (d) the reconstruction by the maximum entropy method. The solid line refers always to the theoretical spectrum.

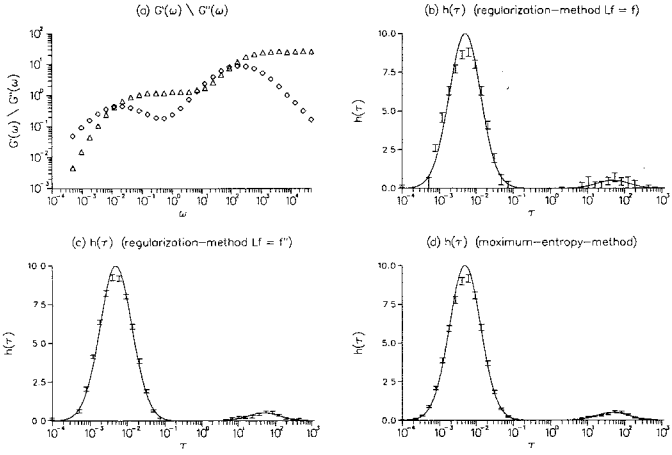

Figure 3.5: Simulated experimental data (the peaks of the spectrum are of very different heigths) (a) and reconstructions of the spectrum (markers with error bars): in (b) by the regularization method with $L = 1$, in (c) with L equal to the second derivative and in (d) the reconstruction by the maximum entropy method. The solid line refers always to the theoretical spectrnm.

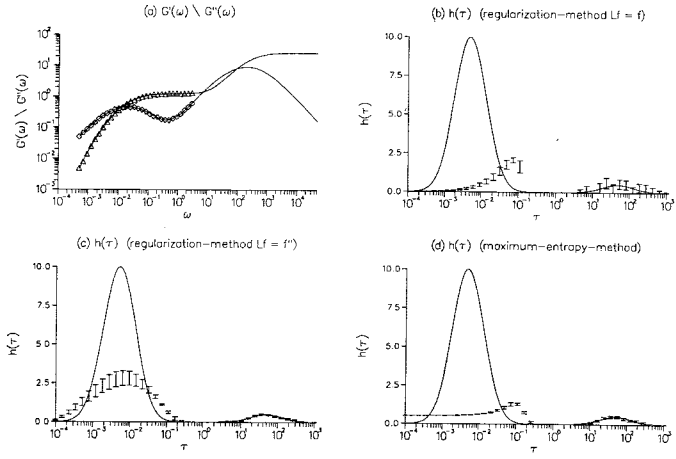

Figure 3.6: Recoustructions with incomplete data for the cases treated in fig. 3.4.

is allowed to be unknown. It can be determined by the methods, but the dependence of the errors on the number of data points, i.e. the variation of the errors has to be known in order to apply the method because the relative weights of the individual discrepancies are determined by the errors.

Very frequently this variation is also not known, it has to be estimated from the data too. Work on this problem is in progress.

Chapter 4

Stochastic Processes in Rheology

F. Petruccione

In this chapter the mathematical definition of a stochastic process is given. We describe under which conditions the important Markov processes are obtained. Markov processes are described by a Master equation. The special class of diffusion processes can be described by a Fokker-Planck equation. For diffusion processes we show that an equivalent description with the help of stochastic differential equations (Langevin equations) is possible. Semi-Markov processes which are a special class of non-Markovian processes are briefly introduced.

All these mathematical concepts can be found in rheological models, as for instance the Rouse model, the Doi-Edwards model, the Orwoll-Stockmeyer model, or the Lodge model. This is described in great detail in the following sections. The concentration on the stochastic concepts underlying these well-known models opens the door for more realistic generalizations and thus for a better understanding of the complex rheological behaviour of polymer melts.

4.1 Stochastic processes

4.1.1 Markov processes

We consider systems which evolve probabilistically in time, that is sytems in which a certain time-dependent random variable $X(t)$ exists. Such systems are called stochastic processes.

In order to characterize such processes we can measure at times $t_1, t_2, t_3, \ldots$ the realizations $x_1, x_2, x_3, \ldots$ of $X(t)$. The system can be described by a set of joint probability densities $p(x_1, t_1; x_2, t_2; x_3, t_3; \ldots)$ which determine the probability of finding the realization x_1 at time t_1, x_2 at time t_2, and so on. In terms of the joint probability densities we can also define conditional probability densities

$$p(x_1, t_1; x_2, t_2; x_3, t_3; \ldots \mid y_1, \tau_1; y_2, \tau_2; \ldots) = \frac{p(x_1, t_1; x_2, t_2; x_3, t_3; \ldots; y_1, \tau_1; y_2, \tau_2; \ldots)}{p(y_1, \tau_1; y_2, \tau_2; \ldots)} \,. \tag{4.1}$$

The concept of a dynamical evolution equation leads us to consider the conditional probabilities as predictions of the future values of $X(t)$ (i.e. $x_1, x_2, \ldots$ at times $t_1, t_2, \ldots$) given the knowledge of the past (values $y_1, y_2, \ldots$ at $\tau_1, \tau_2, \ldots$).

The most simple case occurs when the value of X at time t is completely independent of its value in the past or future, that is

$$p(x_1, t_1; x_2, t_2; x_3, t_3; \ldots) = \prod_i p(x_i, t_i) \tag{4.2}$$

If furthermore $p(x,t)$ is a stationary distribution function $p(x,t) \equiv p(x)$ then one speaks of an independently and identically distributed random variable $X(t) \sim IID(0, \sigma^2)$ where σ^2 is the variance of $p(x)$. If $p(x)$ is a Gaussian probability distribution $p(x) = p_G(0, \sigma^2; x)$ with zero mean and variance σ^2 the stochastic process is called Gaussian white noise: $X(t) \sim WN(0, \sigma^2)$.

We know from the central limit theorem that a sum of random variables can be approximated well by a Gaussian random variable. If we now consider a physical system subject to many fluctuating impacts the resultant effect will be modelled with good accuracy by a Gaussian distributed random variable at each time. If the typical time scale of the system is larger than the time scale of the fluctuations one can neglect time correlations of the random variables. The global effect of the fluctuations will then

be modelled by Gaussian white noise. For this reason white noise plays a very fundamental role.

The next simple process is the Markov process in which the knowledge of only the present determines the future. To formulate the Markov assumption we require that the times satisfy the ordering $t_1 \geq t_2 \geq \ldots \geq \tau_1 \geq \tau_2 \geq \ldots$. The conditional probability is determined entirely by the knowledge of the most recent condition, i.e.,

$$p(x_1,t_1;x_2,t_2;x_3,t_3;\ldots \mid y_1,\tau_1;y_2,\tau_2;\ldots) = p(x_1,t_1;x_2,t_2;x_3,t_3;\ldots \mid y_1,\tau_1). \quad (4.3)$$

The above assumption means that we can define everything in terms of the simple conditional probabilities $p(x_1,t_1 \mid y_1,\tau_1)$. As a consequence one can easily show that

$$p(x_3,t_3 \mid x_1,t_1) = \int dx_2\, p(x_3,t_3 \mid x_2,t_2)p(x_2,t_2 \mid x_1,t_1). \quad (4.4)$$

The above equation is called the Chapman-Kolmogorov equation. The transition probabilities of any Markov process must obey this equation.

Let us conclude this section with the following remarks. It can be shown that for Markov processes the waiting time of a random variable to jump into a specified state is exponentially distributed. Markov processes can be generalized by allowing other waiting time distributions. This generalized class of models is known as semi-Markov processes.

4.1.2 The Master equation

We now want to derive the Master equation which is an equivalent form of the Chapman-Kolmogorov equation for Markov processes. The Master equation is a differential equation for the time development of the probability distribution. It is thus more directly related to physical problems. The equation is obtained by going to the limit of vanishing time difference τ between the events. Let us now suppose that the transition probability $p(x,t+\tau \mid x',t)$ has the following form for small τ

$$p(x,t+\tau \mid x',t) = [1-a(x,t)\tau]\delta(x-x') + \tau w(x,x',t) + O(\tau^2). \quad (4.5)$$

In the above equation $w(x,x',t)$ is the transition probability per unit time to go from x' to x and hence $w(x,x',t) \geq 0$. The coefficient $1-a(x,t)\tau$ in

front of the delta function is the probabilty that no transition takes place during τ and therefore

$$a(x',t) = \int dx\, w(x,x',t). \tag{4.6}$$

Inserting the expression (4.5) into the Chapman-Kolmogorov equation (4.4), divide by τ and going to the limit of vanishing τ we obtain the so called Master equation

$$\frac{\partial}{\partial t}p(x,t) = \int dx' w(x,x',t)p(x',t) - \int dx' w(x',x,t)p(x,t). \tag{4.7}$$

If the range of the random variable X is a discrete set of states labeled with the integer n the Master equation is usually written in the form

$$\frac{d}{dt}p_n(t) = \sum_{n'} \left(w_{nn'}(t)p_{n'}(t) - w_{n'n}(t)p_n(t)\right). \tag{4.8}$$

In this form the meaning of the Master equation becomes very clear: it is a gain and loss equation for the probability of each state n.

In many physical applications one knows the probability for a transition during a short time interval. With the help of the Master equation it is now possible to calculate transition probabilities for large (finite) times.

The class of diffusion processes can be described by another fundamental equation: the Fokker-Planck equation. This equation is a special type of Master equation, and can be obtained by assuming that only small jumps occur and that the probability distribution function $p(\boldsymbol{x},t)$ varies slowly with $\boldsymbol{x}$. Such diffusive processes are characterized by the following constraints on the transition probabilities for short times

$$\int d\boldsymbol{y}\,(y-x)_i p(\boldsymbol{y},t+\tau \mid \boldsymbol{x},t) = A_i(\boldsymbol{x},t)\tau + o(\tau), \tag{4.9}$$

$$\int d\boldsymbol{y}\,(y-x)_i(y-x)_j p(\boldsymbol{y},t+\tau \mid \boldsymbol{x},t) = D_{ij}(\boldsymbol{x},t)\tau + o(\tau), \tag{4.10}$$

$$\int d\boldsymbol{y}\,(y-x)_{i_1}\cdots(y-x)_{i_n} p(\boldsymbol{y},t+\tau \mid \boldsymbol{x},t) = o(\tau), \quad \text{for } n>2. \tag{4.11}$$

In other words the transition probability for short times is given by a Gaussian distribution with mean $\boldsymbol{A}(\boldsymbol{x},t)$ and variances $D_{ij}(\boldsymbol{x},t)$. With the

help of the above assumptions and of the Chapman-Kolmogorov equation one can derive the Fokker-Planck equation for the probability density $p(\boldsymbol{x},t)$

$$\frac{\partial}{\partial t}p(\boldsymbol{x},t) = \Big[-\frac{\partial}{\partial \boldsymbol{x}_i}A_i(\boldsymbol{x},t) + \frac{1}{2}\frac{\partial^2}{\partial \boldsymbol{x}_i \partial \boldsymbol{x}_j}D_{ij}(\boldsymbol{x},t)\Big]p(\boldsymbol{x},t). \tag{4.12}$$

The Fokker-Planck equation plays a fundamental role in the kinetic theory of polymer solutions and melts.

4.1.3 Stochastic differential equations

When a system is subject to fluctuating external forces, its equation of motion is given by a differential equation with stochastic coefficients. Probably the best known stochastic differential equation is the Langevin equation that describes Brownian motion. A Brownian particle of mass m feels two forces: a viscous drag, as it is known from macroscopic hydrodynamics, $-6\pi\eta a\frac{d\boldsymbol{x}}{dt}$ (η being the viscosity, and a the radius of the particle), and a fluctuating force F, which represents the impacts of the molecules of the liquid on the Brownian particle. Thus the equation of motion for the Brownian particle is given by

$$m\frac{d^2\boldsymbol{x}}{dt^2} = -6\pi\eta a\frac{d\boldsymbol{x}}{dt} + F. \tag{4.13}$$

The above equation is a stochastic differential equation with additive noise. Let us now consider the equation

$$\dot{X}_t = a(X_t,t) + \eta_t; \qquad \eta_t \sim WN(0,\sigma^2) \tag{4.14}$$

for the random variable X_t. The increment dX_t during a small time interval dt is given by

$$dX_t = a(X_t,t)dt + dW_t, \tag{4.15}$$

where

$$dW_t = \int_t^{t+dt} dt'\,\eta_{t'}. \tag{4.16}$$

W_t is called the Wiener process. As dW_t is a sum of Gaussian distributed random numbers it is itself Gaussian distributed. The mean and the variance are given by

$$< dW_t >= 0, \tag{4.17}$$

and

$$< (dW_t)^2 >= \int_t^{t+dt} dt_1 \int_t^{t+dt} dt_2 < \eta_{t_1}\eta_{t_2} >= \sigma^2 dt. \tag{4.18}$$

If $[t, t+dt] \cap [t', t'+dt'] = 0$ then $< dW_t dW_{t'} >= 0$. From Eq.(4.18) we can now determine a very important relation. It is fundamental to realize that dW_t can be written as

$$dW_t = \sigma \eta_t \sqrt{dt}\,; \qquad \eta_t \sim WN(0,1)\,. \tag{4.19}$$

This means that the stochastic increment in an infinitesimal time step is proportional to the square root of the time step. In the next chapter we will see what consequences this fact has on the numerical integration of stochastic differential equations.

In realistic applications, as we will see later on, one often encounters stochastic differential equations with multiplicative noise, that is equations of the form

$$\dot{X}_t = a(X_t, t) + b(X_t, t)\eta_t\,; \qquad \eta_t \sim WN(0, \sigma^2), \tag{4.20}$$

or, equivalently in differential form

$$dX_t = \int_t^{t+dt} dt'\, a(X'_t, t') + \int_t^{t+dt} dt'\, b(X_{t'}, t')\eta_{t'}\,. \tag{4.21}$$

The above equation only makes sense if a definition of the stochastic integrals is given. One can evaluate the stochastic integral with the help of the well known Cauchy-Euler procedure. One takes the value of the integrand at the beginning of the interval $[t, t+dt]$ and multiplies it with the length of the interval. One can then show that

$$dX_t = a(X_t, t)dt + b(X_t, t)\eta_t \sqrt{dt}. \tag{4.22}$$

This result corresponds to the treatment we have already introduced for stochastic differential equations with additive noise. It is customary to call this approach the Ito interpretation of the stochastic differential equation. Another definition of Eq. (4.21) is obtained by taking the value of the integrand in the middle of the interval. It can then be shown that this so called Stratonovich interpretation of the stochastic differential equation leads to the following differential expression

$$dX_t = \left[a(X_t, t) + \frac{1}{2} b'(X_t, t) b(X_t, t)\right] dt + b(X_t, t)\eta_t \sqrt{dt}. \tag{4.23}$$

As the Ito and the Stratonovich version of the stochastic differential equation differ in the form of the drift term, they obviously lead to different results. Thus a stochastic differential equation with multiplicative noise only makes sense if one specifies the interpretation of the stochastic integrals.

We conclude this section by establishing a very important relationship. The Langevin equation is an equation for the random variable X_t. As an example we might again consider

$$dX_t = a(X_t,t)dt + \sigma\eta_t\sqrt{dt}\,, \qquad \eta_t \sim WN(0,1). \tag{4.24}$$

It is now interesting to find an equation which describes the dynamical behaviour of the probability density $p(x,t)$. If X_t is known, dX_t is just a normally distributed random number with mean $a(x,t)dt$ and variance $\sigma^2 dt$. These conditions are exactly the constraints on the transition probability for short times that characterize diffusion processes, and which lead to a Fokker-Planck equation. In our example the corresponding Fokker-Planck equation would be

$$\frac{\partial}{\partial t}p(x,t) = [-\frac{\partial}{\partial x}a(x,t) + \frac{1}{2}\sigma^2\frac{\partial^2}{\partial x^2}]p(x,t). \tag{4.25}$$

Thus in a formal sense the Langevin and the Fokker-Planck approaches are equivalent. For practical reasons one may prefer the one or the other. To describe the dynamics of polymer melts the Langevin approach might be more appropriate, as it can easily be implemented on a computer for a numerical evaluation. Obviously the equivalence can be generalized to the three dimensional case, as well as for stochastic differential equations with multiplicative noise.

A more detailed exposition of the fundamental equations arising in the description of stochastic processes can be found in Refs. [1, 3, 2]. There one can also find a description of the analytical tools required to treat these equations. An introduction to the powerful numerical approach will be given in the next chapter.

In the next sections we will show that in the theories describing polymer melts stochastic concepts arise quite naturally. Some theories were originally developed with the help of stochastic tools, for some other theories a stochastic reinterpretation will be necessary.

4.2 Stochastic differential equations in rheology

4.2.1 The Rouse model

Polymer kinetic theory is associated with the model developed by Rouse [18]. As it contains all fundamental ideas of polymer kinetic theory we will start our discussion with a short review of this model.

In the Rouse model a linear polymer chain is described by replacing a portion of the chain containing many fundamental atomic units by a spring and concentrating the masses of the atoms in beads. This model is also called the freely jointed bead-spring chain. In its simplest version one takes into consideration only the global orientation and length of the macromolecule as degrees of freedom. Each polymer is then regarded as a flexible dumbbell consisting of two beads connected by a Hookean spring. The polymer is fully characterized by the vector $\boldsymbol{Q}$ that joins the two beads. In addition to the internal entropic force $F(\boldsymbol{Q}) = H\boldsymbol{Q}$, where H is the spring constant, the beads experience a hydrodynamic drag proportional to their velocity $\boldsymbol{v}$ relative to the flow field, which is customarily described by Stoke's law,

$$\boldsymbol{F}_{drag} = \zeta(\boldsymbol{v} - \dot{\boldsymbol{Q}}). \tag{4.26}$$

Here ζ is a friction coefficient and we will consider homogeneous flow fields $\boldsymbol{v}$ of the form $\boldsymbol{v}(\boldsymbol{Q},t) = \boldsymbol{\kappa}(t)\cdot\boldsymbol{Q}(t)$, where $\boldsymbol{\kappa}$ is the traceless transpose velocity gradient tensor. The dumbbell also feels Brownian forces due to the thermal fluctuations of the surrounding solvent molecules or polymers. These are modelled by a stochastic force $\boldsymbol{\eta}(t)$, which is here assumed to be a Gaussian white noise with zero mean and two time correlations

$$< \eta_i(t)\eta_j(t') >= D\delta_{ij}\delta(t-t'), \tag{4.27}$$

where $D = \frac{4kT}{\zeta}$ (T is the temperature, k is Boltzmann's constant). Neglecting the acceleration terms the equation of motion for $\boldsymbol{Q}(t)$ reads

$$\dot{\boldsymbol{Q}}(t) = \boldsymbol{\kappa}(t)\cdot\boldsymbol{Q}(t) - \frac{2}{\zeta}\mathbf{F}(\boldsymbol{Q}(t)) + \boldsymbol{\eta}(t), \tag{4.28}$$

which is a Langevin equation with additive noise. The equivalent Fokker-Planck equation for the probability distribution $\Psi(\boldsymbol{Q},t)$ is

$$\frac{\partial}{\partial t}\Psi + \frac{\partial}{\partial \boldsymbol{Q}}\cdot\left(\boldsymbol{\kappa}\cdot\boldsymbol{Q}\Psi - \frac{2}{\zeta}\mathbf{F}\Psi - \frac{2kT}{\zeta}\frac{\partial}{\partial \boldsymbol{Q}}\Psi\right) = 0 \quad . \tag{4.29}$$

From the above equation one can see that the special choice of the diffusion constant D ensures the equilibrium distribution Ψ_{eq} to be

$$\Psi_{eq}(\boldsymbol{Q}) = const \exp\left(-\frac{H\boldsymbol{Q}^2}{2kT}\right) \quad . \tag{4.30}$$

The Hookean dumbbell model can be trivially generalized to a bead-spring chain model, the proper Rouse model. Let us therefore give the equations of motion of a chain consisting of N identical beads. Let $\boldsymbol{r}_\nu$ be the coordinate of bead ν, and let $\boldsymbol{Q}_\nu = \boldsymbol{r}_{\nu+1} - \boldsymbol{r}_\nu$ for $\nu = 1, \cdots, N-1$, be the connector vector between bead $\nu+1$ and ν. The Ito-Langevin equation for the ν-th connector $\boldsymbol{Q}_\nu$ is given by

$$\dot{\boldsymbol{Q}}_\nu(t) = \boldsymbol{\kappa}(t) \cdot \boldsymbol{Q}_\nu(t) - \frac{H}{\zeta} \sum_\sigma \boldsymbol{A}_{\nu\sigma} \cdot \boldsymbol{Q}_\sigma(t) + \sum_\sigma \mathbf{B}_{\nu\sigma} \cdot \boldsymbol{\eta}_\sigma(t). \tag{4.31}$$

Here the vectors $\boldsymbol{\eta}_\sigma(t)$ have the same two time correlations as in Eq.(4.27). The 3×3 matrices $\boldsymbol{A}_{\nu\sigma}$ and $\boldsymbol{B}_{\nu\sigma}$ are given by

$$\boldsymbol{A}_{\nu\sigma} = (2\delta_{\nu,\sigma} - \delta_{\nu,\sigma\pm1})\mathbf{1} \quad , \quad \boldsymbol{B}_{\nu\sigma} = \sqrt{1/2}(\delta_{\nu,\sigma} - \delta_{\nu,\sigma-1})\mathbf{1} \tag{4.32}$$

They can be interpreted as the elements of $(N-1) \times (N-1)$ dimensional supermatrices $\hat{\boldsymbol{A}}$ and $\hat{\boldsymbol{B}}$. Due to the fluctuation-dissipation theorem, which asserts that the frictional dissipation is balanced by the fluctuations to keep the temperature constant at equilibrium, these supermatrices obey the equation

$$\hat{\boldsymbol{B}} \cdot \hat{\boldsymbol{B}}^T = \frac{1}{2}\hat{\boldsymbol{A}} \tag{4.33}$$

The Fokker-Planck equation equivalent to the Langevin equation is

$$\frac{\partial}{\partial t}\Psi = -\sum_\nu \partial_\nu \cdot (\boldsymbol{\kappa} \cdot \boldsymbol{Q}_\nu \Psi) + \frac{H}{\zeta} \sum_{\nu\sigma} \partial_\nu \cdot (\boldsymbol{A}_{\nu\sigma} \cdot \boldsymbol{Q}_\sigma \Psi) + \frac{kT}{\zeta} \sum_{\nu\sigma} \partial_\nu \partial_\sigma \boldsymbol{A}_{\nu\sigma} \Psi \quad . \tag{4.34}$$

Here the symbol ∂_ν is an abbreviation for $\frac{\partial}{\partial \boldsymbol{Q}_\nu}$.

Again one can see that the stationary equilibrium solution is given by

$$\Psi_{eq}(\boldsymbol{Q}) = const \exp\left(-\frac{V}{kT}\right) \quad , \tag{4.35}$$

where $V = \sum_\nu \frac{1}{2} H \boldsymbol{Q}_\nu^2$.

In rheology one is mainly interested in the evaluation of the stress tensor σ. For the Rouse model it is defined (apart from an isotropic term) as

$$\sigma = nH \sum_{\nu} < Q_\nu Q_\nu > \tag{4.36}$$

where n is the number density of polymer chains and the angular brackets denote an average with respect to the distribution function Ψ. Unfortunately, the predictions of the Rouse model are not very satisfactory. The material functions, which are linear combinations of components of the stress tensor, turn out to be constant, in contrast to the experimental observation. Nevertheless, the Rouse model is very useful. It allowed us to introduce the fundamental stochastic ingredients, which are also common to more refined kinetic models.

4.2.2 The Doi-Edwards model

As we have seen the Rouse model is only a very crude approximation for the dynamical behavior of a polymer in a melt. In fact many kinetic theories for polymer melts make additional assumptions for the motion of a single macromolecule. One postulates a mean field built by all the other macromolecules which constitute the environment of the described single polymer. The effect is the reduction of the complicated many-chain problem to a much easier one chain problem. The price to be paid for this simplification is the introduction of a mean field which is not determined self-consistently but only postulated. For concentrated solutions and melts one usually supposes that the neighborhood of a randomly chosen macromolecule has the effect that motions perpendicular to its contour are strongly hindered. In the reptation picture of de Gennes [19, 20] a macromolecule is confined to a tube-like region and only diffusion along its contour is possible. This assumption is the starting point for the well-known Doi-Edwards model for polymer melts [21].

We will now discuss the basic equations of the Doi-Edwards model and their stochastic interpretation. The original Doi-Edwards model describes a single polymer chain in a highly entangled state. Ignoring the small scale wiggling motions of the real chain one describes the large scale diffusive motion with a more basic so-called primitive chain which represents only the bare topological structure. Based on the reptation picture one assumes

that the motion of the primitive chain is hindered by the other chains such that only motion along the contour is possible. The ends of the chain may move in any random direction. In a flow field described by a tensor $\boldsymbol{\kappa}$ there is an additional deformation of the primitive chain. The dynamics is then described by the following diffusion equation for the probability density $p(\boldsymbol{u}, s; t)$ [23]

$$\frac{\partial p}{\partial t} = -\frac{\partial}{\partial \boldsymbol{u}} \cdot (\boldsymbol{\kappa} \cdot \boldsymbol{u} - \boldsymbol{\kappa} : \boldsymbol{uuu})\, p + D \frac{\partial^2 p}{\partial s^2} \quad . \tag{4.37}$$

In the above equation $\boldsymbol{u}(s)$ is the unit vector tangent to the primitive chain at the point of arclength s with $0 \leq s \leq L$, where L is the contour length of the primitive chain and D is the diffusion coefficient. The quantity $p(\boldsymbol{u}, s; t) d^2u ds$ is the probability of finding a tangent vector with orientation between $\boldsymbol{u}$ and $\boldsymbol{u} + d\boldsymbol{u}$ at a position between s and $s + ds$ at time t . The first term on the right hand side describes the flow induced deformation of the primitive chain within the independent alignment approximation and the second term describes the diffusive motion. The boundary conditions for the diffusion equation are

$$p(\boldsymbol{u}, 0; t) = p(\boldsymbol{u}, L; t) = \frac{1}{4\pi} \quad , \tag{4.38}$$

which describe the random orientation of the end vectors. The stress tensor can be obtained from a formula of rubber elasticity (apart from an isotropic term) as

$$\boldsymbol{\sigma}(t) = G_0 < \boldsymbol{u}(s,t)\boldsymbol{u}(s,t) > \quad , \tag{4.39}$$

where G_0 is a constant with the dimensions of the rigidity modulus and the brackets denote an average with respect to $p(\boldsymbol{u}, s; t)$ at fixed time.

In a work by Öttinger [24] the stochastic picture that underlies the diffusion equation (4.37) is clearly demonstrated by interpreting this equation as a Fokker-Planck equation. In this interpretation one has two stochastic processes $\boldsymbol{U}(t)$ and $S(t)$. The process $\boldsymbol{U}(t)$ describes the motion of a unit vector $\boldsymbol{U}$ which obeys the deterministic equation of motion

$$\frac{d\boldsymbol{U}}{dt} = \boldsymbol{\kappa} \cdot \boldsymbol{U} - \boldsymbol{\kappa} : \boldsymbol{UUU} \quad , \tag{4.40}$$

and the process $S(t)$ describes the dynamics of a real number S (corresponding to s/L) lying between 0 and 1 which obeys the stochastic differential equation

$$dS(t) = \frac{\sqrt{2D}}{L}\, dW(t) \quad . \tag{4.41}$$

where $W(t)$ is the Wiener process. The process $S(t)$ is simulated with reflecting boundaries at $S = 0$ and $S = 1$.

The important point is that the variable S now plays an active dynamical role in contrast to the pure labelling in the Doi-Edwards interpretation. In this way it is demonstrated that it suffices to simulate one single vector $\boldsymbol{U}$ so that in fact the Doi-Edwards model (with independent alignment) is a one link theory. The two processes $\boldsymbol{U}(t)$ and $S(t)$ are coupled through the boundary condition Eq.(4.38). When $S(t)$ reaches one of the boundaries, then $\boldsymbol{U}(t)$ has to be newly chosen as a random unit vector.

The Doi-Edwards model has been a major contribution to the understanding of the dynamics of polymer melts.

Another major approach in the description of polymer melts is the model of Curtiss and Bird [25], which is based on the kinetic theory in phase space. A polymer molecule is modelled as a Kramers chain consisting of identical beads connected by rigid rods. The other molecules provide anisotropic friction on adjacent beads. The theory obtains a constitutive equation for the stress on the basis of the mild curvature assumption. This assumption effectively reduces the one-chain theory to a one-segment one. The dynamics of this segment is in fact identical to that of the vector $\boldsymbol{U}$ in the Doi-Edwards model so that the two models are very similar in their stochastic contents despite their different motivations. An advantage of the Cutriss-Bird theory is that it provides an explicit mesoscopic expression for the stress tensor, which differs in one additional term from the stress tensor in the Doi-Edwards theory, and leads therefore to different predictions. As we are only interested in the stochastic contents of the theories here, we refer to the literature [25] for a more detailed description of the Curtiss-Bird model.

4.2.3 A dumbbell model with anisotropic friction

The idea of reptation has been very successful. It is therefore interesting to see if it can be used to improve the Rouse model. We will start by studying a generalization of the Hookean dumbbell model. The model treats a representative polymer in a mean field. The ansatz for the mean field is that the environment of the test polymer leads to an anisotropic hydrodynamic drag force on the beads. In the kinetic theory frame of Bird

et al. [25] the ansatz for this hydrodynamic force is

$$\mathbf{F}_\nu^h = -\zeta \boldsymbol{\mu}^{-1} \cdot (\dot{\boldsymbol{r}}_\nu - \boldsymbol{\kappa} \cdot \boldsymbol{r}_\nu). \tag{4.42}$$

Here instead of a scalar friction coefficient ζ an anisotropic friction tensor $\zeta\boldsymbol{\mu}^{-1}$ appears with a dimensionless tensor $\boldsymbol{\mu}$ to be specified later. For $\boldsymbol{\mu} = \mathbf{1}$ one obtains the Hookean dumbbell model. The correct Fokker-Planck equation with tensorial friction has already been given by Baxandall [26]. It reads

$$\frac{\partial}{\partial t}\Psi = -\frac{\partial}{\partial \boldsymbol{Q}} \cdot \left(\left(\boldsymbol{\kappa} \cdot \boldsymbol{Q} - \frac{2H}{\zeta} \boldsymbol{\mu} \cdot \boldsymbol{Q} \right) \Psi \right) + \frac{2kT}{\zeta} \frac{\partial}{\partial \boldsymbol{Q}} \cdot \boldsymbol{\mu} \cdot \frac{\partial}{\partial \boldsymbol{Q}} \Psi \quad . \tag{4.43}$$

The position of the tensor $\boldsymbol{\mu}$ between the two derivatives is not surprising, the same is found for the diffusion of a particle in a medium with space dependent mobility [3]. One can see immediately that the solution for equilibrium is the Gaussian one that we already know. The Fokker-Planck equation can now be transformed into an equivalent Langevin equation for $\boldsymbol{Q}$. Since we will study mobilities which depend on $\boldsymbol{Q}$ this has to be done with great care, because the result is a stochastic equation with multiplicative noise. The Ito-Langevin equation corresponding to the above Fokker-Planck equation is

$$\dot{\boldsymbol{Q}}(t) = \boldsymbol{\kappa}(t) \cdot \boldsymbol{Q}(t) - \frac{2H}{\zeta} \boldsymbol{\mu}(t) \cdot \boldsymbol{Q}(t) + \frac{2kT}{\zeta} \frac{\partial}{\partial \boldsymbol{Q}} \cdot \boldsymbol{\mu}(t) + \boldsymbol{B}(t) \cdot \boldsymbol{\eta}(t). \tag{4.44}$$

The stochastic force $\boldsymbol{\eta}$ in the last term of the above equation is Gaussian white noise with zero mean and the two time correlation functions as in Eq.(4.27) and the matrix $\boldsymbol{B}$ has to fulfil

$$\boldsymbol{B} \cdot \boldsymbol{B}^T = \boldsymbol{\mu}, \tag{4.45}$$

because of the fluctuation-dissipation theorem.

To conclude the definition of our dumbbell model with anisotropic friction we must specify the tensor $\boldsymbol{\mu}$. Following [26, 27, 28, 29] we choose

$$\boldsymbol{\mu} = (1 - \alpha)\,\mathbf{1} + \alpha \mathbf{u}\mathbf{u}. \tag{4.46}$$

Here $\boldsymbol{u}$ is the unit vector in the direction of $\boldsymbol{Q}$ and α $(0 \leq \alpha \leq 1)$ is a dimensionless parameter which is a measure for the anisotropy. For $\alpha = 0$ one gets the isotropic friction tensor, as in the Hookean dumbbell model.

For all α the mobility in the direction of $\boldsymbol{u}$ is $1/\zeta$ and the mobility in a direction perpendicular to $\boldsymbol{u}$ is $(1-\alpha)/\zeta$ so that for $\alpha \neq 0$ motions along the direction of the dumbbell are favored. For the extreme case of $\alpha = 1$ all motions perpendicular to $\boldsymbol{u}$ are suppressed because the mobility in these directions is zero.

As an alternative ansatz one could also consider the tensor

$$\boldsymbol{\mu} = (1-\alpha)\,\mathbf{1} + \alpha \frac{H}{kT} \boldsymbol{Q}\boldsymbol{Q}. \tag{4.47}$$

A similar ansatz has been used in the works of Volkov [29] and of Giesekus [30, 31]. It is of the same form as Eq. (4.46) but with $\boldsymbol{Q}$ instead of $\boldsymbol{u}$. This has the effect that the mobility depends not only on the direction of the dumbbell's connector but also on its length. For two dumbbells with unequal length but the same direction the mobility for the longer one is greater then for the shorter one.

The predictions for both mobilities were studied with the help of Brownian Dynamics simulations [32]. The ansatz of Eq.(4.47) where the mobility increases with increasing length of the dumbbell is more successful. In a rough way this may incorporate the effect that under high shear rates the mobility of the polymer increases. As the dumbbell model for a polymer is very crude it will be necessary to study the effects of an anisotropic mobility also in a chain model.

4.2.4 A chain model with anisotropic mobility

It is now straightforward to generalize our dumbbell model with configuration dependent tensorial mobility to a bead-spring chain model. The intermolecular interactions are treated as a mean-field acting on the chain. To this end we must introduce anisotropic mobility tensors for the beads. The ansatz for these tensors corresponds very closely to the assumption in the Curtiss-Bird model. A major difference lies in the fact that in the present model the number of beads is a physical quantity which measures the degree of entanglements in the polymer system. Again we have chosen a simple Hookean force law for the springs and Brownian forces that follow from the fluctuation dissipation theorem. In this section we will therefore only sketch briefly the corresponding Langevin and Fokker-Planck equations. A more detailed derivation can be found in Ref. [33]

As a mesoscopic model for the chain we choose N identical beads connected by Hookean springs with spring constant H. All other chains are treated as a mean-field by assuming that the chain moves more easily along its contour than in other directions on an appropriate length scale. The Fokker-Planck equation for the probabilty distribution function $\Psi(\boldsymbol{Q}_1, \cdots, \boldsymbol{Q}_{N-1}, t)$ is given by

$$\frac{\partial}{\partial t}\Psi = -\sum_{\nu} \partial_\nu \cdot (\boldsymbol{\kappa} \cdot \boldsymbol{Q}_\nu \Psi) + \frac{H}{\zeta} \sum_{\nu\sigma} \partial_\nu \cdot (\boldsymbol{A}_{\nu\sigma} \cdot \boldsymbol{Q}_\sigma \Psi) + \frac{kT}{\zeta} \sum_{\nu\sigma} \partial_\nu \cdot \boldsymbol{A}_{\nu\sigma} \cdot \partial_\sigma \Psi \quad . \tag{4.48}$$

The summation indices run from 1 to $N-1$. The 3×3 matrices $\boldsymbol{A}_{\nu\sigma}$ are elements of the symmetric $(N-1) \times (N-1)$ supermatrix $\hat{\boldsymbol{A}}$ which follows from the matrix representation of the mobility tensors of the beads as

$$\hat{\boldsymbol{A}} = \begin{pmatrix} \boldsymbol{\mu}_1 + \boldsymbol{\mu}_2 & -\boldsymbol{\mu}_2 & 0 & \cdots & 0 & \cdots & 0 \\ -\boldsymbol{\mu}_2 & \boldsymbol{\mu}_2 + \boldsymbol{\mu}_3 & -\boldsymbol{\mu}_3 & \cdots & 0 & \cdots & 0 \\ \vdots & \vdots & \vdots & \vdots & \vdots & \vdots & \vdots \\ 0 & \cdots & 0 & \cdots & -\boldsymbol{\mu}_{N-2} & \boldsymbol{\mu}_{N-2} + \boldsymbol{\mu}_{N-1} & -\boldsymbol{\mu}_{N-1} \\ 0 & \cdots & 0 & \cdots & 0 & -\boldsymbol{\mu}_{N-1} & \boldsymbol{\mu}_{N-1} + \boldsymbol{\mu}_N \end{pmatrix}.$$

The corresponding Langevin equation is given by

$$\dot{\boldsymbol{Q}}_\nu(t) = \boldsymbol{\kappa}(t) \cdot \boldsymbol{Q}_\nu(t) - \frac{H}{\zeta} \sum_{\sigma} \boldsymbol{A}_{\nu\sigma} \cdot \boldsymbol{Q}_\sigma + \frac{kT}{\zeta} \sum_{\sigma} \partial_\sigma \cdot \boldsymbol{A}_{\nu\sigma} + \sum_{\sigma} \mathbf{B}_{\nu\sigma} \cdot \boldsymbol{\eta}_\sigma. \tag{4.49}$$

Here the first two terms on the right-hand side are the drift terms originating from the flow field and the intramolecular forces. The third term is an additional drift term which is a consequence of the Ito interpretation of the Langevin equation. It vanishes if the mobility tensors of the beads, and thus the matix $\hat{\boldsymbol{A}}$, are independent of the variables $\boldsymbol{Q}_\nu$. In the last term of Eq. (4.49) the $N-1$ vectors $\boldsymbol{\eta}_\sigma$ describe the effects of the Brownian forces. They are modelled as Gaussian white noise with zero mean and the two time correlation functions as in Eq.(4.27). The 3×3 matrices $\mathbf{B}_{\nu\sigma}$ are the elements of the $(N-1) \times (N-1)$ dimensional supermatrix $\hat{\boldsymbol{B}}$ which as for the isotropic case has to fulfil the condition Eq.(4.33) which is an expression of the fluctuation dissipation theorem.

In order to complete the model an ansatz for the anisotropic mobility tensors has to be given. For instance, one could choose the tensors $\boldsymbol{\mu}_\nu$ as

$$\boldsymbol{\mu}_\nu = (1 - \alpha_\nu)\,\mathbf{1} + \alpha_\nu \boldsymbol{u}_\nu \boldsymbol{u}_\nu \quad , (\nu = 1, \cdots, N), \tag{4.50}$$

where the α_ν are dimensionless parameters with $0 \leq \alpha_\nu \leq 1$. The unit vectors $\boldsymbol{u}_\nu$ are defined for $\nu = 1, \cdots, N$ by

$$\boldsymbol{u}_\nu = \begin{cases} \boldsymbol{Q}_1 / \mid \boldsymbol{Q}_1 \mid & \text{for } \nu = 1 \\ (\boldsymbol{Q}_{\nu-1} + \boldsymbol{Q}_\nu) / \mid \boldsymbol{Q}_{\nu-1} + \boldsymbol{Q}_\nu \mid & \text{for } \nu = 2, \cdots, N-1 \\ \boldsymbol{Q}_{N-1} / \mid \boldsymbol{Q}_{N-1} \mid & \text{for } \nu = N \end{cases} \tag{4.51}$$

The effect of this ansatz is that for a motion in the direction $\boldsymbol{u}_\nu$ the bead ν feels a friction ζ , while for a motion in a direction perpendicular to $\boldsymbol{u}_\nu$ it feels a friction $\zeta/(1-\alpha_\nu)$, which is greater for $\alpha_\nu \neq 0$. In this way a motion along the contour of the chain is favoured. In principle the parameters α_ν could be different for each bead. In Ref. [33] two cases were studied. In the first one all parameters assumed the same value. In the second one the parameters for bead 1 and bead N were set equal to 0 to study the influence of the mobility of the chain ends. The model was found to be a real improvement over the Rouse model. The time dependence of the material functions is satisfactory, as an overshoot is predicted. However the experimentally observed shear thinning effect cannot be explained for larger shear rates.

4.3 Master equations in rheology

4.3.1 Transient network theories

Concentrated polymer solutions and melts can also be described with the help of an approach that originated from the theory of rubber elasticity. A vulcanized rubber consists of strands which are permanently cross linked at junctions. To allow the description of the liquid-like behaviour, which is typical for polymer melts, one has to assume that the junctions, which represent the entanglements in the polymer system are temporary. In transient network theories junctions break up and reform continuously.

Let us now assume that the junctions are connected by elastic strands. These strands are idealized as Hookean springs. Their length and orientation is given by $\boldsymbol{Q}$. For simplicity let us assume that we have only one type of strand, with spring constant H. The vectors $\boldsymbol{Q}$ are distributed independently according to the distribution function $\Psi(\boldsymbol{Q},t)$. $\Psi(\boldsymbol{Q},t)\,d^3Q$ gives the probability of finding $n(t)$ network strands joining two entanglements with

a configuration around $\boldsymbol{Q}$ at time t in unit volume. The number density of strands $n(t)$ is thus defined as

$$n(t) = \int d^3Q \; \Psi(\boldsymbol{Q}, t) \quad , \tag{4.52}$$

and is generally a function of time. As the internal force law of the strands that make up the network was assumed to be linear, the distribution function $\Psi_0(\boldsymbol{Q})$ at equilibrium will simply be a Gaussian one, that is

$$\Psi_0(\boldsymbol{Q}) = \frac{n_0}{(2\pi\sigma^2)^{3/2}} \exp\left(-\frac{\boldsymbol{Q}^2}{2\sigma^2}\right) \quad . \tag{4.53}$$

Here $\sigma^2 = kT/H$ is one third of the mean square equilibrium length of the strands (with k Boltzmann's constant and T the temperature) and n_0 gives the equilibrium number density of strands.

At equilibrium the rate of junction creation should be equal to the rate of junction loss. It is therefore plausible that the distribution function $\Psi(\boldsymbol{Q})$ obeys the following Master equation

$$\frac{\partial}{\partial t}\Psi(\boldsymbol{Q}, t) = h(\boldsymbol{Q})[\Psi_0(\boldsymbol{Q}) - \Psi(\boldsymbol{Q}, t)] \quad . \tag{4.54}$$

The terms on the right hand side describe the creation and the destruction of the strands. Note that here new strands are created from the equilibrium ensemble, as is usually assumed in transient network theories. The function $h(\boldsymbol{Q})$ determines the rate of the creation and destruction of the strands. The above equation is in fact the Master equation describing a birth and death process for each strand $\boldsymbol{Q}$. Such processes are also known under the name of one-step processes.

As we are mainly interested in the flow properties of polymer melts we have to describe the motion of a strand $\boldsymbol{Q}$. For a Gaussian network the junctions can be shown [34] to move affinely with the deformation, as obviously does the strand vector joining two of them. The deformation of the strands which is induced by the flow field is thus given by the deterministic differential equation

$$\dot{\boldsymbol{Q}} = \boldsymbol{\kappa} \cdot \boldsymbol{Q} \quad , \tag{4.55}$$

where $\boldsymbol{\kappa}$ is the transpose of the velocity gradient. The equation of continuity determining the distribution function $\Psi(\boldsymbol{Q}, t)$ as a consequence of the

affine deformation is given by

$$\frac{\partial}{\partial t}\Psi + \frac{\partial}{\partial \boldsymbol{Q}} \cdot (\boldsymbol{\kappa} \cdot \boldsymbol{Q}\Psi) = 0 \quad . \tag{4.56}$$

If we now allow that during the flow the strands may be lost and created we have to combine Eq.(4.54) with Eq.(4.56). Doing so we finally get the so-called convection equation [25] for the configurational distribution function $\Psi(\boldsymbol{Q},t)$, which plays a fundamental role in polymer network theories ,

$$\frac{\partial}{\partial t}\Psi(\boldsymbol{Q},t) + \frac{\partial}{\partial \boldsymbol{Q}} \cdot [\boldsymbol{\kappa} \cdot \boldsymbol{Q}\Psi(\boldsymbol{Q},t)] = h(\boldsymbol{Q})\,[\Psi_0(\boldsymbol{Q}) - \Psi(\boldsymbol{Q},t)] \quad . \tag{4.57}$$

The convection equation is a balance equation for the flow, the loss, and the creation of strands.

The quantity we want to determine to characterize the rheological behaviour of transient polymer network theories is the stress tensor $\boldsymbol{\sigma}$, which for a Gaussian network with strands of only one type is defined as [25]

$$\boldsymbol{\sigma} = H < \boldsymbol{QQ} > \quad . \tag{4.58}$$

Here the brackets denote an average over an ensemble described by the distribution function $\Psi(\boldsymbol{Q},t)$.

Transient network theories can be classified by the chosen ansatz for the function $h(\boldsymbol{Q})$. For $h = constant$ one obtains the well-known model of Green and Tobolsky [35]. In this case the stress tensor can be evaluated analytically from a closed constitutive equation. In order to improve the predictions of the Green-Tobolsky model, several models have been proposed, in which the strand creation and destruction probabilities depend on the instantaneous stress. One example is the model of Phan-Thien and Tanner [36, 37, 38]. For this model it is also possible to derive closed constitutive equations, because the rates depend on some mean properties of the ensemble, such as $< \boldsymbol{Q}^2 >$. Models where the creation and destruction rates depend on the history of stress or the history of strain rate have also been proposed (for a review see ref. [39]). All the above-mentioned models have in common that the rates depend on global (or averaged) quantities. From a physical point of view it is much more plausible to assume that the rates depend on the local configuration of the strands. In these Yamamoto-type models [40, 41, 42, 43, 44], where the destruction probability depends on the strand extension, it is not possible to write

down a closed constitutive equation. It is exactly this class of network models for which simulation algorithms will be particularly useful. In fact the simulation of such network models leads to very satisfactory rheological predictions [45, 46].

Let us conclude this section with the following remark. The convection equation (4.57) which usually describes the dynamical behaviour of transient network theories is not a proper Master equation. It is as we have seen a combination of a Liouville equation with a Master equation for a birth and death process. It is nevertheless possible to generalize the convection equation to a proper Master equation. To this end one has to reconsider the dynamics of a single strand. In Gaussian transient network theories the strand is modelled as a Hookean spring, which is deformed affinely in a flow situation. At equilibrium the only dynamics is represented by the birth and death process. One could now describe the dynamics of a strand by a dumbbell model. Doing so the strand does not only feel the affine deformation, but also a retractive force and Brownian motion. The Hookean dumbbell model fulfills the above requirements, although one could also consider nonlinear dumbbell models. The transient network is thus formally modelled by an ensemble of dumbbells. The strands evolve stochastically in time according to a proper Langevin equation, as for instance

$$\dot{\boldsymbol{Q}}(t) = \boldsymbol{\kappa}(t) \cdot \boldsymbol{Q}(t) - \frac{2}{\zeta}\mathbf{F}(\boldsymbol{Q}(t)) + \boldsymbol{\eta}(t), \tag{4.59}$$

which is typical for molecular kinetic polymer models. If we allow again the strands to be generated and removed with certain rates as is typical for transient network models, then our new model can be described by the following equation for the distribution function $\Psi(\boldsymbol{Q},t)$ [47]

$$\frac{\partial}{\partial t}\Psi + \frac{\partial}{\partial \boldsymbol{Q}} \cdot \left(\boldsymbol{\kappa} \cdot \boldsymbol{Q}\Psi - \frac{2}{\zeta}\mathbf{F}\Psi - \frac{2kT}{\zeta}\frac{\partial}{\partial \boldsymbol{Q}}\Psi\right) = h(\boldsymbol{Q})[\Psi_0(\boldsymbol{Q}) - \Psi(\boldsymbol{Q})] \quad . \tag{4.60}$$

which is a Master equation describing a diffusive process (Fokker-Planck equation) and a birth and death process. This approach gives us therefore a theoretical framework in which the two different points of view of molecular kinetic theories and of transient network theories can be unified. This approach is very promising as it naturally allows the study of non-Gaussian transient network theories by considering nonlinear internal force laws [47].

4.3.2 The Orwoll-Stockmayer model

Master equations arise also in another class of models we want to introduce briefly. Let us consider a polymer chain as a freely jointed chain made out of $N+1$ beads. The beads are separated by a constant bond distance b. Let us denote the connector vector joining bead $i-1$ to bead i $b\boldsymbol{u}_i$, where $\boldsymbol{u}_i$ is a unit vector. This so called Kramers chain makes elemental jumps of the following type. When an interior bead moves, the vectors $\boldsymbol{u}_i$, and $\boldsymbol{u}_{i+1}$ before the flip are transformed to the vectors $\boldsymbol{u}'_i$ and $\boldsymbol{u}'_{i+1}$ according to the following rule

$$\boldsymbol{u}'_i = \boldsymbol{u}_{i+1} \qquad \textit{and} \qquad \boldsymbol{u}'_{i+1} = \boldsymbol{u}_i. \tag{4.61}$$

That is, beads on the interior of the chain can suddenly jump to positions attained by a 180° rotation of the connecting rods, while the neighboring beads are held still. Orwoll and Stockmayer [48] specify the terminal beads 0 and N to move so that

$$\boldsymbol{u}'_1 = -\boldsymbol{u}_1 \qquad \textit{and} \qquad \boldsymbol{u}'_N = -\boldsymbol{u}_N. \tag{4.62}$$

The model is completely defined if one also specifies the probabilities w_i per unit time that the i-th bead jumps. In the model of Orwoll and Stockmayer these are given by

$$w_i = \alpha\,(1 - a\boldsymbol{u}_i\boldsymbol{u}_{i+1}), \tag{4.63}$$

with $a \leq 1$. The flip probability for an end bead is assigned a constant value

$$w_0 = w_N = \alpha. \tag{4.64}$$

The jumping probabilities depend on the chain configuration. The motion of the chain may be described by a Master equation that is configuration dependent. One finds that the probability distribution function obeys the following Master-equation

$$\begin{aligned}\frac{d}{dt}p(\boldsymbol{u}_1,\cdots,\boldsymbol{u}_N,t) \;=\; & -p(\boldsymbol{u}_1,\cdots,\boldsymbol{u}_N,t)\left(\sum_{i=0}^{N} w_i\right) + w_0 p(-\boldsymbol{u}_1,\boldsymbol{u}_2,\cdots,\boldsymbol{u}_N,t) \\ & + \sum_{i=1}^{N-1} w_i(\boldsymbol{u}_{i+1},\boldsymbol{u}_i)p(\boldsymbol{u}_1,\cdots,\boldsymbol{u}_{i+1},\boldsymbol{u}_i,\cdots,\boldsymbol{u}_N,t) \\ & + w_N p(\boldsymbol{u}_1,\cdots,\boldsymbol{u}_{N-1},-\boldsymbol{u}_N,t).\end{aligned} \tag{4.65}$$

The first term on the right-hand side of the above equation describes the loss of the configuration $(\boldsymbol{u}_1, \cdots, \boldsymbol{u}_N)$ as a consequence of the flip of one of the $N+1$ beads. The other terms on the right hand-side describe the creation of the configuration $(\boldsymbol{u}_1, \cdots, \boldsymbol{u}_N)$ from all the other chain configurations.

We have briefly reviewed the dynamics of the Orwoll-Stockmayer model as it is of fundamental importance for the understanding of a new semi-Markovian model that we will describe in the next section.

4.4 Semi-Markov processes

In concentrated polymer solutions and melts the motion of a chain is strongly hindered due to the presence of the other chains. In Freiburg we developed a new model which is based on the following assumption [49] . A given polymer chain is frozen in space until it meets with a "gap", *i.e.*, a portion of free volume in the melt. When a gap reaches a segment of chain the corresponding segment may jump to a new position, while the rest of the chain remains stationary. Note that the exact forms of the gaps are not specified, and not even considered, except for how they influence the movement of the chain. In the description of the chain dynamics the waiting time between two succesive jumps of the same segment plays a fundamental role. When one specifies the possible motions of the chains, along with their relative probabilities, the type of chain, and the waiting time distributions, the equilibrium model is completely specified.

Our model is based on a generalization of the Orwoll-Stockmayer model [48]. In the original Orwoll-Stockmayer model the probability for a given bead to jump may depend upon the angle made by the two connecting-rods adjoining it. We remove this dependence, and allow all beads to jump with equal probability independent of the configuration of the chain.

Furthermore we allow the motion of the end beads to be more general: The bead may jump to any point on the sphere of radius a centered on the adjoining bead. In other words, the unit vector pointing from the second-to-the-end bead to the end bead may suddenly jump to a random orientation chosen from a uniform distribution on the unit sphere. This generalization allows all possible orientations of the rods independent of the initial chain configuration. The stochastic kinematics of the original

model are a Markovian process. Thus, the probability of a bead making a jump is dependent only upon the current configuration of the chain, and not upon the past jumps of the chain. Such an assumption implies that the times between successive jumps of a bead are much shorter than the time scale of interest, namely the time scale of the motion of chains. However, in the theory presented above, the motion of the segments of the chain are governed by the motions of neighboring chains on longer time scales. Thus, the time scale characteristic for a chain segment to meet up with a gap may be much longer than the time scale of interest, and thus, the waiting times for bead jumps are assumed to be fractal. For this reason the model describes a semi-Markovian process. The assumption of a fractal waiting time distribution has turned out to be very fruitful in a similar problem, namely the relaxation of concentrated solutions of electric dipoles [51]. Unfortunately, we can no longer write a Master Equation for the time evolution of the probability distribution function for the chain, and an analytic solution no longer seems possible.

All that remains to complete the model is the specification of the waiting time distribution function for the beads. It is defined as:

$$\psi(t)dt := \text{Prob}\{\text{the time between successive jumps for a given bead is between } t \text{ and } t+dt\}. \quad (4.66)$$

For simplicity, we assume that this probability is configuration independent and independent of the time of day. Actually, we expect some segments to be effectively screened by other segments, and thus to have a lower probability of jumping. Also, we expect that chain segments that are near in space to other segments that have recently jumped to have greater probability of jumping. We also ignore, for the time being, excluded volume effects. One fractal distribution is:

$$\psi(t) = \frac{1}{\beta(1+t)^{\beta+1}}. \quad (4.67)$$

For $0 < \beta \leq 1$, the waiting times have no first moment, and thus, no characteristic time scale.

It is also useful to define another distribution function:

$$P(t)dt = \text{Prob}\{\text{when examining any given bead at any given time, the time one must wait until the bead jumps is} \quad (4.68)$$

between t and $t+dt$}

$$= \sum_{\text{all } t'>t} \text{Prob\{the total jump is } t' \text{ in this interval}\} \times \text{Prob\{time } t-t' \text{ has passed in this interval}\}$$

$$= J\int_t^\infty \psi(t')dt'dt,$$

where J is the proper normalization constant. For the simple distribution given by Eq.[4.67], $P(t)$ has the form:

$$P(t) = \frac{J}{(1+t)^\beta}. \tag{4.69}$$

Note that if $\beta < 1$, $P(t)$ is not normalizable, and is thus no proper probability function. We will therefore consider only chains for which $\beta > 1$. We may then find the normalization function J as

$$\begin{aligned} J &= \frac{1}{\int_0^\infty \frac{1}{(1+t)^\beta}dt}, \quad \beta > 1 \\ &= \beta - 1. \end{aligned} \tag{4.70}$$

Our simplified model has only two parameters: β and N, the number of beads in the chain. However, we may interpret the beads in the chains as entanglement points, which we may expect to be roughly related to the entanglement molecular weight, M_e (similar to the Doi-Edwards model):

$$N = M/M_e - 1, \tag{4.71}$$

where M is the molecular weight of the chain. This leaves the parameter β as the only adjustable parameter in the model, which is related to the gap diffusion. It may be closely related to the concept of free volume often invoked by physical chemists. However, we leave it open for now as an adjustable parameter to be fixed by one experiment, such as diffusion.

The Freiburg model is certainly not a reptation model. In fact, the probability for a chain making even one reptative-like motion is vanishingly small for longer chains. Nevertheless the chain kinematics considered here are similar to those of the Curtiss-Bird [25] and Giesekus [52, 30] models, since chain segments move independently. However, here the segments have no preferred anisotropic motion, and the process is non-Markovian. Also, since the full chain kinematics are considered (and simulated) here,

the predictions of the model for diffusion are unambiguous. At equilibrium the model predicts non-Fickian diffusion in agreement with experimental data. A more detailed discussion of the predictions of the model can be found in Refs. [49, 50]

The model may be also interpreted as a network model with the beads representing entanglements, and bead jumps as the simultaneous destruction and creation of segments. However, here we have a connection to chain properties, and the destruction and creation rates are allowed to be non-Markovian. The latter point suggests that the model is more realistic, since the junction lifetimes are on the same time scales as the chain motions themselves.

4.5 Summary

The description of a complex dynamical system, such as a polymer melt requires the introduction of stochastical concepts. To this end we have briefly reviewed the fundamental equations describing the dynamics of stochastic processes. The Chapmann-Kolmogorov equation was shown to characterize the properties of the very fundamental class of Markov processes, whose dynamics is generally described by a Master equation. For the restricted class of diffusive processes the Master equation is approximated by a Fokker-Planck equation for the probability distribution function. In this case the diffusive system can be equivalenty described by a stochastic differential equation for the stochastic variable. This equivalence is fundamental for the Brownian Dynamics simulation approach to polymer melts. Semi-Markov processes were briefly introduced.

Stochastic differential equations arise very naturally in the theoretical description of polymer chains in a melt. If the chain is modelled as a bead-spring chain the single bead, neglecting inertial effects, feels a hydrodynamic drag, an internal force law, and a stochastic force which represents the effect of the interaction with the surrounding molecules. As stochastic differential equations can be very efficiently solved numerically one can introduce configuration dependent mobilities in the theories, which lead to a more realistic modelling. Also well established theories as the Doi-Edwards theory can be shown to be based on stochastic differential equations.

Master equations also occur in rheology. Transient network theories are usually described by a convection equation. Introducing an additional diffusive motion of the strands, that is by modelling the strand as a dumbbell, these theories can be shown to be described by a Master equation for both a diffusive and a birth and death process. Another model, the Orwoll-Stockmayer model is also described by a Master equation.

A new model, which was developed in Freiburg, is based on semi-Markov processes. Unfortunately the predictions of this model cannot be calculated analytically. For a Kramers chain the jump probabilities no longer depend on the configuration. One must specify the waiting time distribution for the jumps to occur. This is assumed to be fractal.

Chapter 5

Simulation of Stochastic Processes

P. Biller

In this lecture the powerful numerical method of computer simulations of stochastic processes is introduced and explained. The idea of a computer simulation is to follow a particle subject to the stochastic process under study. Generally one introduces small discrete time steps and calculates the changes the particle will make during such time steps. The particle is registered up to a desired final time and in this way one obtains a single realization of the stochastic process. Usually the interesting quantities are defined as certain averages of the stochastic process. Therefore one has to repeat the simulation until a large number of realizations is obtained from which the desired quantities, together with their statistical errors, can be calculated. In the following we will give the details of such a procedure for the Langevin equations and Master equations, as well as for the semi-Markov processes that arise in the description of the rheological behaviour of polymers. Before we begin with this programme let us make some introductory remarks on the generation of random numbers on a computer.

5.1 The generation of random numbers

Random numbers are one of the most important ingredients in any computer simulation. One may ask: how can a deterministic machine like a computer provide true random numbers? The answer is that the computer uses simple laws to generate a series of numbers which have statistical properties, such as the absence of correlations, that resemble those of true random numbers. So the more appropriate term for the stochastic quantities appearing in computer simulations would be pseudo random numbers.

The generation of equally distributed random numbers in the unit interval $[0,1]$ is a fundamental task. A method frequently employed is the linear congruential method [53] which works as follows. For prescribed parameters a, b, m one chooses an initial value r_0 (which for example may be a function of the instant of time when the generation of the random numbers is started) and then constructs the series of numbers r_n using the recursion formula

$$r_{n+1} = (ar_n + b) \bmod m \ . \tag{5.1}$$

The n-th random number is then defined as

$$x_n = r_n/m. \tag{5.2}$$

It obviously lies in the unit interval. The quality of the random numbers generated in this way strongly depends on the choice of the parameters a, b, m. For instance, m has to be chosen very large, for it gives the maximum possible number of different random numbers. For example, a good random number generator is obtained with the parameters $a = 513, b = 297410973$, and $m = 2^{47}$. More details on the choice of the parameters, as well as the various methods to test the quality of a generator can be found in the literature [53]. There one can also find alternatives to the linear congruential method. Tested subroutines for the generation of random numbers equally distributed in the unit interval can be found in any program library.

With the help of the random numbers x_n equally distributed in the unit interval one can easily generate equally distributed random numbers x'_n in the general interval $[\alpha, \beta]$ by the operation

$$x'_n = \alpha + (\beta - \alpha)x_n \ . \tag{5.3}$$

In the simulation of Gaussian white noise to be treated soon, Gaussian random numbers are used instead of equally distributed ones. Without proof we give the following simple recipe for their generation known as the Box-Müller method [53]. Given two equally distributed random numbers x_1, x_2 from the unit interval one can build two random numbers y_1, y_2 through

$$y_1 = \sqrt{-2\ln x_1}\cos(2\pi x_2) \ , \quad y_2 = \sqrt{-2\ln x_1}\sin(2\pi x_2) \tag{5.4}$$

which represent two independent realizations of a variable that is normally distributed. Random numbers η_n described by a Gaussian distribution with mean μ and variance σ^2 can then easily be obtained as

$$\eta_n = \mu + \sigma y_n \ . \tag{5.5}$$

Sometimes one has to draw random numbers z_n from an arbitrary normalized probability distribution $p(z)$ (with say $0 \leq z < \infty$). There are several possibilities to do this [5]. Here we introduce the so-called inversion method: pick a random number x_n equally distributed in the unit interval and solve the equation

$$P(z) \equiv \int_0^z dy \ p(y) = x_n \tag{5.6}$$

for z. This solution defines the random number z_n which is a realization of a stochastic variable z with the probability distribution $p(z)$.

5.2 The simulation of Langevin equations

This section explains the general method for a computer simulation of a stochastic differential equation, also known as Brownian dynamics simulation. As an example we will first consider the stochastic process of a Hookean dumbbell and then some generalized models. Throughout this section we will study the typical flow situation of inception of steady shear flow at time zero where κ takes on the form

$$\kappa(t) = \dot{\gamma} \begin{pmatrix} 0 & 1 & 0 \\ 0 & 0 & 0 \\ 0 & 0 & 0 \end{pmatrix} \theta(t) \ . \tag{5.7}$$

Here $\dot{\gamma}$ is the constant imposed shear rate and θ is the Heaviside step function. The quantity of interest in rheology is the stress tensor σ which for the Hookean dumbbell model is simply given by

$$\sigma = nH < \boldsymbol{QQ} > \quad . \tag{5.8}$$

Here n denotes the number density of polymers. The definition of the stress tensor for the generalized models treated later can be found in the literature [25]. Here it is not the precise form that is important but the fact that σ is always defined as an average over the stochastic process. For the inception of steady shear flow one concentrates on the determination of the material functions η^+,ψ_1^+,ψ_2^+ which are defined by

$$\begin{aligned} \eta^+(t,\dot{\gamma}) &= \sigma_{xy}(t)/\dot{\gamma} \ , \\ \psi_1^+(t,\dot{\gamma}) &= \big(\sigma_{xx}(t) - \sigma_{yy}(t)\big)/\dot{\gamma}^2 \ , \\ \psi_2^+(t,\dot{\gamma}) &= \big(\sigma_{yy}(t) - \sigma_{zz}(t)\big)/\dot{\gamma}^2 \ . \end{aligned} \tag{5.9}$$

The steady state values for $t \to \infty$ are denoted by η,ψ_1,ψ_2. These are the material functions for the characterization of steady shear flow.

5.2.1 The algorithm for the Hookean dumbbell model

According to the last chapter the stochastic motion of a Hookean dumbbell is described by the Langevin equation

$$\dot{\boldsymbol{Q}} = \boldsymbol{\kappa} \cdot \boldsymbol{Q} - \frac{2H}{\zeta}\boldsymbol{Q} + \boldsymbol{\eta} \ , \tag{5.10}$$

where the stochastic forces $\boldsymbol{\eta}$ are modelled as a Gaussian white noise with zero mean and the two time correlations

$$\langle \eta_i(t)\eta_j(t')\rangle = \frac{4kT}{\zeta}\delta_{ij}\delta(t-t') \ . \tag{5.11}$$

Before the simulation can begin one first has to introduce dimensionless quantities. Fixing the energy scale kT, the length scale $\sqrt{kT/H}$ (which is one third of the mean-square equilibrium length of the dumbbell) and the time scale $\lambda_H = \zeta/4H$ one arrives at

$$\dot{\boldsymbol{Q}} = \boldsymbol{\kappa} \cdot \boldsymbol{Q} - \frac{1}{2}\boldsymbol{Q} + \boldsymbol{\eta} \ , \tag{5.12}$$

where

$$\langle \eta_i(t)\eta_j(t')\rangle = \delta_{ij}\delta(t-t') \ . \tag{5.13}$$

In the above equations all quantities should be interpreted as dimensionless, although we have not introduced new symbols for simplicity.

The next step before the simulation is the discretization of the dimensionless Langevin equation by the introduction of finite time steps which leads to

$$\boldsymbol{Q}(t+\Delta t) = \boldsymbol{Q}(t) + \Delta t[\boldsymbol{\kappa}(t)\cdot\boldsymbol{Q}(t) - \frac{1}{2}\boldsymbol{Q}(t)] + \sqrt{\Delta t}\,\boldsymbol{f}(t) \ . \tag{5.14}$$

Here Δt is the time step and each component of the vector $\boldsymbol{f}(t)$ is a normally distributed random number. The latter vectors are uncorrelated for different times. The above equation is known as the Euler discretization of the original Langevin equation and resembles the corresponding discretization for an ordinary differential equation. It gives the increment of the quantity $\boldsymbol{Q}$ in a small time step. This increment is a sum of a deterministic part and a stochastic part. It is important to note that the stochastic increment is not proportional to the time step, but to its square-root. This follows from the well-known fact that in an ordinary Wiener process the variance grows proportional to the time.

The discretized equation is the starting point of the computer simulation. It allows the determination of the stochastic quantity $\boldsymbol{Q}$ at the time $t+\Delta t$ if its value is known at time t. One starts at time zero with a vector $\boldsymbol{Q}_0$ that is randomly drawn from the known Gaussian equilibrium distribution. Then the succesive application of the discretized Langevin equation leads to one particular realization of the stochastic process. Since we are interested in the stress tensor which is an average over the stochastic process this single realization is not enough and we have to repeat the simulation for a large number of times M. Then we can calculate an estimator for a quantity q (which may be time dependent) by the ensemble average

$$\langle q\rangle = \frac{1}{M}\sum_{i=1}^{M} q_i \ , \tag{5.15}$$

where i labels the different realizations. An estimator for the statistical error of the ensemble average is given by the square-root σ of the following

expression

$$\sigma^2 = \frac{1}{M}[\langle q^2 \rangle - \langle q \rangle^2] = \frac{1}{M^2} \sum_{i=1}^{M} (q_i - \langle q \rangle)^2 \ . \tag{5.16}$$

One can see that the estimator for the error σ asymptotically varies as $M^{-1/2}$ so that one needs four times as many realizations in order to reduce the error by a factor of two. The obtained results clearly depend on the time step chosen. Therefore the whole simulation is run for different time steps and the results are then extrapolated to time step zero to obtain the final results. For the Euler scheme used here the extrapolation has to be linear [54]. The structure of the program is summarized in the following flow diagram:

S1: Choose a random vector $\boldsymbol{Q}_0$ from the equilibrium distribution. This is the initial configuration of the dumbbell.

S2: Calculate the new configuration after a small time step Δt with the use of the discretized Langevin equation.

S3: If you are interested in measuring some quantity q at the present time, then calculate the value of this quantity for this realization and add it up to the contributions of the former realizations. Do the same for the quantity q^2.

S4: If the time has not reached the final time, then go back to S2, otherwise the calculation of this realization is finished and you proceed to S5.

S5: If the number of realizations has not reached the prescribed value M, then repeat the simulation steps S1-S4, otherwise proceed to S6.

S6: Calculate the estimators of the interesting quantities and their statistical errors.

S7: Repeat the whole simulation S1-S6 for other values of the time step and determine the final results by an extrapolation to time step zero.

This is the general way to do a Brownian dynamics simulation for the Hookean dumbbell model. Let us end this description with a few remarks. First, we are not really interested in stochastic trajectories itself, but only in averages of the stochastic process. For such a situation one can show [54] that only the first two moments of the random numbers appearing

in the stochastic increment have to be correct. So, instead of normally distributed random numbers one may work with equally distributed random numbers in the interval $[-\sqrt{3}, \sqrt{3}]$. Depending on the machine, this can reduce the necessary computer time up to one order of magnitude. Second, there is an easier simulation method if one has a steady flow, or if one is only interested in the steady state values that are approached after the inception of the flow. Then it is sufficient to simulate only one single realization over a very large time and instead of an ensemble average one builds a time average to obtain the (time step dependent) results. In this way one implicitly assumes that the system is ergodic. The determination of the statistical error is slightly more complicated and can be found in the literature [55]. Third, methods of higher order than the first order Euler integration scheme may also be used. For this point we again refer to the literature [2].

5.2.2 The algorithm for the Rouse model

Now we want to generalize the Hookean dumbbell model to the original Rouse model where the polymer is modelled as a chain consisting of N beads connected by $N-1$ Hookean springs. The Langevin equation for this model was given in (4.31) in the last chapter. Using the same length, time, and energy scale as above, it is easy to derive the dimensionless Langevin equation for the $\nu - th$ connector vector ($\nu = 1, ..., N-1$). After discretization we arrive at

$$\boldsymbol{Q}_\nu(t+\Delta t) = \boldsymbol{Q}_\nu(t) + \Delta t[\kappa(t)\cdot\boldsymbol{Q}_\nu(t) - \frac{1}{4}\sum_{\sigma=1}^{N-1}\boldsymbol{A}_{\nu\sigma}\cdot\boldsymbol{Q}_\sigma(t)] + \sqrt{\Delta t}\sum_{\sigma=1}^{N-1}\boldsymbol{B}_{\nu\sigma}\cdot\boldsymbol{f}_\sigma(t)\ . \quad (5.17)$$

As before, each component of the three dimensional vector $\boldsymbol{f}_\sigma(t)$ is a normally distributed random number. The matrices $\boldsymbol{A}_{\nu\sigma}$ and $\boldsymbol{B}_{\nu\sigma}$ are given by

$$\boldsymbol{A}_{\nu\sigma} = (2\delta_{\nu,\sigma} - \delta_{\nu,\sigma\pm1})\,\mathbf{1} \quad , \quad \boldsymbol{B}_{\nu\sigma} = \sqrt{1/2}(\delta_{\nu,\sigma} - \delta_{\nu,\sigma-1})\,\mathbf{1}. \quad (5.18)$$

As indicated in the last chapter they are the elements of supermatrices $\hat{\boldsymbol{A}}$ and $\hat{\boldsymbol{B}}$ that obey the equation $\hat{\boldsymbol{B}}\cdot\hat{\boldsymbol{B}}^T = \frac{1}{2}\hat{\boldsymbol{A}}$ as a consequence of the fluctuation-dissipation theorem.

All quantities appearing in the discretized Langevin equation are defined and we are ready to start the Brownian dynamics simulation. The

program runs exactly the same way as described above for the Hookean dumbbell model. The only difference is that now we have $N-1$ times as many stochastic variables as before. Moreover, the interesting phenomena occur on a time scale which scales quadratically with the number of beads. So one has to simulate a much longer time and for practical reasons the maximum bead number is limited to values of about 50.

Let us now turn to the results of the simulation. Both the Hookean dumbbell model and the Rouse model lead to predictions that are not at all satisfactory. For example, the viscosity η and the first normal stress coefficient ψ_1 are independent of the shear rate, and the second normal stress coefficient ψ_2 vanishes. All this is in contradiction to experimental data. Moreover the models are simple enough to be solved analytically [25]. So one may wonder: why do we make such a complicated simulation program for a model that can be solved analytically and moreover leads to disappointing results? The answer is simple. First, it is a great advantage that the computer simulation can be checked when analytical results are available. Second, the Hookean dumbbell model and the Rouse model are ideal starting points for more sophisticated models. For instance, one may argue that a linear force law for the springs is inadequate because the polymer is only finitely extensible. With a nonlinear force law the model cannot be solved analytically any more. However, a simulation is straightforward since only very few lines in the program have to be changed slightly. The inclusion of such a nonlinear force law along these lines has been treated in Ref. [56] and there it was found that the viscosity and the first normal stress coefficient decrease with increasing shear rate, in accordance with experiment. Here we want to discuss another generalization of the Hookean dumbbell model and the Rouse model, namely the inclusion of anisotropic mobility tensors as motivated in the last chapter.

5.2.3 The algorithm for the dumbbell model with anisotropic mobility

We begin with the implementation of the dumbbell model. Let the inverse of the scalar friction coefficient be substituted by an anisotropic mobility tensor of the form $\frac{1}{\zeta}\boldsymbol{\mu}$. In the last chapter we have learned that this leads to a stochastic differential equation with multiplicative noise which can be interpreted in different ways, either according to Ito or to Stratonovich. For the simulation it is essential to discretize the Ito-Langevin equation because only in this version are the stochastic Brownian forces, that are added in a small time step, uncorrelated with the actual stochastic variable $\boldsymbol{Q}(t)$. The Ito-Langevin equation was given in Eq.(4.44) in the last chapter. After the introduction of dimensionless quantities and discretization we get

$$\boldsymbol{Q}(t+\Delta t) = \boldsymbol{Q}(t) + \Delta t[\boldsymbol{\kappa}(t)\cdot\boldsymbol{Q}(t) - \frac{1}{2}\boldsymbol{\mu}\cdot\boldsymbol{Q}(t) + \frac{1}{2}\frac{\partial}{\partial\boldsymbol{Q}}\cdot\boldsymbol{\mu}] + \sqrt{\Delta t}\,\boldsymbol{B}\cdot\boldsymbol{f}(t)\ . \quad (5.19)$$

We can see immediately that the general simulation algorithm described for the Hookean dumbbell model also works for this more complicated model if one takes into account the following modifications. The anisotropic tensor $\boldsymbol{\mu}$ appearing in the discretized Langevin equation is configuration dependent and therefore depends on the actual value of the stochastic variable $\boldsymbol{Q}(t)$. So this quantity is not fixed throughout the simulation as in the Hookean dumbbell model where it was simply the unit tensor but time dependent. Therefore it has to be calculated anew in each time step. The same is true for the additional drift term in the Langevin equation and for the matrix $\boldsymbol{B}$ which is defined by $\boldsymbol{B}\cdot\boldsymbol{B}^T = \boldsymbol{\mu}$. The calculation of $\boldsymbol{B}$ is straightforward since the elements of $\boldsymbol{B}$ can be given analytically in terms of the elements of $\boldsymbol{\mu}$.

5.2.4 The algorithm for the chain model with anisotropic mobility

For the chain model with anisotropic mobility tensors one has to modify the computer program for the Rouse chain. Again the mobility tensors which now appear in the supermatrix $\hat{\boldsymbol{A}}$ depend on the actual values of the stochastic variables so that they have to be calculated anew in each time step. Also the elements of the supermatrix $\hat{\boldsymbol{B}}$ have to be calculated anew

in each time step from the equation $\hat{\boldsymbol{B}} \cdot \hat{\boldsymbol{B}}^T = \frac{1}{2}\hat{\boldsymbol{A}}$. This can be done with the so-called Cholesky decomposition algorithm. The additional calculations that become necessary in each time step increase the computation time significantly. Even for a chain with only ten beads a supercomputer like the CRAY2 needs about one hour of CPU time for one single run.

For a suitablly chosen ansatz for the anisotropic mobility all qualitative predictions of the models are in full agreement with experimental findings. In particular, shear rate dependent material functions, including a nonvanishing second normal stress, with an overshoot in their time dependence for high shear rates, are found. The results are described and analysed in great detail in Ref. [32] for the dumbbell model and in Ref. [33] for the chain model.

5.3 The simulation of Master equations

5.3.1 The general algorithm for network models

In this section we will give the details of a computer simulation of the convection equation that arises in network theories of polymer melts. This serves as an example for a program for other more general Master equations. As in the simulation of the Langevin equations in the last section one follows the stochastic motion of particles in small time steps. Typical for a process described by a Master equation is that the small time behaviour is characterized by jumps between different states. In our concrete example network strands can be generated or destroyed in a small time step. The probabilities for these events depend on the creation and loss rates. Fixing the equilibrium distribution to be Gaussian, the single loss rate function h specifies the whole stochastic process, as explained in the last chapter. We do not want to specify the functional form of this function here but we have in mind the particularly interesting situation that h depends on the actual configuration $\boldsymbol{Q}$ of a strand. In addition to the stochastic jumping from the equilibrium generation reservoir to existence and from existence to death we also have the deterministic change of the configuration of strands due to the flow that has to be taken into account in each time step. All these effects are now simulated for a large ensemble of network strands. The first step is again the introduction of

dimensionless quantities. As in the last section the energy scale is kT, the length scale is $\sqrt{kT/H}$, and the time scale λ is taken from the definition of the loss rate function h. Then the simulation proceeds as indicated in the following flow diagram:

S1: Generate the Gaussian equilibrium ensemble consisting of M strands at time zero. This ensemble is followed in the simulation and a copy of it serves as the ensemble from which strands are generated.

S2: For each strand in the actual ensemble calculate the new configuration vector after a small time step: $\boldsymbol{Q}(t+\Delta t) = \boldsymbol{Q}(t) + \Delta t\, \boldsymbol{\kappa}(t) \cdot \boldsymbol{Q}(t)$.

S3: For each strand in the actual ensemble calculate the configuration dependent probability $h' = 1 - \exp[-h(\boldsymbol{Q}(t))\Delta t]$ that the strand is destroyed in the time step Δt. Remove strands from the actual ensemble according to the calculated probabilities.

S4: For each strand in the Gaussian generation ensemble calculate the configuration dependent probability h' that the strand is created in the time step Δt. Bring strands into the ensemble according to the calculated probabilities.

S5: If you are interested in measuring the stress tensor at the present time, then evaluate the corresponding average over the actual ensemble and its statistical error according to the rules in the last section, otherwise proceed to S6.

S6: If the time has not reached the final time, then go back to S2.

Also in this simulation the results depend on the time step chosen. In general one can show that with decreasing time step the results tend to the exact values. More quantitative details on this problem can be found in Ref. [57].

The main difference from the simulation of the Hookean dumbbell model in the last chapter is that the change of the configuration vector is much easier because it is only deterministic but that now one has the additional possibility that strands are generated or destroyed in a time step. Therefore the number of particles in the ensemble may not be constant but time dependent. This is the reason for simulating the whole ensemble over

successive time steps instead of generating single realizations one after the other as in the simulations of the last chapter.

Let us briefly discuss different network models classified by the function h. The Lodge model where the function h is constant is simple enough to be solved analytically. In a similar way as the Hookean dumbbell model was helpful for a test of the computer program of Langevin equations the Lodge model serves as a check for the algorithm for network models. In analytical theories one generalizes the Lodge model by the assumption that the rate h depends on some averaged quantities, such as the mean-square equilibrium length. However, physically it is much more plausible to assume that h depends on the configuration of each single strand. For example, one can imagine that longer strands will break more easily than shorter ones. Such a theory with configuration dependent rates is not analytically solvable any more but it is very easy to modify the program for the Lodge model in order to solve it numerically. From symmetry arguments one argues that the loss rate should be a function of Q^2. So the simplest ansatz for a model with configuration dependent rates is

$$h = \frac{1}{\lambda}(1 + \epsilon \frac{HQ^2}{kT}) \,. \tag{5.20}$$

Here ϵ is a positive dimensionless parameter characterizing the strength of the configuration dependence. For $\epsilon = 0$ one reobtains the Lodge model. The qualitative predictions of the model turn out to be very satisfactory for both the shear rate dependence and the time dependence of the material functions. In particular, it turns out that the nonvanishing second normal stress difference can be directly traced back to the configuration dependence of the loss rate function. A more detailed description of the results can be found in Ref. [45].

5.3.2 The continuous time algorithm for network models

The simulation algorithm presented above works for the most general network models. In special cases a much more efficient method is possible which avoids the introduction of time steps [58]. It is therefore called continuous time simulation. What is the central idea behind this alternative algorithm? Instead of testing at each time step whether strands enter or leave the actual ensemble, one determines beforehand how long a single

strand lives in the ensemble. The lifetime τ is a stochastic quantity and so we have to determine the whole probability distribution function of lifetimes.

Let us assume a strand to be generated at time t_0 out of the Gaussian distribution with configuration $\boldsymbol{Q}_0$. The probability that this strand is still in the ensemble at time t is given by

$$P(t;t_0) \equiv \exp\left[-I(t;t_0)\right] = \exp\left[-\int_{t_0}^{t} ds\ h(\boldsymbol{Q}(s))\right] \quad . \tag{5.21}$$

For time-independent loss rates this reduces to an equation which is well-known, for instance in the connection with radioactive decay processes. The above formula is then the obvious generalization to time-dependent loss rates. The time-dependent configuration vector appearing in the above equation obeys the differential equation $\dot{\boldsymbol{Q}} = \boldsymbol{\kappa} \cdot \boldsymbol{Q}$ with the additional initial condition $\boldsymbol{Q}(t_0) = \boldsymbol{Q}_0$. For sufficiently simple flows, such as the inception of steady shear flow, this differential equation can be analytically solved leading to

$$\boldsymbol{Q}(t) = \begin{pmatrix} Q_{0x} + \dot{\gamma} f(t;t_0) Q_{0y} \\ Q_{0y} \\ Q_{0z} \end{pmatrix} \quad , \tag{5.22}$$

with

$$f(t;t_0) = \begin{cases} 0 & , \text{if } t_0 \le t \le 0 \\ t & , \text{if } t_0 \le 0 \text{ and } t \ge 0 \\ t - t_0 & , \text{if } 0 \le t_0 \le t \end{cases} \quad . \tag{5.23}$$

Note that $P(t;t_0)$ is identical to the probability that the lifetime τ of the strand is at least $t - t_0$. We want to know the probability $p(\tau;t_0)\,d\tau$ that the lifetime is between τ and $\tau + d\tau$. So the strand lives up to the time $t_0 + \tau$ but not to time $t_0 + \tau + d\tau$. It follows that

$$p(\tau;t_0) = -\dot{P}(t;t_0)\big|_{t=t_0+\tau} = h\big(\boldsymbol{Q}(t_0+\tau)\big) P(t_0+\tau;t_0) \quad . \tag{5.24}$$

We have now obtained the desired probability distribution function from which the lifetime of the strand will be chosen randomly during the simulation. It is interesting to see that this quantity not only depends on the time t_0 when the strands under study entered the ensemble but through $I(t;t_0)$ and h on all configurations $\boldsymbol{Q}$ from time t_0 up to the time $t_0 + \tau$ and thus on $\boldsymbol{Q}_0$ and the shear rate.

The main steps in the continuous time simulation are then the following:

S1: Define a series of measurement times at which you like to measure the stress tensor.

S2: Choose a random time t_0 equally distributed in an appropriately chosen time interval. The time t_0 represents the time at which the new strand enters the ensemble.

S3: Choose a random vector $\boldsymbol{Q}_0$ from the equilibrium ensemble. This is the initial configuration of the new strand.

S4: Choose a lifetime τ randomly from the correct probability distribution $p(\tau; t_0)$. Thus the strand will live from time t_0 until time $t_0 + \tau$.

S5: Calculate the configuration $\boldsymbol{Q}(t)$ at those measurement times where the strand exists. From this determine the contribution to the interesting quantities at these times and add these contributions to those obtained for the earlier strands. Do the same for the squares of the interesting quantities. Update the number of contributing strands at the measurement times where the strand lives.

S6: If the number of simulated strands has not reached a prescribed value M, then repeat the simulation steps S2-S5, otherwise proceed to S7.

S7: Evaluate the interesting quantities and their statistical errors as ensemble averages at the chosen measurement times.

Let us make some remark on the above program. As the number of strands that enter the ensemble with the given configuration $\boldsymbol{Q}_0$ is proportional to the rate $h(\boldsymbol{Q}_0)$, one can think that instead of one strand $h(\boldsymbol{Q}_0)$ strands enter the ensemble. This is the easiest way to take the configuration dependent generation rate into consideration in the simulation. So in step S5 instead of one we add $h(\boldsymbol{Q}_0)$ when counting the number of contributing strands and for the same reason also the contributions to the measured quantities are weighted with the same factor before adding them to earlier contributions. The determination of the random lifetimes τ in step S4 is the central point in the simulation. These are drawn randomly from the distribution $p(\tau; t_0)$ with the inversion method described in section 5.1. For our problem at hand this strategy leads to the equation

$$I(\tau + t_0; t_0) + \ln(x_n) = 0 \tag{5.25}$$

with a random number x_n equally distributed in the unit interval. This equation has to be solved for τ. For simple models like that where the function h quadratically increases with $\boldsymbol{Q}^2$ this can be done analytically. In more complicated situations a numerical determination of τ is straightforward.

Note the main differences to the general algorithm introduced above. In the continuous time simulation it is possible to follow the evolution of single strands one after the other. More important is the fact, that no discrete time steps are introduced and so one does not have errors due to time discretization. Furthermore, there are no time consuming tests at each time step whether strands are created or destroyed. So the continuous time algorithm is much more efficient. Its only disadvantage is that it only works in special cases. First, the differential equation for the deterministic motion of the strand must have an analytical solution. However, this is true for homogeneous flows that are usually studied. More stringent is the necessary condition that the probability distribution of lifetimes must be calculated beforehand analytically. This is only possible in cases where the functional form of the loss rate function h, as well as of the flow field, are very simple.

5.3.3 The continuous time algorithm for the Doi-Edwards model

At the end of this long chapter let us mention another interesting application of the continuous time simulation, namely the simulation of the Doi-Edwards model. In the last chapter the stochastic picture that underlies the Doi-Edwards model was explained. One has a vector $\boldsymbol{U}$ obeying the deterministic equation of motion $\dot{\boldsymbol{U}} = \boldsymbol{\kappa} \cdot \boldsymbol{U} - \boldsymbol{\kappa} : \boldsymbol{UUU}$ and a stochastic quantity S controlled by a Wiener process with reflecting boundaries. Each time the variable S reaches one of its boundaries the vector $\boldsymbol{U}$ has to be chosen new as a random unit vector. We note the similarity to the network model: we again have a configuration vector that has a specific lifetime during which it is changed deterministically by the flow field. The lifetime of the vector is now controlled by a Wiener process. One could have the idea to simulate this Wiener process with the simulation algorithm introduced for Langevin equations in order to determine the times

when the stochastic quantity S reaches one of its boundaries. This is indeed possible and has been done in Ref.[24]. However, it is not necessary to simulate the process S explicitly because for the determination of the stress tensor at time t only the value of the process $\boldsymbol{U}(t)$ has to be known while the value of the process $S(t)$ is irrelevant. Moreover, the Wiener process with reflecting boundaries is simple enough to calculate all necessary quantities analytically. Therefore a much more elegant way is the direct application of the continuous time simulation approach.

Suppose that one wants to measure the stress tensor at time t. For technical reasons it is easier in the following to work with birth times instead of lifetimes. For a vector $\boldsymbol{U}(t)$ that exists at time t, the process S controls the stochastic birth time t' when this vector was created with random orientation. Now let $\mu(t-t')dt'$ be the probability that this birth time is between t' and $t'+dt'$. This is equivalent to the probability that, given the value $S(t)$ at time t, the last reflection at a boundary occurred between times t' and $t'+dt'$. The analytical expression for $\mu(t-t')$ can be found in the works of Doi and Edwards and is given by [23]

$$\mu(t-t') = \sum_{p \ odd} \frac{8}{\pi^2 T_d} \exp\left(-\frac{p^2(t-t')}{T_d}\right) \quad , \tag{5.26}$$

where T_d is called the disengagement time. So the quantity $\mu(t-t')$ can directly be interpreted as a probability distribution for the stochastic variable t'. The continuous time simulation for the Doi-Edwards model then runs as follows:

S1: Choose a random time t' from the probability distribution $\mu(t-t')$. The time t' is the time when the process $S(t)$ reached one of the boundaries the last time before t and hence when the vector $\boldsymbol{U}(t)$ was born with random orientation.

S2: Choose a random orientation over the unit sphere. This defines the vector $\boldsymbol{U}(t')$.

S3: Calculate the orientation $\boldsymbol{U}(t)$ of the vector at the present time t with the analytical solution of the differential equation of motion.

S4: Calculate the contribution of this vector to the stress tensor and add this contribution to those obtained for the earlier realizations. Do the same for the squares of the measured quantities.

S5: If the number of simulated realizations has not reached a prescribed value M, then repeat the simulation steps S1-S4, otherwise proceed to S6.

S6: Evaluate the interesting quantities and their statistical errors as ensemble averages at the chosen measurement times.

Note that in order to allow a continuous time simulation the nonlinear deterministic equation of motion of the vector $\boldsymbol{U}$ must be solvable analytically. To this end the flow tensor $\boldsymbol{\kappa}$ has to be simple enough.

More details on the algorithm and the comparison of the obtained results with those of other numerical approaches can be found in Ref. [59].

5.4 The simulation of semi-Markov processes

In this section of the chapter we are going to describe a simulation algorithm for the semi-Markov process which was introduced in the last chapter and which is briefly recapitulated here. The model for the polymer is a Kramers chain with N beads that make elementary jump motions of the Orwoll Stockmayer type. Up to now the model only treats the equilibrium case so that the chain remains motionless inbetween jumps. Each bead jumps according to the waiting time distribution

$$\psi(t) = \frac{\beta}{(1+t)^{\beta+1}} , \tag{5.27}$$

with a free adjustable parameter $\beta > 1$. The slowly decaying function ψ has no higher moments than the first which makes the model non-Markovian, in contrast to the original Orwoll-Stockmayer model for which the waiting time distribution is exponential.

Since the waiting time distribution is given analytically and the deterministic motion inbetween jumps is trivial one can use the continuous time simulation approach introduced in the last section. As before, we simulate one chain at a time. A sufficient number of chains are simulated to obtain the desired statistics, and the results of all chains are averaged. All units of length are normalized by the rod-length a, and time is already made dimensionless through the expression for $\psi(t)$. At the beginning of the simulation one has to define initial values of the bead jump times. One

can show [49] that these have to be drawn from the distribution function $P(t)$ given by

$$P(t) = \frac{\beta - 1}{(1+t)^{\beta}} \ . \tag{5.28}$$

This can easily be done with the method of inversion. The jump order is then found from the selected jump times, and stored in a table. The table is ordered only once at the beginning of the simulation and then updated throughout. Thus, the next bead to jump is always given by the first entry in the table. During the simulation new jump times are always drawn randomly from the distribution ψ which is again done using the inversion method.

For the equilibrium situation considered here it is interesting to study the diffusive behaviour of the center-of-mass and the autocorrelation of the end-to-end vector.

The simulation thus proceeds in the following steps:

S1: Define the times at which you like to measure the interesting quantities.

S2: Choose the initial configuration of the chain from a random walk of unit step length. Calculate the initial end-to-end vector and set the initial center-of-mass position arbitrarily to $\mathbf{0}$. Draw initial values of the bead jump times from the distribution function $P(t)$ and build the jump table.

S3: The length of the current time step is given by the jump time of the bead in the first entry of the jump table. Advance the simulation time counter by this time step.

S4: If the simulation time counter has advanced past some of the measurement times, then add the interesting quantities (and their squares) at these times to those of the previous chains, else go to S5.

S5: Change the configuration. Calculate the new center-of-mass position, and the new end-to-end vector (if an end bead jumps).

S6: Decrease all jump times by the current time step, select a new jump time for the bead that just jumped, and update the jumping order table.

S7: If the time has not reached the desired final time, then go back to S3, otherwise proceed to S8.

S8: If the number of simulated chains has not reached a prescribed value M, then repeat the simulation steps S2-S7, otherwise proceed to S9.

S9: Evaluate the interesting quantities and their statistical errors as ensemble averages at the chosen measurement times.

To check the entire simulation, $\psi(t)$ can be replaced by the (dimensionless) exponential form $\psi_{OS}(t) = exp(-t)$ to make the model Markovian, and the simulation results compared with the analytic results for the Orwoll-Stockmayer model.

The results of the model are very interesting. One finds that the model predicts non-Fickian diffusion in an intermediate time region ($\langle r_c(t)^2 \rangle \sim t^\alpha$ with α dependent on β), in agreement with experimental data. For longer times the diffusion is Fickian and scales with the chain length N as $N^{1-2/\alpha}$, where α is a function of β. For example, for $\beta = 1.3$ one finds for the diffusion coefficient $D \sim N^{-2.28}$. The autocorrelation of the end-to-end vector of the chain has a stretched exponential form ($\exp[-(t/\tau)^\gamma]$, with γ a function of β and N) with a time constant τ that scales as $N^{3.3}$ for $\beta = 1.3$. A thorough discussion of the predictions can be found in Ref. [49]. For the future it is planned to generalize the model to investigate also non-equilibrium conditions.

5.5 Conclusions

At the end of this long chapter on stochastic simulation algorithms for the investigation of models for polymer melts let us remark that we only have described some aspects of the field. For instance, we have not at all considered the important Monte-Carlo calculations on a lattice. Let us briefly summarize the main results.

- Typically only oversimplified models can be solved analytically and more realistic models have to be treated numerically.
- Instead of solving the partial differential equations (*e.g.*, Fokker-Planck equation, convection equation) numerically, it is preferable to simulate directly the stochastic dynamics underlying these equations.

- Very often the programs for the realistic models do not differ much from those of the simple models with analytical solutions. So the known solutions of the simple models serve as a check of the computer programs.
- The simulation of the stochastic process is straightforward: generally one follows the evolution in small time steps to get one realization. The results follow as averages over many such realizations.
- A careful error analysis is necessary: one has statistical errors and errors due to time discretization (the latter vanish in continuous time simulations).
- A more and more detailed model building (and thus a better understanding of the system) is only limited by the necessary amount of computer time.

The author hopes to have shown that simulation methods are a very powerful and valuable (and perhaps the most promising) tool to study such complex dynamical systems as polymer melts.

Bibliography

[1] C.W. Gardiner, *Handbook of Stochastic Methods*, (Springer-Verlag, New York 1985).

[2] J. Honerkamp, *Stochastische Dynamische Systeme*, (VCH-Verlag Weinheim 1990).

[3] N.G. van Kampen, *Stochastic Processes in Physics and Chemistry*, (North-Holland, Amsterdam 1985).

[4] R.B. Bird, R.C. Armstrong and O. Hassager, *Dynamics of Polymeric Liquids, Vol.1 Fluid Mechanics*, (Wiley, New York 1977).

[5] W. H. Press, B. F. Flannery, S. A. Teukolsky, and W. T. Vetterling, *Numerical Recipes* (Cambridge University, Cambridge, 1986).

[6] J.D. Ferry, *Viscoelastic properties of Polymers*, (Wiley, New York 1980).

[7] H. M. Laun, Rheol. Acta **17** (1978) 1.

[8] M. H. Wagner, Rheol. Acta **18** (1979) 33.

[9] S.F. Gull and J. Skilling, IEE Proc. **131** (1984) 646.

[10] A.K. Livesey, P. Licinio and M. Delaye, J. Chem. Phys. **84** (1986) 5102.

[11] A.K. Louis, *Inverse und schlecht gestellte Probleme*, (Teubner Studienbücher, Stuttgart 1989).

[12] A.N. Tikhonov and V.Y. Arsenin, *Solutions of ill- posed problems*, (Wiley, New York 1977).

[13] C.W. Groetsch, *The theory of Tikhonov regularization for Fredholm equations of the first kind*, (Pitman, Boston 1984) .

[14] L. Delves and J. Walsh, *Numerical Solution of Integral Equations*, (Clarendon Press, Oxford 1974).

[15] J. Honerkamp and J. Weese, Macromol. **22** (1989) 4372-4377.

[16] J. Honerkamp and J. Weese, Cont.Mech.and Therm. **2** (1990) 17-30.

[17] C. Elster and J. Honerkamp, *A modified maximum entropy method and its application to creep data*, Freiburg preprint 1990.

[18] P. E. Rouse,jr., J. Chem. Phys. **21** (1953) 1272.

[19] P. G. de Gennes, J. Chem. Phys. **55** (1971) 572.

[20] P. G. de Gennes, *Scaling Concepts in Polymer Physics* (Cornell University Press, Ithaca, 1979).

[21] M. Doi and S. F. Edwards, *The Theory of Polymer Dynamics* (Clarendon Press, Oxford 1986).

[22] M. Doi and S. F. Edwards, *The Theory of Polymer Dynamics* (Clarendon Press, Oxford 1986).

[23] M. Doi and S. F. Edwards, J. Chem. Soc. Faraday Trans. 2 **74** (1978) 1789; **75** (1978) 381.

[24] H. C. Öttinger, J. Chem. Phys. **91** (1989) 6455.

[25] R. B. Bird,C. F. Curtiss,R. C. Armstrong,and O. Hassager, *Dynamics of Polymeric Liquids, Volume 2, Kinetic Theory*, 2nd ed. (Wiley, New York, 1987).

[26] L. G. Baxandall, J. Chem. Phys. **87** (1987) 2297.

[27] R. B. Bird and J. R. De Aguiar, Journal Non-Newtonian Fluid Mech. **13** (1983) 149.

[28] X. J. Fan, Journal Non-Newtonian Fluid Mech. **17** (1985) 251.

[29] V. S. Volkov and G. V. Vinogradov, Rheol. Acta **23** (1984) 231.

[30] H. Giesekus, Journal Non-Newtonian Fluid Mech. **11** (1982) 69.

[31] H. Giesekus, Journal Non-Newtonian Fluid Mech. **17** (1985) 349.

[32] P. Biller and F. Petruccione, J. Chem. Phys. **89** (1988) 2412.

[33] P. Biller, Continuum Mech. Thermodyn. **1** (1989) 53.

[34] A. S. Lodge,Proceedings of the VIIth International Congress of Rheology, Chalmers University of Technology, Gothenburg, Sweden, edited by C. Klason and J. Kubat, 1976, p.79.

[35] M. S. Green and A.V. Tobolsky, J. Chem. Phys. **14** (1946) 89.

[36] N. Phan-Thien and R. I. Tanner, J. Non-Newtonian Fluid Mech. **2** (1977) 353.

[37] N. Phan-Thien , J. Rheology **22** (1978) 259.

[38] R. I. Tanner, J. Non-Newtonian Fluid Mech. **5** (1979) 103.

[39] R.G. Larson, *Constitutive Equations for Polymer Melts and Solutions* (Butherworths, Boston, 1988).

[40] M. Yamamoto, J. Phys. Soc. Jpn. **11** (1956) 413.

[41] M. Yamamoto, J. Phys. Soc. Jpn. **12** (1957) 1148.

[42] M. Yamamoto, J. Phys. Soc. Jpn. **13** (1958) 1200.

[43] F. W. Wiegel, Physica **42** (1969) 156.

[44] F. W. Wiegel and F. Th. De Bats, Physica **43** (1969) 33.

[45] F. Petruccione and P. Biller, J. Chem. Phys. **85** (1988) 577.

[46] F. Petruccione and P. Biller, Rheol. Acta **27** (1988) 559.

[47] F. Petruccione, Continuum Mech. Thermodyn. **1** (1989) 97.

[48] R. A. Orwoll and W. H. Stockmayer, Adv. Chem. Phys. **15** (1969) 305.

[49] J. D. Schieber, P. Biller, and F. Petruccione, *A new model for polymer melts and concentrated solutions*, to appear in J. Chem. Phys.

[50] J. D. Schieber, F. Petruccione, and P. Biller, *A new model for polymer melts and concentrated solutions II. Excluded volume effects*, (preprint, Freiburg,1990).

[51] M. F. Shlesinger, Ann. Rev. Phys. Chem. **39** (1988) 269.

[52] H. Giesekus, Rheol. Acta **5** (1966) 29.

[53] D.E. Knuth, *The art of computer programming, Vol. 2*, (Addison-Wesley, Reading, Mass., 1969).

[54] A. Greiner, W. Strittmatter, and J. Honerkamp, J. Stat. Phys. **51** (1988) 95.

[55] M. Bishop and S. Frinks, J. Chem. Phys. **87** (1987) 3675.

[56] P. Biller, F. Petruccione, J. Honerkamp, and H.C. Öttinger, J. Non-Newtonian Fluid Mech. **22** (1987) 309.

[57] D. Bedeaux, K. Latakos-Lindenberg, and K. Shuler, J. Math. Phys. **12** (1971) 2116.

[58] P. Biller and F. Petruccione, J. Chem. Phys. **92** (1990) 6327.

[59] F. Petruccione und P. Biller, J. Chem. Phys. **92** (1990) 6332.

ISTITUTO ITALIANO PER GLI STUDI FILOSOFICI

SEMINARI E CONVEGNI DI SCIENZE
E DI STORIA DELLE SCIENZE

SEMINARI

EMILIO SEGRÉ, premio Nobel per la Fisica: « Metodi e problemi della fisica di oggi »; ILYA PRIGOGINE dell'Università di Bruxelles, premio Nobel per la Chimica: « Filosofia e Scienza »; « Tempo, entropia, evoluzione »; ALFONSO MARIA LIQUORI dell'Università di Roma: « 'Ordine', 'simmetria' e 'organizzazione': categorie diverse nello studio della struttura e dell'evoluzione dei sistemi naturali »; CARL HENRY OPPENHEIMER della University of Texas: « Ecologia e conoscenza del mondo »; JACQUES ROGER dell'Università della Sorbona: « Morfologia ed evoluzione » (in collaborazione con l'Istituto di Fisica della Facoltà di Scienze dell'Università di Napoli); HIROOMI UMEZAWA della University of Alberta: « Il concetto di unificazione nella fisica »; CHARLES C. GILLISPIE dell'Università di Princeton: « I fratelli Montgolfier e l'invenzione dell'aviazione: apparenza e realtà » (in collaborazione con l'Istituto di Fisica Teorica dell'Università di Napoli); PIERRE COSTABEL dell'Ecole de Hautes Etudes en Sciences Sociales: « L'esperimento cruciale nella scienza classica » (in collaborazione con l'Osservatorio Astronomico di Capodimonte); PIETRO OMODEO dell'Università di Padova: « Idee per una teoria del vivente »; PETER G. BERGMANN della New York University: « Albert Einstein e la teoria della relatività: I - La mia collaborazione con Albert Einstein; II - La teoria della relatività di Einstein oggi »; N. MUKUNDA dell'Indian Institute of Science di Bangalore: « Il ruolo della matematica nella fisica contemporanea »; DINO DINELLI: « Ricerca e società »; ALFONSO MARIA LIQUORI dell'Università di Roma: « L'evoluzione molecolare »; ALFONSO MARIA LIQUORI dell'Università di Roma: « Evoluzione prebiotica ed evoluzione biologica: le origini chimiche della vita: I - La struttura primaria dei geni e delle proteine; II - Trascrizione, traduzione chimica e stereo-

chimica di un gene in una proteina; III - Le proteine come « molecole cristallo »; IV - Proteine omologhe e proteine analoghe »; ELENA GAGLIASSO, MASSIMO STANZIONE, ALFONSO MARIA LIQUORI e VITTORIO SOMENZI: « Evoluzione e modelli: il concetto di adattamento nelle teorie dei sistemi biologici, culturali ed artificiali »; CESARE MUSATTI dell'Università di Milano: « Introduzione alla lettura dell'opera di Sigmund Freud: I - La fondazione della psicoanalisi; II - La dottrina degli istinti; III - La metapsicologia e la struttura dell'apparato psichico; IV - Psicologia dell'arte e psicologia sociale »; ALBERTO MONROY dell'Università di Palermo: « Origine ed evoluzione della sessualità negli animali »; MARCELLO PERA: « I pericoli della scienza senza fondamento »; KARL R. POPPER: « La scienza e i suoi nemici »; E.C.G. SUDARSHAN del Center for Particles Theory, University of Texas at Austin: « Unità e unificazione nella fisica »; « La geometrizzazione della fisica »; ALBERTO MONROY dell'Università di Palermo: « Orizzonti della biologia »; ABHAY ASHTEKAR dell'Institute Henri Poincaré, Syracuse University: « From General Relativity to Quantum Gravity: I - Quantum Gravity: What and Why; Canonical Quantization; II - Achievements; Canonical Quantization: Problems; III - Asymptotic Quantization and Applications; IV - Back to Canonical Methods via Self-Duality »; PETER G. BERGMANN della New York University: « Classical Aspects of General Relativity and the Kaluza-Klein Theory: I - General Relativity and Hamiltonian Formalism; II - Einstein-Infeld-Hoffmann Theory; III - Unitary Field Theory: Weyl; IV - Unitary Field Theory: Kaluza-Klein; Experiments and Observations »; RITA LEVI MONTALCINI, premio Nobel per la Medicina: « Aspetti evolutivi del sistema nervoso: I - Principi evolutivi del sistema nervoso; II - Processi cognitivi nei due emisferi cerebrali dell'*homo sapiens*; III - Nuove frontiere nella neurobiologia »; STEVEN WEINBERG dell'University of Texas at Austin, premio Nobel per la Fisica: « The Role of Beauty in Physics »; JOHN ARCHIBALD WHEELER del Center for Theoretical Physics, University of Texas at Austin: « Foundation Problems in Physics: I - Bohr's Elementary Quantum Phenomenon; From 'Complementarity' and 'Distinguishability' to the Probability Amplitudes of Quantum Theory; II -

From Quantum Phase to Physical Fields; III - The Vanishing of the Boundary of a Boundary as Foundation Principle of Field Theory; IV - 'Physics' and 'Meaning' »; CESARE MUSATTI dell'Università di Milano: « Scienza e mito: una inversione di tendenza » (in collaborazione con la Stazione Zoologica di Napoli); VINCENZO CAPPELLETTI dell'Università di Roma: « Un mito per la scienza » (in collaborazione con la Stazione Zoologica di Napoli); MASSIMO PIATTELLI PALMARINI, Direttore del Centro fiorentino di storia e filosofia della scienza: « Verità e plausibilità » (in collaborazione con la Stazione Zoologica di Napoli); SARA BISEL: « Nuove scoperte antropologiche a Ercolano » (in collaborazione con la Stazione Zoologica di Napoli); RENATO GUTTUSO: « Leonardo: l'armonia del sapere » (in collaborazione con la Stazione Zoologica di Napoli); SERGIO FUBINI del CERN di Ginevra: « Da Democrito ai quark »; MARIA LUISA ALTIERI BIAGI dell'Università di Bologna: « Letteratura e lingua scientifica dopo Galileo » (in collaborazione con la Stazione Zoologica di Napoli); CARLO BERNARDINI dell'Università di Roma: « Rigore scientifico e qualità letteraria » (in collaborazione con la Stazione Zoologica di Napoli); ENZO TIEZZI dell'Università di Siena: « Tempi storici, tempi biologici » (in collaborazione con il Dipartimento di Chimica dell'Università di Napoli); VITTORIO DE ALFARO dell'Università di Torino: « Le forze nella natura e la loro unità »; ROBERTO FIESCHI: « Scienziati e armamenti » (in collaborazione con la Stazione Zoologica di Napoli); MARCELLO PERA dell'Università di Pisa: « Prove e argomentazioni nella preferenza delle teorie scientifiche » (in collaborazione con la Stazione Zoologica di Napoli); MIRKO D. GRMEK dell'Ecole Pratique des Hautes Etudes: « Miti e realtà nella morte di Plinio » (in collaborazione con la Stazione Zoologica di Napoli); DAVIDE MARIA TUROLDO: « Le mani sulla vita » (in collaborazione con la Stazione Zoologica di Napoli); FRANCO BONAUDI del CERN di Ginevra: « Il CERN di Ginevra: il grande laboratorio europeo per lo studio della fisica delle particelle »; FORTUNATO TITO ARECCHI dell'Università di Firenze: « Dal caos all'ordine in fisica »; ENRICO BELLONE: « Scienza e modelli storiografici » (in collaborazione con la Stazione Zoologica di Napoli); CARLO RUB-

BIA, premio Nobel per la Fisica: « La trasformazione dell'energia in materia: l'alchimia dei tempi moderni? » (in collaborazione con il Dipartimento di Fisica dell'Università di Napoli); EDUARDO CAIANIELLO, GIORGIO CEVENINI, ANTONIO D'AURIA: « Intelligenza artificiale e formazione: I - La lunga via dell'intelligenza; II - Tecnologia e formazione; III - Intelligenza artificiale e strutture produttive » (in collaborazione con la rivista « Zadig »); AUGUSTO MARINONI: « Leonardo: una nuova immagine dell'artista-scienziato; I - La lingua di Leonardo; II - La matematica di Leonardo; III - Leonardo e la natura »; E.C.G. SUDARSHAN dell'Università di Madras e dell'University of Texas: « From Fermi Interactions to electroweak interactions; I - Early history of beta decay; II - From beta decay to weak interactions; III - The chiral V-A interactions; IV - Fundamental constituents and fundamental interactions; V - Electroweak interactions » (in collaborazione col Dipartimento di Fisica dell'Università di Napoli); ITALO SABELLI: « Agopuntura oggi »; ALDO CLEMENTI, FRANCESCO GUERRA, LUIGI PESTALOZZA, ALDO PICCIALLI, FAUSTO RAZZI, JEAN CLAUDE RISSET, CURTIS ROADS, JOHANN SUNDBERG e WALTER TORTORETO: « Musica e scienza: un rapporto conflittuale? » (in collaborazione con l'Associazione Informatica Musicale Italiana e con il Dipartimento di Fisica dell'Università di Napoli); BRUNO COPPI del Massachusetts Institute of Technology: « Recenti scoperte della fisica dello spazio e loro implicazioni filosofiche »; R.V. MALLYA dell'Imperial College of Science and Technologies di Londra: « Programmi ed esperienze di *management-science* »; VALENTINO L. TELEGDI dell'Institut für Hochenergiephysik, Zurigo: « La figura e l'opera di Roland Eötvös »; S. ZAPPACOSTA, J.J. VAN ROOD, M. SIMONSEN: « Nuove frontiere della biologia: il complesso maggiore d'istocompatibilità (MHC): I - Il complesso maggiore d'istocompatibilità al di là dell'istocompatibilità; II - The Relevance of the MHC in Biology and Medicine; III - Evolutionary Aspects of the MHC » (in collaborazione con il Dipartimento di Biologia e Patologia Cellulare e Molecolare « L. Califano » dell'Università di Napoli); VITTORIO G. VACCARO dell'Università di Napoli: « La ricerca e i suoi strumenti nella fisica delle particelle »; SHELDON L. GLASHOW, premio Nobel

per la Fisica: « La sfida della fisica delle particelle »; BRUNO ROSSI del Massachusetts Institute of Technology: « La scoperta del vento solare »; G. BARONE, G. DELLA GATTA, G. NEMETHY, F. LELJ: « Ruolo dell'acqua nelle interazioni fra molecole biologiche: I - Interazioni in soluzione acquose di amminoacidi, ammidi e peptidi modello; II - Entalpie di idratazione di ammini e uree; III - Modelli di idratazione negli studi conformazionali di peptidi; IV - Il ruolo del solvente nell'aggregazione di ammini e uree: simulazioni numeriche »; CHEN JING-HUA della Società di agopuntura tradizionale della Repubblica Popolare Cinese: « Il trattamento delle malattie respiratorie con l'agopuntura e le erbe cinesi »; HUMBERTO MATURANA: « Riflessioni sulla cognizione come fenomeno biologico »; PAOLO DE LUCA, DENNIS W. STEVENSON, JAMES E. MICKLE: « Attualità dello studio della Paleobotanica e dell'Etnobotanica » (in collaborazione con l'Orto Botanico di Napoli); GIORGIO BERNARDI del Laboratoire de génétique moléculaire - Institut Jacques Monod di Parigi: « Il caso e la necessità nell'evoluzione»; I.M. KHALATNIKOV e V. BELINSKI dell'Istituto Landau dell'Accademia delle Scienze dell'Unione Sovietica: « Inflationary cosmology »; PAOLA MANACORDA e ABBE MOWSHOWITZ: « Calcolatore e società: I - Lavorare quanto, lavorare come, lavorare per chi? II - L'organizzazione possibile: il futuro con la tecnologia dell'informazione » (in collaborazione con il Dipartimento di Informatica e Sistemistica dell'Università di Napoli); GIANFRANCO CIMMINO, ENNIO DE GIORGI, GIOVANNI PUGLIESE CARRATELLI, LUIGI A. RADICATI DI BROZOLO, CARLO SBORDONE, GIUSEPPE SCORZA DRAGONI, EDOARDO VESENTINI: « Il pensiero matematico del XX secolo e l'opera di Renato Caccioppoli » (in collaborazione con la Scuola Normale Superiore di Pisa); FRANCO RINALDI dell'Università di Napoli: « Recenti prospettive della ricerca in psichiatria » (in collaborazione con l'ADFAOF-AFASP Regione Campania); ALFONSO MARIA LIQUORI dell'Università di Roma: « Dalla biologia molecolare e teorica all'oncologia » (in collaborazione con l'Istituto Italiano per gli Studi Oncologici); ITALO SABELLI: « Esperienze di analgesia con agopuntura »; DAVID GROSS dell'Università di Princeton: « Teorie unificate di ogni genere »; MANFRED FINK dell'University of

Texas: « Elctron Scattering: I-Electron Scattering as a Contributor to Science and Technology; II - High Energy Electron Scattering Images of Atoms and Molecules; III - Low Energy Electron Scattering; IV - Spin Effects in Scattering World; V - Electron Beam Lithography »; FAUSTO MARCHI e ITALO SABELLI dell'Académie Médicale d'Acupuncture di Parigi: « La ricerca in agopuntura oggi »; GIUSEPPE CAGLIOTI, EDUARDO CAIANIELLO, ALFONSO MARIA LIQUORI, MICHELE EMMER: « Simmetria e asimmetria in natura » JEAN CLAUDE DARRAS, Presidente dell'Académie Médicale d'Acupuncture di Parigi: « L'agopuntura: sua pratica, sue indicazioni, suoi limiti »; CHEN JING-HUA della Società di agopuntura tradizionale della Repubblica Popolare Cinese: « Controlled trial of acupuncture for disabling breathlessness ». « Aspetti della fisica contemporanea: esperimenti sulle interazioni fondamentali », seminari in collaborazione col Dipartimento di Scienze Fisiche dell'Università di Napoli coordinati da Paolo Strolin: TIZIANO CAMPORESI del CERN, « Lo sviluppo della fisica sperimentale delle particelle elementari: l'interazione elettromagnetica; ANTONIO EREDITATO del CERN, « L'unificazione delle forse fondamentali: verifiche sperimentali dell'interazione elettrodebole »; FABRIZIO FABBRI dell'Istituto Nazionale di Fisica Nucleare, Bologna, « Esperimenti sulla struttura degli adroni: l'interazione forte »; EUGENIO COCCIA dell'Università di Roma « Tor Vergata », « L'interazione gravitazionale: aspetti sperimentali ».

NUOVE PROSPETTIVE NELLE TEORIE DEI QUANTI E DELLA RELATIVITÀ GENERALE

(in collaborazione con docenti e ricercatori delle Università italiane e con scienziati del CERN di Ginevra)

Napoli-Amalfi, 7-12 maggio 1984

Relazioni di: PAOLO BUDINICH, EDUARDO CAIANIELLO, VITTORIO DE ALFARO, TULLIO REGGE, L. VAN HOVE.

Con la partecipazione di: J. BELL, CERN, Ginevra; P. BUDINICH, SISSA, ICTP Trieste; R.E. MARSHAK, Virginia Polyt. Instit., Presidente della American Physical Society, USA; C. REBBI, Brookhaven National Laboratory, USA; T. REGGE, Università di Torino; E.C.G. SUDARSHAN, University of Texas, Austin, USA; L. VAN HOVE, CERN, Ginevra; B. ZUMINO, Lawrence Berkeley Laboratory, USA.

TEORIA GENERALE DELLE STRUTTURE

(in collaborazione con l'Accademia delle Scienze dell'U.R.S.S. e con il Consiglio Nazionale delle Ricerche)

Napoli, 18 ottobre-Amalfi, 19-21 ottobre 1984

Relazioni di: M.A. AIZERMAN, E. CAIANIELLO, G. DELLA RICCIA e C. TASSO.

Con la partecipazione di: A. ALESKEROV, F. DOROFEYUK, M. MARINARO, G. MUSSO, A. NEGRO, S. PIATNISKIJ, N. POSTIGLIONE, L. ROZONOER, G. SCARPETTA, I. SMIRNOVA, L. TENENBAUM, A. VENTRE, L. VOLSKIY.

PARTICLES AND GEOMETRY

(in collaborazione con il Center for Theoretical Physics, University of Texas at Austin)

Austin, 25 febbraio - 1 marzo 1985

Relazioni di: STEVEN WEINBERG, BRYCE DE WITT, JOSEPH POLCNINSKI, PHILIP CANDELAS, RICHARD MATZNER, WILL FISCHLER, MARC HENNEAUX, CECILE MORETTE-DE WITT, JOHN ARCHIBALD WHEELER.

IL MERIDIONE E LE SCIENZE (secoli XVI-XIX)

(in collaborazione con l'Università degli studi di Palermo e con l'Istituto Gramsci Siciliano)

Palermo 14-16 maggio 1985

Inaugurazione: IGNAZIO MELISENDA, Magnifico Rettore dell'Università di Palermo; FRANCESCO RENDA, Presidente dell'Istituto Gramsci Siciliano.

Relazioni di: PAOLO CASINI, MARCELLO CARAPEZZA, ANNA DELL'OREFICE, CARLO OLMO, GUIDO MASOTTO, ALBERTO MONROY, CHRISTINE GROEBEN, F. PAOLO CASTIGLIONE, FRANCO PALLADINO, FRANCO MARIA RAIMONDO, UGO BALDINI, CORRADO DOLLO, ROSARIO MOSCHEO, PIER DANIELE NAPOLITANI, JOSÉ ELIA, PAOLO RIGUTTI, SILVANA BARRECA, SALVATORE PEDONE, PIETRO OMODEO, FERDINANDO ABBRI, PINA CATALANOTTO, NICOLETTA MORELLO, VLADO ZORIC, EDOARDO BENVENUTO, GIUSEPPE BENTIVEGNA, UMBERTO BOTTAZZINI, PAOLO FREGUGLIA, SANTI VALENTI, CLARA GALLINI, PASQUALE ASSENNATO, GIUSEPPE CASARRUBEA, GIUSEPPE DATO, STEFANIA MISURACA, GIUSEPPE RESTIFO, LUCIO SARNO, GIOVANNI FIUME, GIUSEPPE SICHEL, SALVATORE DI PASQUALE, VALERIA BRUNAZZI, ANTONIETTA JOLE LIMA, AUGUSTO PLACANICA, ANTONINO BUTTITTA, SEBASTIANO DI FAZIO, JOLE GIGANTE, ELIO MANZI, GUGLIEMO BENFRATELLO, ANTONINO BE-

NIGNO, ORAZIO CANCILIA, ROSARIO LA DUCA, SALVATORE PEDONE, MARCELLO RENDA, CONCETTA RIZZO INSERRA, ROSARIO SPAMPINATO.

Tavola rotonda sul tema: *La scienza oggi nel meridione.* Con la partecipazione di: PAOLO ROSSI, CARLO CILIBERTO, IGNAZIO MELISENDA, PAOLO CAVALIERE, ERNESTO DRIOLI, GIUSEPPE GIARRIZZO, GIOVANNI GIUDICE.

ROLE OF DNA IN BRAIN ACTIVITY

(in collaborazione con il Consiglio Nazionale delle Ricerche, la International Society for Neurochemistry, l'Istituto Internazionale di Genetica e Biofisica, la Stazione Zoologica di Napoli e l'Università di Napoli)

Napoli-Ravello, 26-29 maggio 1985

Direzione scientifica: Prof. Antonio Giuditta
Istituto Internazionale di Genetica e Biofisica.

Relazioni di: A. GIUDITTA, H. HYDEN, W. E. HAHN, GREGOR J. SUTCLIFFE, EDWARD HERBER, I.R. BROWN, I. SERRA, A.M. GIUFFRIDA, G. BERNOCCHI, E. SCHERINI, C.C. KUENZLE, K. SUBBA RAO, P. MANDEL, V. MARES, S. REINIS, H. HYDEN, W.E. HAHN, B.B. KAPLAN, J.G. SUTCLIFFE, K.E. DAVIES, I. OBERLÉ, M.R. MORRISON, L. LIM, E.A. BARNARD, J. GIRAUDAT, H. SOREO, J. MALLET, D.K. BATTER, M.W. KILIMANN, L.J. DE GENNARO, E. HERBERT, J. ROBERTS, D. RICHTER, R.J. MILNER, I. GINZBURG, U.Z. LITTAUER, A.C. MAHON, R.H. SCHELLER.

QUANTUM FIELD THEORY

(in collaborazione con l'Università di Salerno, Dipartimento di Fisica Teorica e con l'Università di Alberta - Canada).

Napoli-Positano, 1-8 giugno 1985

Comitato scientifico: S. KAMEFUCHI, F. MANCINI, H. MATSUMOTO, N.Y. PAPASTAMATIOU.

Comitato organizzatore: Istituto Italiano per gli Studi Filosofici, S. DE FILIPPO, M. FUSCO-GIRARD, F. MANCINI, P. SODANO, G. VITIELLO.

Relatori: E. CAIANIELLO, W.J. MC DONALD, F. MANCINI, H.P. DÜRR, H. EZAWA, R.W. JACKIW, S. KAMEFUCHI, K. KIKKAWA, J.R. KLAUDER, J. LOPUSZANSKI, K. MAKI, H. MATSUMOTO, S. ONEDA, N. PAPASTAMATIOU, E.C.G. SUDARSHAN, M. SUZUKI, M. TACHIKI, Y. TAKAHASHI, M. WADATI, H. UMEZAWA.

Partecipanti ai lavori: A. AURILIA (Canada), F. BASSANI (Italia), A.Z. CAPRI (Canada), D. DE. FALCO (Italia), R. FERRARI (Italia), Y. FUJIMOTO (Giappone), G. JONA-LASINIO (Italia), M. KONUMA (Giappone), L. LEPLAE (Stati Uniti), M. MISRA (Belgio), T. MUTA (Giappone), Y. NAKANO (Italia), B. PREZIOSI (Italia), H. SCHIFF (Canada), G.M. SEMENOFF (Canada), V. SRINIVASAN (India), S. TANAKA (Giappone), Y. TOMOZAWA (Stati Uniti), K. YOSHIDA (Italia).

L'OPERA DI EINSTEIN. I - EINSTEIN E IL SUO TEMPO

(in collaborazione con: Istituto Gramsci Veneto,
Goethe Institut, Max-Planck-Institut,
Intercultural Society for Science and Art)

Venezia, 13-14 dicembre 1985

Relazioni di: UMBERTO CURI, JOHN STACHEL, FRANÇOISE BALIBAR, PAOLO BUDINICH, ENRICO BELLONE, FRIEDRICH CRAMER, PAOLO ZELLINI, DENNIS W. SCIAMA, WOLFANG KAEMPFER, JEAN-MARC LEVY-LEBLOND, GERT MATTENKLOTT, REMO BODEI, HEINZ D. KITTSTEINER, MASSIMO CACCIARI.

L'OPERA DI EINSTEIN. II - EINSTEIN E LA FISICA CONTEMPORANEA

(in collaborazione con: Istituto Gramsci Veneto, Dipartimento di Fisica dell'Università di Salerno, Goethe Institut, Max-Planck-Institut, Intercultural Society for Science and Art)

Napoli, 28 febbraio - 1 marzo 1986

Relazioni di: JOHN STACHEL, TULLIO REGGE, FRANCÇOISE BALIBAR, ENRICO BELLONE, ROBERT COHEN, DIETER WANDSCHNEIDER, EDUARDO CAIANIELLO, BRUNO BERTOTTI, JEAN-PIERRE VIGIER, PAOLO BUDINICH, JEAN-MARC LEVI LEBLOND, GIAN VITTORIO PALLOTTINO, DENNIS W. SCIAMA, REMO RUFFINI.

TEORIA UNIFICATA DELLA GRAVITAZIONE

3-7 marzo 1986

Relatori: TULLIO REGGE, PIETRO FRÉ, RICCARDO D'AURIA, JEANNETTE NELSON.

LEGGI DI SIMMETRIA E UNIFICAZIONE DELLE INTERAZIONI FONDAMENTALI

(in collaborazione con il Dipartimento di Fisica Nucleare, Struttura della Materia e Fisica Applicata dell'Università di Napoli)

Napoli, 15-18 aprile 1986

Relazioni di: VITTORIO SILVESTRINI, ADRIANO DI GIACOMO, VALENTINO L. TELEGDI, NICOLA CABIBBO, GUIDO ALTARELLI, UGO AMALDI, GIOVANNI BELLOTTI, LUIGI A. RADICATI DI BROZOLO.

PHYSICS OF COGNITIVE PROCESSES

(in collaborazione con: Istituto Internazionale di Alti Studi Scientifici - Università di Nijmegen - Dipartimento di Fisica Teorica dell'Università di Salerno - Centro Internacional de Fisica, Bogotà)

Napoli-Amalfi, 16-20 giugno 1986

Relazioni di: F.T. Arecchi (Italia), A. Borsellino (Italia), V. Braitenberg (R.F.G.), R. Busa (Italia), G. Gagliotti (Italia), A. Cools (Olanda), E. Hall (USA), H. Haken (R.F.G.), D. Hofstadter (USA), P. Johannesma (Olanda), T. Kohonen (Finlandia), F. Lauria (Italia), D. Mackay (Inghilterra), H. Maturana (Cile), L. Ricciardi (Italia).

ADVANCES OF PHASE TRANSITIONS AND DISORDER PHENOMENA

(in collaborazione col Dipartimento di Fisica Teorica dell'Università di Salerno)

Amalfi, 25-27 giugno 1986

Relazioni di: A. Aharony, K. Binder, A.J. Bray, J. Hertz, A. Coniglio, K. Walesek, D.I. Uzunov, S.W. Koch, C. Di Castro, C. Parisi, A. Zippelius, B. Preziosi, M. Suzuki, H. Matsumoto, H. Arimitsu, I.D. Lawrie.

FONDAMENTI DI INTELLIGENZA ARTIFICIALE

(Seminario internazionale di studi in collaborazione col Dipartimento di Informatica e Sistemistica dell'Università di Napoli, col Dipartimento di Scienze Relazionali e della Comunicazione dell'Università di Napoli e col Progetto Strategico di Intelligenza Artificiale dell'Istituto di Cibernetica - CNR Napoli)

Napoli - 1-5 settembre 1986

Fondamenti di intelligenza artificiale - Il sistema F.O.L. - Strutture cognitive - Rappresentazione della conoscenza - Open system - Sistemi in comunicazione con l'ambiente - Intentional logic - Ambienti multipli, punti di vista - Ambienti di programmazione e linguaggi per l'intelligenza artificiale.

Relazioni di: RICARD WALDINGER, HAROLD WERTZ, RICHARD WEYHRAUCH, YORICK WILKS.

COOPERAZIONE SCIENTIFICA TRA ITALIA, SPAGNA E FRANCIA NEL CAMPO DELLE TECNOLOGIE DELL'INFORMAZIONE: SITUAZIONE ATTUALE E PROGETTI FUTURI

(in collaborazione con l'Istituto di Cibernetica del C.N.R. di Napoli)

Napoli, 6-10 ottobre 1986

L'informatica teorica nello sviluppo delle tecnologie dell'informazione. Complessità, fattibilità e approssimazione. Linguaggi funzionali e logici. L'Intelligenza Artificiale: metodologia ed applicazione.

Interventi: ENRIC TRILLAS, JOSEPH AGUILAR-MARTIN, JAUME AUGUSTÌ, CLAUDI ALSINA, GIORGIO AUSIELLO, ANTONIO BARONE, NADAL BATLE, GIOVANNI CRISCUOLO, JOSÉ CUENA, MIGUEL DELGADO, ALDO DE LUCA, FRANCESC ESTEVA, RAMON LOPEZ DE MANTARAS, ANTONIO MACHÌ, ANTONIO MASSAROTTI, ALFONSO MIOLA, EUGEN NEIDL, DOMINIQUE PERRIN, JEAN FRANÇOIS PERROT, NURIA PIERA, ANTONIO RESTIVO, TERESA RIERA, TON SALES, SETTIMO TERMINI, LLORENC VALVERDE, AMPARO VILLA, HAROLD WERTZ.

RIEDUCARE IL CERVELLO

(in collaborazione con l'Istituto di Scienze Neurologiche dell'Università di Napoli)

Napoli, 23-24 ottobre 1986

Relazioni di: V. Bonavita, G. Gainotti, M.C. Silveri, M.E. Zanobio, R. Job, M.P. de Partz, S. Carlomagno, P. Montella, E. Magno Caldognetto, X. Seron, G. Miceli, D. Grossi, M. Vanderlinden, G. Vallar, F. Coyotte, E. De Renzi.

Interventi di: G.A. Buscaino, A. Basso.

CRYSTALS, GENES AND EVOLUTION
In honour of A.M. Liquori

(in collaborazione con l'Università degli Studi di Napoli)

Napoli, 3 novembre 1986

Relazioni di: A. Ballio, V. Crescenzi, M. Perutz.

Interventi di: D. De Masi, G. Toraldo di Francia.

CONVEGNO INTERNAZIONALE DI PATOLOGIA AMBIENTALE

(in collaborazione con l'Associazione Italiana di Patologia Ambientale e di Ecologia e l'Associazione Italia Nostra)

Napoli, 11-12 dicembre 1986

Presidente: D. Lauria

Relazioni di: G. Salvatore, S. Del Giacco, D. Burkitt, G. Mazzacca, R. Naccarato, M. Mancini, A.R. Bianco,

L. Cacciatore, A. Menotti, G.A. Feruglio, G. De Simone, D. Romeo, D. Lauria, G. D'Amato, G. Lobefalo, A. Ciammaichella, A. La Rocca, A. Tessitore, G. Fasanaro, V. Montrone, G. Martinelli, L. Stella, V. Dell'Aira, C.H. Oppenheimer, P. Dohrn, G. Bombace, G. Viggiani, P. Craveri, C. Cupo, D. Mainardi.

CONVEGNO ITALO-SOVIETICO SULLA SUPERCONDUTTIVITÀ DEBOLE

(in collaborazione con il Consiglio Nazionale delle Ricerche e con l'Accademia della Scienze dell'U.R.S.S.)

Napoli, 5-7 maggio 1987

NEW IDEAS IN ASTRONOMY

(in collaborazione con l'Istituto Veneto di Scienze, Lettere ed Arti, col Dipartimento di Astronomia dell'Università di Padova e con l'Osservatorio Astronomico di Padova)

Venezia, Palazzo Loredan, 5-7 maggio 1987

KOSMOS. LA COSMOLOGIA OGGI TRA FILOSOFIA E SCIENZA

(in collaborazione con l'Istituto Gramsci Veneto e col Goethe Institut)

Venezia, Ca' Dolfin, 8-9 maggio 1987

BIOMATHEMATICS AND RELATED COMPUTATIONAL PROBLEMS

(in collaborazione con il Consiglio Nazionale delle Ricerche, col Dipartimento di Matematica e Applicazioni dell'Università di Napoli e col Dipartimento di Informatica e Applicazioni dell'Università di Salerno)

Napoli-Capri, 25-30 maggio 1987

THE ETHICS OF SCIENTIFIC KNOWLEDGE

(in collaborazione con l'International Centre of Theoretical Biology e con l'Istituto della Enciclopedia Italiana)

Venezia, Palazzo Loredan, 4-6 giugno 1987

Relazioni di: E. Agazzi, M. Aloisi, A. Borsellino, E. Caianiello, V. Cappelletti, P. Cerletti, P. Fasella, R. Grantham, R. Levi Montalcini, A.M. Liquori, G.B. Marini Bettolo, A. Oliverio, M. Pera, M. Piattelli Palmarini, Sir K. Popper, I. Prigogine, G. Prodi, A. Salam, V. Sgaramella, C. Villi, L. Wolpert, E. Zuckerkandl.

LA RESPONSABILITÀ ETICA DELLO SCIENZIATO

(in collaborazione con l'Università di Colonia e con l'Istituto Italiano di Cultura di Colonia)

Colonia, 21-23 aprile 1988

UNITY AND INTERNATIONALISM OF SCIENCES AND HUMANITIES

(in collaborazione col CERN)

Ginevra, 9-10 maggio 1988

SEQUENCES, COMBINATORICS, COMPRESSION, SECURITY AND TRANSMISSION

(in collaborazione con il Dipartimento di Informatica e Applicazioni dell'Università di Salerno)

Napoli-Positano, 6-10 giugno 1988

LA MECCANICA QUANTISTICA DI FEYNMAN A 40 ANNI DALLA SUA PROPOSTA

(in collaborazione con l'Istituto di Ricerca sulle Onde Elettromagnetiche del CNR)

Napoli, 16-18 giugno 1988

IV CONVEGNO NAZIONALE DI TOPOLOGIA

(in collaborazione con il Dipartimento di Matematica e Applicazioni « Renato Caccioppoli » dell'Università di Napoli, col CNR, col Ministero della Pubblica Istruzione)

Conferenze generali di: J. ADAMEK, F. CAMMAROTO, V. FEDERCOUK, M. HENRINKSEN C. GARIBALDI, J. JONES, S. MARDESIC, Y.C. MCCRORY, S.L. MDZINARISHVILI, S. NAIMPALLY, T. NOIORI, C.M. PAREEK, R. PICCINNI, P. SHARMA, P. SIMON, L. STRAMACCIA, R. TALAMO, J. VERMEER.

Comitato scientifico: D. DEMARIA, G. DE MARCO, M. DOLCHER, S. GUAZZONE, G. TIRONI.

ANALISI REALE E TEORIA DELLA MISURA

(in collaborazione con il Gruppo di Ricerca in Analisi Reale e col Dipartimento di Matematica e Applicazioni « Renato Caccioppoli » dell'Università di Napoli)

Capri, 12-16 settembre 1988

SECONDO CONVEGNO INTERNAZIONALE DI PATOLOGIA AMBIENTALE ED ECOLOGIA

(in collaborazione con la II Facoltà di Medicina e Chirurgia dell'Università di Napoli e con l'Associazione Italiana di Patologia Ambientale ed Ecologia)

Napoli, 27-28 ottobre 1988

Relazioni di: L. Cacciatore, F. Paronetto, B.H. Lauterburg, B. Nalpas, P. Marcellin, V. Kostantinovic, V. Rizza, S. Antonello, M. Piazza, A. Menotti, G.A. Feruglio, F. Fidanza, E. Farinaro, D. Lauria, A. Ragozzino, S. Coppola, E. Abatino, L. Capaldo, D. Marino, R. Raimondi, M. Caruso, G. Donatone, L. Giuliani, A. La Rocca, R. Manchisi.

IL PRINCIPIO ANTROPICO

(in collaborazione con l'Istituto Gramsci Veneto, il Goethe Institut, il Dipartimento di Astronomia dell'Università di Padova)

Venezia, 18-19 novembre 1988

LAMARCK E IL LAMARCKISMO

Napoli, 1-3 dicembre 1988

LA SCIENZA COGNITIVA IN ITALIA

(in collaborazione con l'Istituto di Scienze Neurologiche e il Dipartimento di Scienze delle Relazioni dell'Università di Napoli)

Napoli, 7-8 aprile 1989

I FONDAMENTI DELLA MATEMATICA E DELLA FISICA NEL XX SECOLO: LA RINUNCIA ALL'INTUIZIONE

(in collaborazione con il Dipartimento di Matematica dell'Università di Perugia e con il Comitato Nazionale per le Scienze Matematiche del CNR)

Perugia, 27-29 settembre 1989

MECHANISMS OF FERTILIZATION: PLANTS TO HUMANS

Convegno dedicato alla memoria di Alberto Monroy

(in collaborazione con la Stagione Zoologica « Anton Dohrn » di Napoli)

Sorrento, 1-4 ottobre 1989

SECOND IIGB WORKSHOP MOLECULAR BIOLOGY OF DEVELOPMENT

(in collaborazione con l'Istituto Internazionale di Genetica e Biofisica)

Capri, 2-4 ottobre 1989

Relazioni di: M. ASHBURNER, J. CAMPOS-ORTEGA, M. CHALFIE, T. CLINE, E. DE ROBERTIS, D. DUBOULE, W. GEHRING, P. GRUSS, D. HIRSH, R. HORVITZ, M. LEVINE, M. NOLL, A. SPRADLING, C. WU.

Comitato scientifico: P. BAZZICALUPO, E. BONCINELLI, F. GRAZIANI, M.G. PERSICO.

WAVES AND STABILITY IN CONTINUOUS MEDIA

(in collaborazione con il Dipartimento di Matematica e Applicazioni « Renato Caccioppoli » dell'Università di Napoli e col Comitato Nazionale per le Scienze Matematiche del CNR)

Napoli-Sorrento, 9-14 ottobre 1989

Relazioni di: C.J. AMICK, M. ANILE, L. ARKERYD, N. BELLOMO, P.L. CHRISTIANSEN, M. FABRIZIO, A. GRECO, A. HEYWOOD, H. MATSUMURA, A. MORRO, I. MULLER, A.A. NAYFEH, P. PODIO GUIDUGLI, A. QUARTERONI, R.K. RAJAGOPAL, P. RENNO, S. RIONERO, T. RUGGERI, B. TRAUGHAN, R. TEMAN.

Comitato scientifico: M. FABRIZIO, P. RENNO, S. RIONERO, A. ROMANO, G. TOSCANI.

LE ORIGINI DELL'UNIVERSO

Terzo convegno veneziano di filosofia e cosmologia

(in collaborazione con: Istituto Gramsci Veneto, Dipartimento di Astronomia dell'Università di Padova, Goethe Institut)

Venezia, 24-25 novembre 1989

SCUOLA ESTIVA DI TOPOLOGIA 1990
IPERSPAZI E SPAZI UNIFORMI

(in collaborazione con il Dipartimento di Matematica e Applicazioni « Renato Caccioppoli » dell'Università di Napoli, con il CNR e col Ministero dell'Università e della Ricerca Scientifica e Tecnologica)

Napoli, 9-14 luglio 1990

Coordinamento scientifico: GIUSEPPE DI MAIO (Università di Napoli), DAVIDE DEMARIA (Università di Torino), GINO TIRONI (Università di Trieste).

Relazioni di: G.A. BEER, A. DIMOV, L. HOLA, S. LEVI, S.A. NAIMPALLY, R.A. MCCOY, A. THERÀ, H. WEBER.

IV CONVEGNO DI ANALISI REALE
E TEORIA DELLA MISURA

(in collaborazione col Gruppo di Ricerca CNR in Analisi Reale, col Dipartimento di Matematica e Applicazioni « Renato Caccioppoli » dell'Università di Napoli e col Dipartimento di Matematica e Statistica dell'Università di Napoli)

Capri, 10-14 settembre 1990

Coordinamento scientifico: L. Albano (Bari), V. Aversa (Napoli), L. Barone (Lecce), N. Berruti Onesto (Pavia), M. Boni (Modena), B. Bongiorno (Palermo), P. de Lucia (Napoli), E. de Pascale (Cosenza), M. Puglisi (Bari), G. Santagati (Catania), C. Vinti (Perugia), A. Volčič (Trieste), H. Weber (Potenza), C. Zanco (Milano).

REGULATION OF HEAT SHOCK GENE EXPRESSION

(in collaborazione con l'Istituto Internazionale di Genetica e Biofisica e con la Fondazione Viamarconidieci)

Ravello, 17-20 settembre 1990

Coordinamento scientifico: Bruno Maresca, Susan Lindquist.

Relazioni di: O. Bensaude, T. Bosch, J.R. Brown, E.A. Craig, F.J. Dice, G. Georgopulos, C.A. Grossi, R.L. Halberg, G. Hann, P. Harrison, A. Horwich, S.H.E. Kaufman, Gloria Li, J.T. Lis, R.I. Morimoto, N.S. Petersen, N. Pfanner, S.K. Pierce, B. Polla, M.J. Schlesinger, R. Voelmy, D.B. Young, R.A. Young, J.B. Winfield, C. Wu.

METODI DI ANALISI REALE NELLE EQUAZIONI A DERIVATE PARZIALI

(in collaborazione col Dipartimento di Matematica e Applicazioni « Renato Caccioppoli » dell'Università di Napoli, con l'Università di Napoli « Federico II », con l'Accademia di Scienze Fisiche e Matematiche di Napoli, col Ministero della Pubblica Istruzione)

Capri, 17-20 settembre 1990

Relazioni di: A. AVVANTAGGIATI (Università di Roma « La Sapienza »), A. BOJARSKI (Università di Varsavia), A. CANFORA (Università di Napoli), E. DE GIORGI (Scuola Normale Superiore), E. FABES (Università del Minnesota), C. FEFFERMAN (Università di Princeton), F. GUGLIELMINO (Università di Catania), T. IWANIEC (Syracuse University), E. LANCONELLI (Università di Bologna), P.L. LIONS (Università di Parigi), M. MARINO (Università di Catania), S. MATARASSO (Università di Bologna), A. MAUGERI (Università di Catania), F. MURAT (Université Pierre et Marie Curie), C. PARENTI (Università di Bologna), L. RODINO (Università di Torino), E. STEIN (Università di Princeton), G. TALENTI (Università di Firenze), M. TROISI (Università di Salerno), N. TRUDINGER (The Australian National University), I. WIK (Università di Umea), R. WHEEDEN (Rutgers University).

STOCHASTIC DYNAMICAL SYSTEMS

(in collaborazione con la Facoltà di Fisica dell'Università di Friburgo i.B.)

Napoli, 8-9 ottobre 1990

Relazioni di: P. BILLER, J. HONERKAMP, F. PETRUCCIONE.

FRONTIERE DELLA BIOLOGIA (III)

(in collaborazione con l'Istituto Internazionale di Genetica e Biofisica e con la Fondazione Viamarconidieci)

15 febbraio-30 marzo 1991

Relazioni di: C. CILLO, C. MALVA, B. MARESCA, M. D'URSO, U. DI PORZIO.

L'ORDINE NELL'ALGEBRA E NELLA LOGICA

(in collaborazione con l'Istituto di Matematica della Facoltà di Architettura dell'Università di Napoli e col Dipartimento di Scienze dell'Informazione dell'Università di Milano)

Napoli, 5-8 febbraio 1991

Relazioni di: E. CASARI (Firenze), M. CURZIO (Napoli), M.L. DALLA CHIARA (Firenze), A. DE LUCA (Roma), M. DICKMANN (Parigi), A. DI NOLA (Napoli), U. FELGNER (Tubinga), G. GERLA (Potenza), A. MACINTYRE (Oxford), D. MUNDICI (Milano), D. PERRIN (Parigi), P. RIBENBOIM (Kingston, Ontario), G. TALLINI (Roma).

FRONTIERE DELL'ANTROPOLOGIA

(in collaborazione con il Museo di Antropologia dell'Università di Napoli)

Napoli, 28 febbraio - 27 marzo 1991

Relazioni di: F. GIUSTI, F. FEDELE, B. CHIARELLI, A. TARTABINI, J. WOODBURN.

LINEAR SPACES

(in collaborazione con il CNR, il Dipartimento di Matematica e Applicazioni « Renato Caccioppoli » dell'Università di Napoli, il Gruppo Nazionale di Ricerca del MURST « Strutture geometriche, combinatorie, loro applicazioni »)

Napoli-Capri, 26 maggio - 1 giugno 1991

Coordinamento scientifico: A. BEUTELSPACHER (Università di Giessen), F. MAZZOCCA (Università di Napoli), N. MELONE (Università di Napoli), D. OLANDA (Università di Napoli), G. TALLINI (Università di Roma « La Sapienza »).

Fotocomposizione: De Petrillo & Lattuca - Napoli - Tel. 45.97.82
Stampa: Grafitalia srl - Cercola (Napoli) - Gennaio 1991

In questa collana vengono raccolti testi dei seminari di scienze organizzati dall'Istituto Italiano per gli Studi Filosofici.

1. E. Garin, L.A. Radicati di Brozolo, *Considerazioni su Einstein*
2. Luigi Aurigemma, *Recenti studi su esperienze psichiche di morenti*
3. Gaetano Benedetti, *La schizofrenia*
4. I.M. Khalatnikov, V. Belinski, *Inflationary cosmology*
5. AA.VV., *Il pensiero matematico del XX secolo e l'opera di Renato Caccioppoli*
6. David Gross, *Unified Theories of Everything*
7. Mauro Mancia, *Memoria, costruzioni e ricostruzioni*
8. James Tobin, *Price Flexibility and Full Employment*
9. Giovanni Sambin, *Alla ricerca della certezza perduta. Forma-contenuto nei fondamenti della matematica.*
10. P. Biller, J. Honerkamp, F. Petruccione, *Stochastic Dynamical Systems*